

Environmental  
Studies  
Revolving  
Funds

038 Physical Approaches to  
Iceberg Severity Prediction

The Environmental Studies Revolving Funds are financed from special levies on the oil and gas industry and administered by the Canada Oil and Gas Lands Administration for the Minister of Energy, Mines and Resources, and by the Northern Affairs Program for the Minister of Indian Affairs and Northern Development.

The Environmental Studies Revolving Funds and any person acting on their behalf assume no liability arising from the use of the information contained in this document. The opinions expressed are those of the authors and not necessarily reflect those of the Environmental Studies Revolving Funds agencies. The use of trade names or identification of specific products does not constitute an endorsement or recommendation for use.

Environmental Studies Revolving Funds  
Report No. 038  
July, 1986

**PHYSICAL APPROACHES TO  
ICEBERG SEVERITY PREDICTION**

J.R. Marko, D.B. Fissel and J.R. Birch

Arctic Sciences Ltd.  
1986 Mills Road, R.R. 2  
Sidney, B.C.  
V8L 3S1

The correct citation for this report is:

Marko, J.R., D.B. Fissel and J.R. Birch. 1986. Physical Approaches to Iceberg Severity Prediction. Environmental Studies Revolving Funds Report No. 038. Ottawa. 104 p.

Published under the auspices of the  
Environmental Studies Revolving Funds  
ISBN-0-720783-37-6  
© Arctic Sciences Ltd.

## TABLE OF CONTENTS

	<u>Page</u>
LIST OF FIGURES	iv
LIST OF TABLES	ix
ACKNOWLEDGEMENTS	x
EXECUTIVE SUMMARY	xi
ABSTRACT	xv
RESUME	xvi
<b>1. INTRODUCTION</b>	<b>1</b>
<b>2. FACTORS INFLUENCING ICEBERG SEVERITY</b>	<b>8</b>
2.1 SOURCE NUMBERS	8
2.2 ADVECTION	12
2.2.1 CURRENT FORCING	14
2.2.2 WIND FORCING	16
2.2.3 DIRECT MEASUREMENTS OF ICEBERG ADVECTION	16
2.3 DETERIORATION AND LOSS	19
<b>3. PREVIOUS APPROACHES TO ICEBERG SEVERITY MODELLING</b>	<b>24</b>
<b>4. NEW APPROACHES TO SEVERITY PREDICTIONS</b>	<b>37</b>
4.1 INTRODUCTION	37
4.2 PHYSICAL PARAMETERS	39
4.2.1 SEA-ICE EXTENT	39
4.2.2 AIR TEMPERATURE	43
4.2.3 WATER LEVEL	51
4.2.4 WIND FORCING	51
4.2.5 LARGE SCALE ATMOSPHERIC PROCESSES	60
4.3 RATIONALIZATION OF THE ICEBERG SEVERITY RECORD	77
4.4 SEVERITY PREDICTABILITY, AND EVALUATION	81
<b>5. CONCLUSIONS AND RECOMMENDATIONS</b>	<b>90</b>
5.1 SUMMARY AND CONCLUSIONS	90
5.2 RECOMMENDATIONS	91
<b>6. REFERENCES</b>	<b>94</b>

## LIST OF FIGURES

	<u>Page</u>
Figure 1: Drift of icebergs from their source, into the North Atlantic Ocean. The Hibernia drilling site is shown (*), (from Dinsmore, 1972).	2
Figure 2: Iceberg concentrations, per degree square, off Labrador (from Petro-Canada, 1982). The approximate edge of the continental shelf is indicated by the heavy solid line.	3
Figure 3: Flowchart representation of the factors affecting the number of icebergs reaching the Grand Banks.	5
Figure 4: Estimated numbers of icebergs crossing 48°N, 1900 to 1985 (after Ketchen, 1977). The broken-line curve represents the Davis Strait ice extent during January, while the arrow symbols along the time axis indicate years of strong ENSO events.	6
Figure 5: a) The major iceberg-producing regions of Greenland (from Greenland Tech. Org., 1979). b) The major iceberg-producing glaciers of west Greenland (from Greenland Tech. Org., 1979).	9 10
Figure 6: Mean iceberg density distribution, May through October, 1975-1978 (from Greenland Tech. Org., 1979).	13
Figure 7: The main current patterns responsible for the southerly flux of icebergs.	15
Figure 8: Mean sea-level pressure and winds for January (Meserve, 1974 after Petro-Canada, 1982).	17
Figure 9: Tracks of several ice beset vessels and the <u>Polaris</u> floe party (Smith, 1931). Average speeds are shown for major segments of each track.	18

	<u>Page</u>
Figure 10: Large-scale patterns of iceberg drift in eastern Davis Strait, based on summer observations during 1975 through 1978 (from Greenland Tech. Org., 1979).	20
Figure 11: Theoretical strip-volume waterline melting rate due to wave erosion.	22
Figure 12: The nature of the probability density function for icebergs from the source region to the area of final extinction (from Ebbesmeyer, Okubo and Helseth, 1980; after Chandrasekhar, 1943).	27
Figure 13: Probability density of the annual number of icebergs passing south of 48°N (grouped on 250 iceberg classes) (from Ebbesmeyer, Okubo and Helseth, 1980).	28
Figure 14: Histogram showing the number of seasons (1880 to 1972) having a given number of icebergs (from Murty and Bolduc, 1975).	29
Figure 15: Observed (solid) and computed (dashed) iceberg counts passing 48°N (from Post, 1956).	34
Figure 16: Observed (solid) and computed (dashed) iceberg counts based on a correlation of the number of commas in Tellus (from Kinsman, 1957).	35
Figure 17: Area of Davis Strait used for ice extent measurements.	40
Figure 18: Sea ice extent data, normalized to 61,000 nautical miles squared for a) the entire record 1953-1985; b) the period of lower quality data, 1953-1971; and c) the period of higher quality data, 1972-1985.	44

- Figure 19: Scatter plot of both early low quality (upper) and later higher quality (lower) data on the reported numbers of icebergs passing south of  $48^{\circ}\text{N}$  as functions of the corresponding spatial extents of the January sea-ice cover in Davis Strait. Accompanying each data point is a 2-digit number representing the year. The experimental data points corresponding to high severity, i.e. numbers greater than 600 and hence to the right of the drawn vertical boundary, all have normalized ice extents  $\geq 1.0$ . The absence or presence of high severity entries for intermediate sea-ice extents depends on the precise specification of the high/intermediate extent boundary. No such ambiguity exists with respect to the data points associated with the low,  $< 0.87$ , sea-ice extent regime. High iceberg severity was never observed to follow such conditions. 45
- Figure 20: a) January air temperatures at Frobisher Bay versus yearly iceberg count. b) 700-1000 mb separations, at  $65^{\circ}\text{N}$ ,  $60^{\circ}\text{W}$  for December and January, versus the yearly iceberg count. Accompanying each data point is a 2-digit number representing the year. 47  
48
- Figure 21: Probability distributions of Frobisher Bay air temperatures (January). 49
- Figure 22: Probability distributions of 700-1000 mb separations, January.
- Figure 23: Frobisher Bay air temperature versus off-shore sea-ice extent, January. Accompanying each data point is a 2-digit number representing the year. 52
- Figure 24: Frobisher Bay air temperature (December) versus the sea-ice extent in January. Accompanying each data point is a 2-digit number representing the year. 53



- Figure 25: Anomaly in the longshore component of the winter (Dec.-Feb.) wind stress, computed for offshore Labrador (57°N, 58°W), plotted versus the yearly number of icebergs crossing 48°N. Positive anomalies represent an above-normal wind stress from the northwest. Accompanying each data point is a 2-digit number representing the year. 55
- Figure 26: January-March wind run ( $\times 10^3$  km), computed from OWS Bravo data, versus iceberg counts for a) alongshore and b) cross-shore. 57
- Figure 27: Example of wind-run progressive vector diagrams used to determine cumulative iceberg displacements. The numbers accompanying the dots are month indicators. Assuming a 1-2% iceberg-to-wind response, a wind run of 10,000 km would correspond to an iceberg displacement of 100 to 200 km. 58
- Figure 28: Deviation of northern hemisphere mean air temperature from mid-1880 values (after Mitchell, 1963). 62
- Figure 29: Change of mean winter (Dec.-Feb.) sea-level air pressures (mbar) between the periods: a) 1900-39 and 1956-65; b) 1956-65 and 1966-70; c) 1966-70 and 1971-74; and d) 1900-39 and 1971-74 (from Dickson et al., 1975). 63
- Figure 30: 19-year running average of iceberg counts, March-July (upper), and (lower) 19-year average of December-March Belle Isle (Nfld.) minus Ivigtut (Greenland) pressure difference (after Morgan, 1974). 64
- Figure 31: Schematic representation of the North Atlantic Oscillation (after Wallace and Gutzler, 1981). 66

	<u>Page</u>
Figure 32: Schematic map showing isopleths of correlation of monthly mean station pressure with that of Djakarta, Indonesia (DJ). Other localities shown are Cocos Island (CO), Port Darwin (D), Nauru (N), Ocean Island (O), Palmyra (P), Christmas Island (X), Fanning (F), Malden Island (M), Apia, Samoa (A), Tahiti (T), Easter Island (E), Puerto Chicama (PC), Lima (L) and Santiago (S). (from Julian and Chervin, 1978 after Berlage, 1966).	68
Figure 33: Winter wind stress anomaly patterns associated with years of strong ENSO events, 1957, 1972 and 1983 (data from Thompson and Hazen, 1983).	73
Figure 34: Three winter wind stress anomaly patterns (1953, 1965 and 1976) representative of years of moderate ENSO events (data from Thompson and Hazen, 1983).	74
Figure 35: Northern-hemispheric teleconnection patterns; North Atlantic East Asia (NAEA) and Central Pacific-East North America (CPNA) (after Nobre, Moura and Norbe, 1985).	75
Figure 36: Probability distribution of icebergs counts, 1969-1985.	79
Figure 37: Normalized probability distribution for rationalized iceberg severity in the period 1953-1985.	80
Figure 38: Predicted and observed severity levels (low, moderate or high) for the tested indicators. The dotted prediction curves are visible only when they differ from the observed 3-level severity value.	84
Figure 39: Predicted and observed severity levels for the sea-ice parameter, using optimized partitioning.	87

## LIST OF TABLES

	<u>Page</u>
Table 1: Predictor statistics.	xiii
Table 2: Monthly average fluxes of icebergs across each latitude from Newfoundland to Cape Dyer.	26
Table 3: Predicted and observed iceberg severity for the years 1926-1930 (Smith, 1931).	30
Table 4: Sources of sea-ice extent data.	41
Table 5: Tabulation of annual iceberg severity counts and other parameters which may be related to iceberg severity.	42
Table 6: AES, Canada temperature data and periods of coverage.	46
Table 7: Tabulation of wind "event" observed at OWS Bravo from December to May, inclusive, 1950 to 1972.	59
Table 8: Year of onset of El Nino type events, 1725-1983, as classified according to event intensity by Eguiguren (1894), Quinn et al. (1978) and Rasmusson (1984).	71
Table 9: The boundaries between the high, low and intermediate categories of each predictor assuming approximate equality between the total fractional probabilities associated with subportions of the corresponding parameter distributions and those associated with iceberg severity.	83
Table 10: Predictor statistics in terms of mean and standard errors (in levels) and percentage distribution of error magnitude.	85

**ACKNOWLEDGEMENTS**

The completion of this project in its final form was made possible by the active cooperation of many members of the North American sea-ice and iceberg research community. Particular acknowledgements are due to Messrs. D. Mudry, F. Geddes, P. Cote and H. McRuer of AES Canada; Commander N. Edwards of the International Ice Patrol; Dr. J. Walsh of the University of Illinois; Mr. L. Davidson of Seaconsult Ltd.; and Dr. W. Quinn of Oregon State University, for significant provisions of data and/or comments and discussions of the severity problem.

We also would like to express our appreciation to Mr. J. Miller of Petro-Canada Explorations and Mr. Peter Wood of the ESRF supervisory organization for their encouragement and unfailing assistance in overcoming difficulties.

**EXECUTIVE SUMMARY**

The large degree of interannual variability in the number of icebergs present in the waters off Canada's southern East Coast presents difficulties for the exploration and production of offshore oil and gas. The objectives of this study were to:

1. review and evaluate procedures for long-range predictions of iceberg season severity in Newfoundland waters;
2. develop an optimum approach for iceberg severity prediction based on physically understandable relationships to measurable environmental parameters; and
3. provide recommendations for future research directed at improvements to iceberg severity prediction capabilities.

Following an extensive review of previous attempts at iceberg severity prediction, our approach concentrated on a joint examination of both a coarsened version on the historical iceberg severity record and the best available interannual time series data on a selected set of physical parameters. The criterion used in selecting these parameters was that in each case the parameter could be expected to have a source of variability in common with the iceberg severity index. The coarsening of the severity record was regarded as essential to reduce the contributions of year-to-year variations in the levels of detection effort and/or effectiveness. The coarsening criteria, although somewhat arbitrary, were chosen to maintain consistency with the general qualitative assessments of seasonal hazard as deduced from the corresponding annual IIP reports. Thus low and high severities were judged to be attained in all years where the reported numbers respectively were equal to or less than 200, or equal to or greater than 600. An intermediate category, corresponding to iceberg counts in the 200 to 600 range, contained both truly intermediate severities as well as those low and high severity years which were over- and under-counted, respectively.

The most useful parameters for testing were found to include:

1. the maximum January sea-ice extent in Davis Strait (1953-1985);

2. the January air temperatures in Frobisher Bay (1946-1984);
3. the recorded occurrences of strong El Nino-Southern Oscillation (ENSO) indices as defined by Quinn et al. (1978) and Rasmusson, (1984) (1940-1985);
4. the alongshore and cross-shore windages calculated from the 1945-1972 Ocean Weather Station Bravo daily wind record;
5. the wind stress anomalies corresponding to the calculated deviations of the along- and cross-shore geostrophic winds from the mean December to February (1950-1980) at 56°N, 58°W.

Some expectations of the relevance of sea-ice extent could be anticipated from Smith's original (1931) observation of a high correlation between iceberg severity and Newfoundland sea-ice concentration. In addition, more recent evidence (limited comparisons of iceberg and ice floe velocities) and calculations indicate that icebergs and the surrounding sea-ice cover generally have a common velocity. The coastal temperatures would also be expected to be linked to the sea-ice extent either through the proximity-dependent effects associated with the warmer water at the offshore ice edge. The wind connections have been noted in almost all previous efforts to develop models. Finally, connections to the ENSO phenomenon were based on previously suggested associations between the North Atlantic Oscillation (NAO) and ENSO (Berlage and de Boer, 1960) and, as well, because of the obvious coincidence between high iceberg counts and the well-documented large ENSO events. A physical connection between ENSO and iceberg variability could be attributable to linkages between the chains of alternating long-term average pressure cyclones and anti-cyclones which girdle the earth. This linkage is currently the subject of much active research effort. At present, it can only be stated that the shifts in the pressure systems associated with a strong ENSO event would appear to have their counterparts in the NAO which corresponds to alternating and opposing positive and negative shifts in the mean pressure associated with the adjoining Icelandic cyclone and the Azore anti-cyclone. The corresponding deepening or shallowing of the Iceland 'Low' would again be expected to respectively strengthen or weaken the southeastward iceberg flux and hence affect the observed severity.

By insisting that the probability distributions for the low, high and intermediate categories of each test parameter be identical to the corresponding distribution among the three severity categories, simple non-optimal predictions were possible in which the categorization of the predictor variable coincided with the category of the predicted severity output. Such a scheme was not possible with the binary (yes/no) ENSO indicator and in this case, high severity levels were predicted for years coincident with the occurrence of a strong ENSO event, as well as for years which were preceded by two successive years of strong ENSO events.

The comparisons of the predicted and recorded severities are given in terms of the individual predictor statistics of Table 1. The latter include mean and standard errors (in levels) and the percentages of zero-, one- and two-level errors. The data show generally good performance by all predictors, although the agreements achieved with the sea-ice extent and ENSO indicators were particularly impressive. It should be noted that optimization of the sea-ice extent predictor led to correct predictions in 29 of the 33 years tested. In addition, three of the four noted errors occurred prior to 1961 when according to the data sources (Walsh, 1979), accurate ice concentrations were not available in the Davis Strait region. It is important to note that in all tested years, the sea-ice extent predictor never underestimated severity by more than one level.

**Table 1:** Predictor statistics.

Predictor	Mean Error	Standard Deviation	% Correct	% Correct or One Level Error	% Two Level Error
Sea-Ice Extent	-0.03	0.53	82	97	3
ENSO	-0.22	0.75	72	89	11
Air Temperature	-0.08	0.83	56	95	5
Wind Stress Anomaly	0.0	0.97	70	88	12
Bravo Windage	0.17	1.24	61	87	13

The good performance of the tested indicators suggests the existence of a common atmospheric source for all the observed parameter variabilities which could be linked to large-scale periodicities in the global pressure distribution.

Recommendations for future research are presented. Of particular importance are: improvements to existing iceberg survey techniques; research into the relationship between iceberg numbers and the extent and movements of sea-ice; and an improved understanding of iceberg deterioration mechanisms in more southerly waters.



**ABSTRACT**

Previously developed statistical techniques for forecasting iceberg numbers arriving at latitudes of 48°N or less were reviewed and found to be inadequate for operational use in conjunction with Grand Banks hydrocarbon exploration. Several alternative, more physically-based forecasting methods were then developed based on comparisons of the existing severity data with corresponding good quality data sets for physical parameters which were suspected to be closely related to the physical mechanisms which control iceberg severity. Useful parameters were found to be the January sea-ice extent in Davis Strait, the ENSO (El Nino Southern Oscillation) strength index, winter sea-surface and coastal temperature in Davis Strait and the Labrador Sea wind and wind stress anomaly values. The results of comparisons against a rationalized three-level iceberg severity appeared to be consistent with a common global scale atmospheric source of severity variability. Although the data were rather limited, it would appear that the occurrence of high levels of the ENSO strength index tends to precede by several months the occurrence of high iceberg severity. The best actual performance as an indicator was achieved with the Davis Strait sea-ice extent which over a 25-year period, for which good sea-ice data were available, produced only one hindcast error on the three-level severity scale. Recommendations are provided with regard to obtaining improved understanding of interrelationships among sea-ice extent, sea-ice velocity, iceberg numbers and the rates of iceberg deterioration.

**RESUMÉ**

Nous avons étudié les techniques statistiques, déjà développées pour la prévision des nombres d'icebergs qui arrivent à la latitude de 48°N ou moins, et nous avons conclu qu'ils sont inadéquats pour utilisation opérationnelle dans l'exploration pour hydrocarbures sur les Grand Bancs de Terre Neuve. Nous avons développé plusieurs autres méthodes de prévision qui sont basées sur des mécanismes plus physiques. Ils sont déduits des comparaisons entre le nombre d'icebergs et de bonnes informations sur les paramètres soupçonnés d'être pertinents. Les paramètres qui sont avérés les plus pertinents, sont la quantité de glace dans l'Étroit de Davis en Janvier, un index exprimant l'intensité de ENSO (El Nino Southern Oscillation), la température de la surface de la mer et de la côte dans l'Étroit de Davis pendant l'hiver, et les déviations par rapport aux valeurs moyennes du vent et de la contrainte du vent dans le Mer du Labrador.

Les résultats des comparaisons avec un index de sévérité des icebergs, rationalisé et à trois niveaux, sont consistants avec une source atmosphérique d'échelle globale. Les données sont limitées, mais elles suggèrent qu'un index ENSO élevé précède par quelques mois les périodes de forte concentration des icebergs. Comme indicateur, le meilleur paramètre fut la quantité de glace dans l'Étroit de Davis. Lorsque comparé avec l'indicateur de sévérité de trois niveaux, il n'a produit qu'une seule erreur pendant 25 ans pour lesquelles de bonnes données sont disponibles.

Nous faisons des recommandations pour mieux comprendre les relations entre la quantité de glace de mer, sa vitesse, le nombre d'icebergs et leurs vitesses de détérioration.

## 1. INTRODUCTION

Technological advances have greatly increased the ease with which man carries out his complex activities in the harsh northern marine environment. Nevertheless, the degree to which these activities are safely conducted with minimum impact on environmental quality, requires careful planning to insure the adequacy and optimal use of logistical resources.

In the Labrador Sea and Grand Banks areas, the planning efforts of mariners, fishermen, and hydrocarbon exploration syndicates have often been confounded by the large interannual variability of the regional iceberg population. This report examines the feasibility of forecasting, several months in advance, the annual numbers of icebergs to be encountered in the Grand Banks region.

The ocean circulation patterns which bring icebergs to the Grand Banks were first reported in detail by Smith (1931) as part of the U.S. Coast Guard and International Ice Patrol (IIP) attempt to prevent recurrences of the 1912 Titanic tragedy. The deduced flow, as confirmed and augmented by more modern tracking experiments (Figure 1), reflects the overall cyclonic circulation which dominates the water bodies of Baffin Bay, Davis Strait and the Labrador Sea. This circulation moves the icebergs from their principal source areas, the glacial fronts of central and northern West Greenland, northward and westward into the strong southward flows of the Baffin and Labrador currents. These currents and the corresponding iceberg flows tend to be concentrated over the continental slope and outer shelf regions as indicated by the plots of average seasonal counts off the Labrador Coast (Figure 2).

The average time for an iceberg to travel from the staging areas of West Greenland to the final extinction zones off Labrador and Newfoundland is estimated to be 3 years or longer (Marko, Birch and Wilson, 1982). This estimate is not consistent with travel times of 150 to 200 days, derived from observed typical drifter speeds (25 km/day) in the main Current cores. The discrepancy of actual to expected transit times was attributed (Marko, Birch and Wilson, 1982) to frequent diversions of icebergs into adjacent weaker current regimes. In particular, groundings in shallow water areas and entrapment by the growth of landfast ice shelves significantly impede the overall rate of southward advection during the life history of individual icebergs.

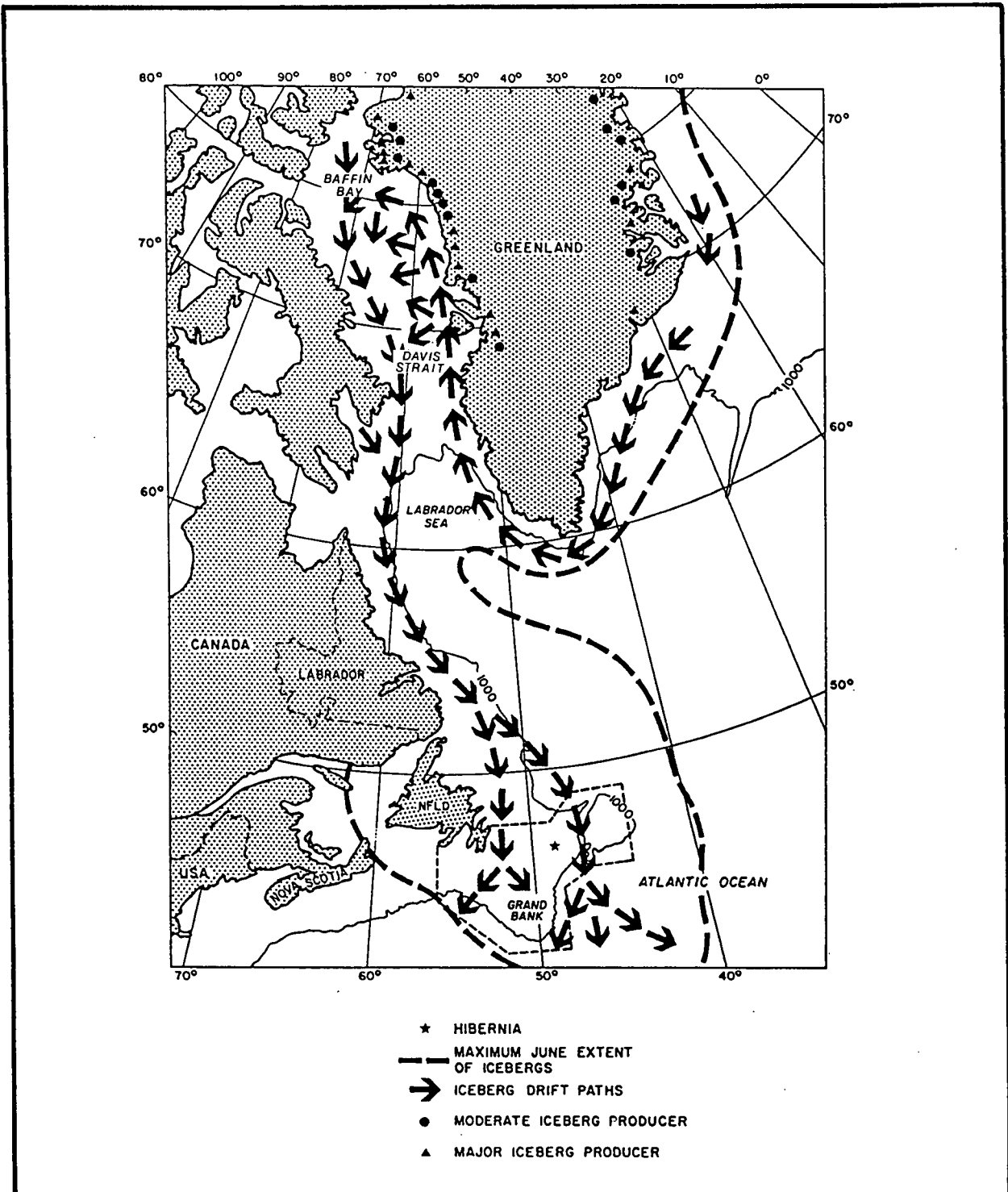


Figure 1: Drift of icebergs from their source, into the North Atlantic Ocean. The Hibernia drilling site is shown (\*), (from Dinsmore, 1972).

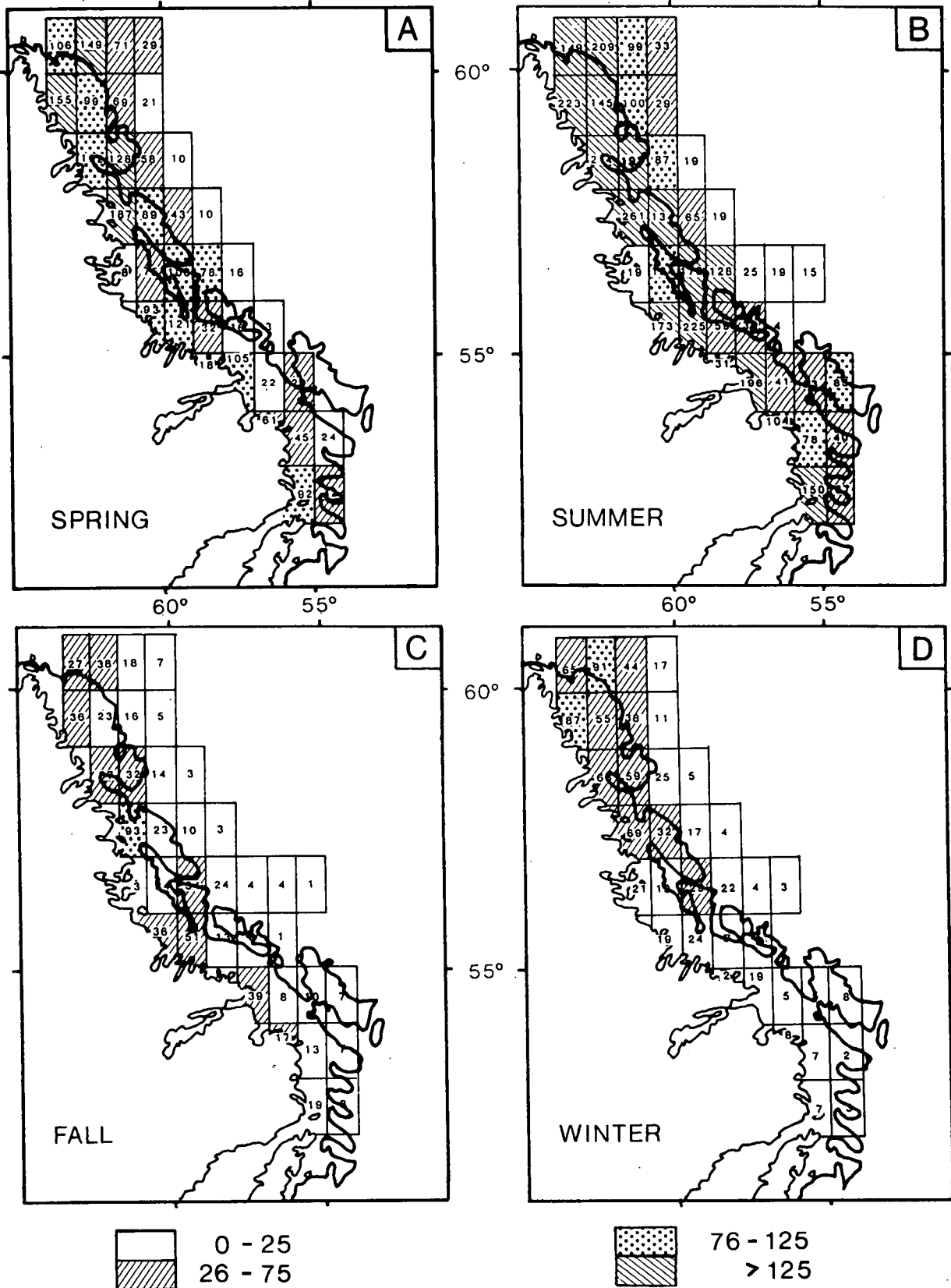


Figure 2: Iceberg concentrations, per degree square, off Labrador (from Petro-Canada, 1982). The approximate edge of the continental shelf is indicated by the heavy solid line.

The International Ice Patrol has found it useful to attribute the variability in the annual numbers of icebergs reaching the normal endpoint of this circulation to corresponding variations in three major factors:

1. The numbers and sizes of icebergs in upstream source areas during the winter period preceding the annual iceberg season.
2. The advection, or the rate at which icebergs move southward toward the Labrador-Grand Banks region.
3. The changes in iceberg numbers associated with melting and the calving of small and large iceberg fragments.

The linkage between these factors and the observed iceberg severity is illustrated for convenience by the flowchart of Figure 3. The severity end-product in the Figure has traditionally been expressed in terms of the annual numbers of icebergs observed at latitudes lower than 48°N. Records of these numbers, dating back to 1880 (Mecking, 1906), have been utilized in numerous prior studies of the variability problem. Early data were obtained from sums of the observations recorded in shipboard logs. After correction for multiple sightings of individual icebergs, these data were combined with subsequent annual counts by the IIP to provide, in principle, a continuous record of annual counts for the 1880-1985 period. It is important to note that this record consists of data obtained with successively increasing levels of sampling effort and technology. The record includes, at one time or another, observations from sailing ships, Coast Guard survey vessels, airborne visual observation, airborne radar observation and most recently, side-looking airborne radar (SLAR). Thus, for example, the record high counts of 1984, can be attributed in part, to the extra search effort associated with the IIP operation, BERGSEARCH '84. Forty-nine per cent of the reported sightings were made with SLAR instruments. As a result, even the most commonly cited IIP post-1900 record of iceberg severity (Figure 4) has its own internal inconsistencies and inaccuracies which must somehow be taken into account in any meaningful usage.

This report will begin with a review (Section 2) of relevant details of the mechanisms which govern the characteristics of the three basic factors cited in Figure 3. This treatment will be followed by a consideration of previous prediction models (Section 3) prior to the presentation (Section 4) of our own arguments for a more physically-based approach which might hope to avoid some of the difficulties inherent in the predominantly

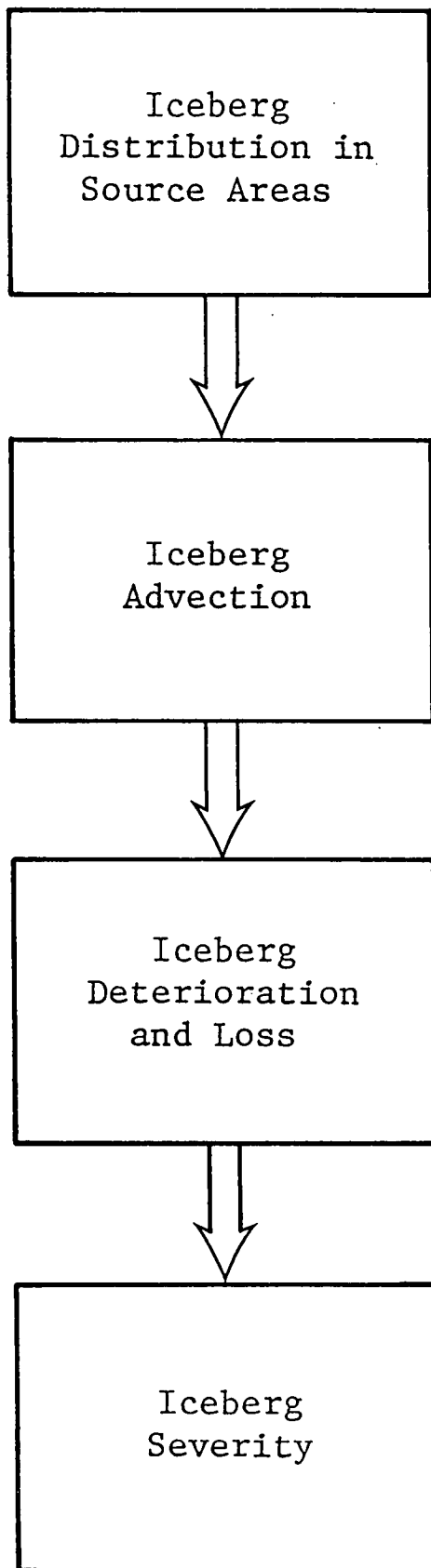


Figure 3: Flowchart representation of the factors affecting the number of icebergs reaching the Grand Banks.

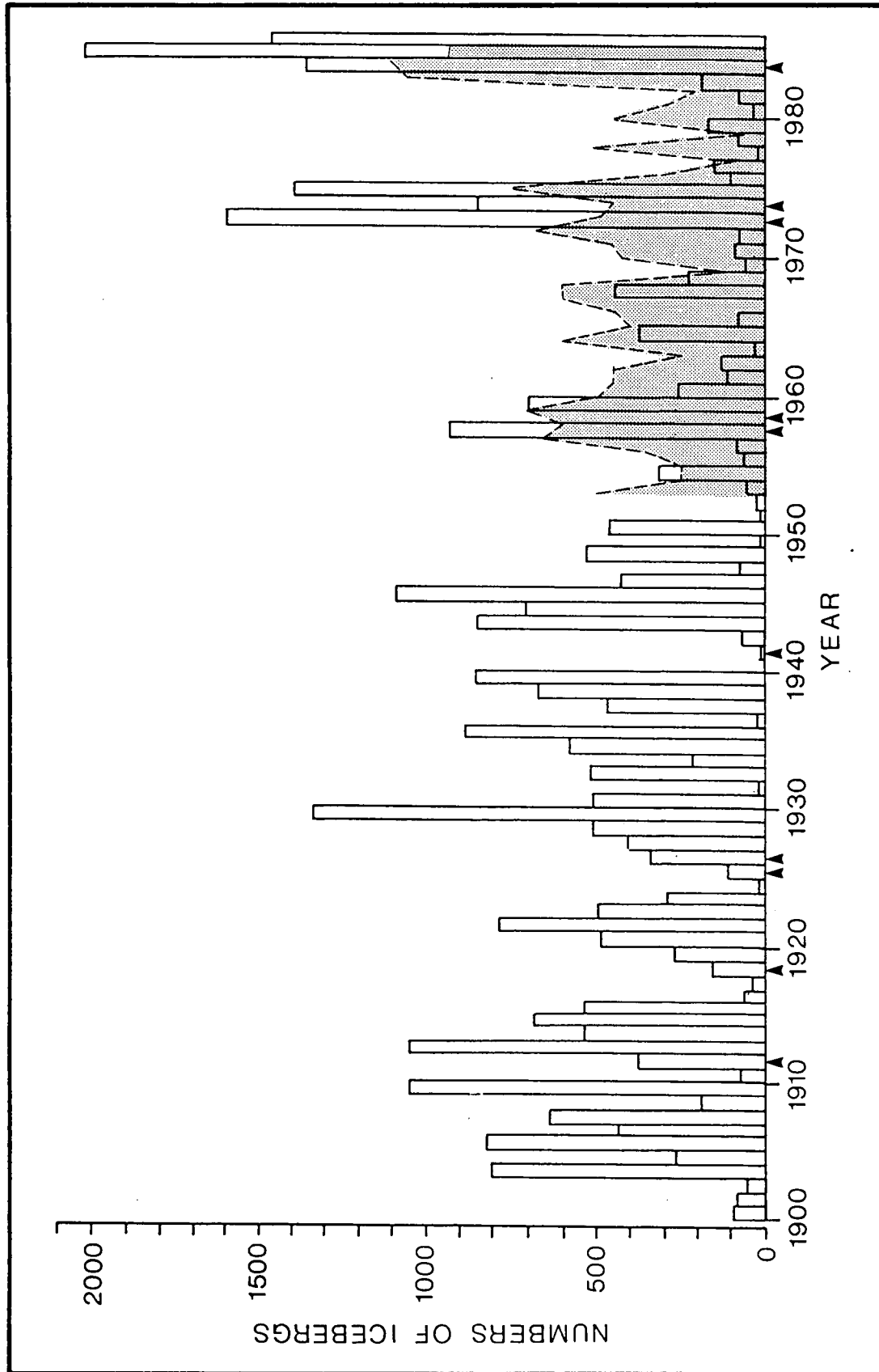


Figure 4: Estimated numbers of icebergs crossing  $48^{\circ}\text{N}$ , 1900 to 1985 (after Ketchen, 1977). The broken-line curve represents the Davis Strait ice extent during January, while the arrow symbols along the time axis indicate years of strong ENSO events.



statistical methodology of the previous work. The results obtained with this approach are then discussed in detail. A closing section (Section 5) summarizes the new results obtained in this report and presents recommendations for further research and testing.

## 2. FACTORS INFLUENCING ICEBERG SEVERITY

### 2.1 SOURCE NUMBERS

It is generally believed (Dinsmore, 1972) that roughly 85% of the icebergs which reach the Grand Banks of Newfoundland originate from the tidewater glaciers of West Greenland (Figure 5). These glaciers annually calve some 10,000 to 20,000 icebergs into the adjoining waters of Baffin Bay. Other contributions to the Newfoundland iceberg population arise from the glacier fields of East Greenland (estimated as 10%) and the glaciers and ice shelves of Ellesmere, Devon and Bylot islands (estimated as 5%).

Quantitative estimates of the interannual variability of iceberg production in these primary source areas have heretofore been inhibited by the vast numbers of icebergs involved. Thus, it has not been uncommon for counts in the areas immediately adjacent to the glacial front production zones to be expressed in terms of qualitative judgements such as "very many". Moreover, the size criteria for inclusion in the count of icebergs in such areas tend to be elevated relative to less populated zones.

In any case, this lack of knowledge in primary source variability is carried over into the secondary source areas which are of most immediate interest to the development of 3 to 6 month severity forecasts. Such source areas encompass the upstream regions occupied in December and January by those icebergs which pass south of 48°N during the subsequent March to July period. Assuming that an iceberg observed at 48°N in early July had moved southward at a 20 km/day average speed, one would expect the northern boundary of the secondary source regions to be in the vicinity of 68°N. Similar drift rates were used to guide the IIP pre-season survey program during the 1971-1978 period. Thus, until 1973, surveys were carried out to 67°N and subsequently to 71°N. Unfortunately, the results of these surveys are not very useful for detailed secondary source characterization. Particular difficulties in the data could be associated with the incompleteness of the survey coverage (typically only 10% to 20% of each grid square was actually surveyed) and with a frequent inability to distinguish between icebergs and other radar targets (i.e. fishing boats). In addition, no separate designation was given to those icebergs which were trapped in fast ice. Such icebergs were generally not mobile and were unlikely to contribute to the following season's iceberg flux at 48°N. Additionally, there were obvious inconsistencies between the reported annual iceberg counts as a function of latitude both in comparison to corresponding counts recorded in February and with regard to plotted average values for the preceding 10 year

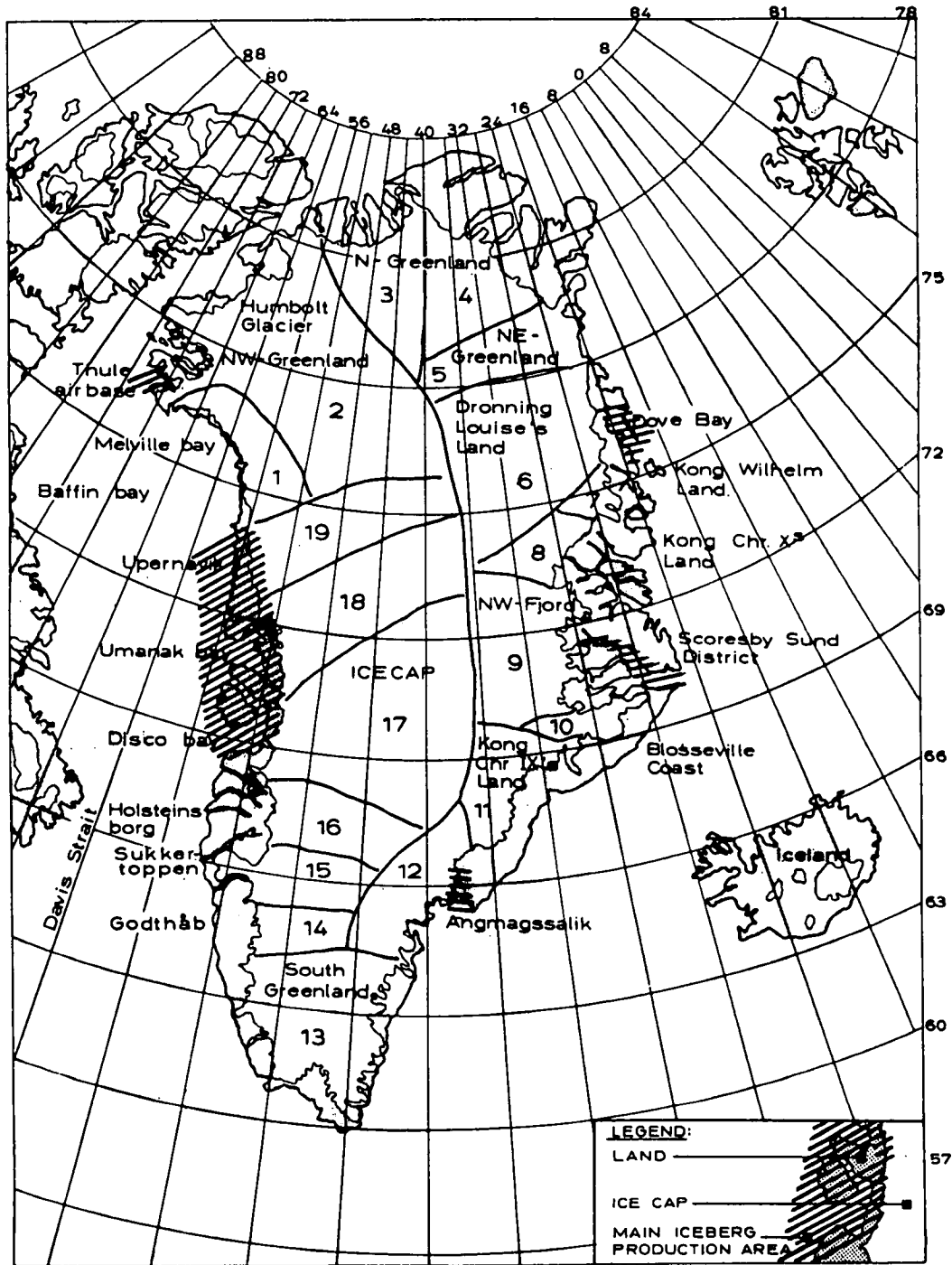


Figure 5: a) The major iceberg-producing regions of Greenland (from Greenland Tech. Org., 1979).

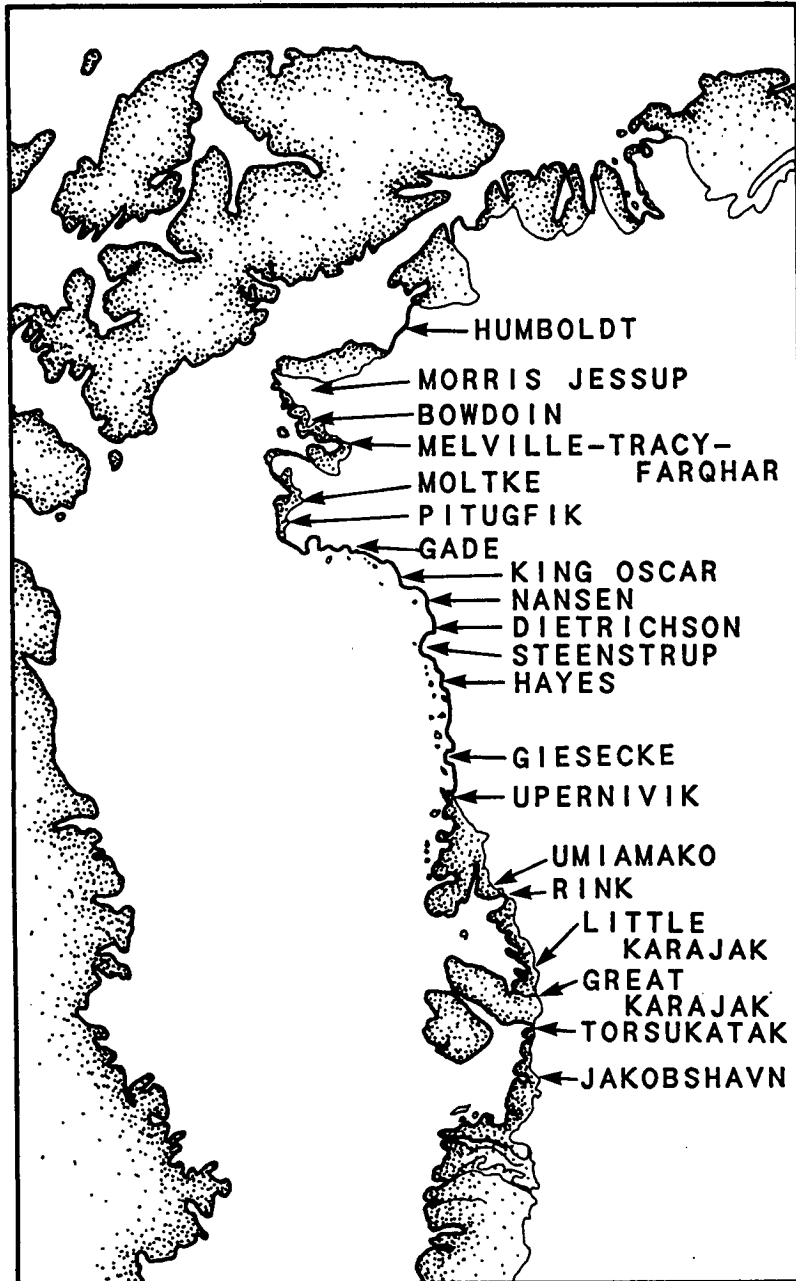


Figure 5: b) The major iceberg-producing glaciers of west Greenland (from Greenland Tech. Org., 1979).

period. With only one exception, the overall total of January icebergs always fell below the preceding 10-year January average.

The IIP record of winter iceberg counts contains some useful observations, such as the presence of a large release of icebergs from Melville Bay over the 1966-1969 period and anomalously low iceberg numbers in the secondary source region prior to the 1975 season. However, the incompleteness and uncertainty of the record must be recognized in the application of this data set to prediction model development.

Several other reports of iceberg survey data were also reviewed with respect to their potential for characterizing the secondary iceberg source. Summaries of the respective contents, deficiencies and contributions are given in the following paragraphs.

1. Labrador Iceberg Baseline Study, 1981 (Hengeveld, AES Ice Branch, 1981). This study, conducted by the Atmospheric Environment Service and Petro-Canada Resources, presented data on iceberg observations recorded during 5 flights of the AES SLAR instrument over the July-November period of 1981. Detailed data were confined to latitudes below 60° and the only flight of possible immediate interest to this study, that of November 7, 1981, was flown with a 100 km range setting which precluded a comprehensive mapping of the Labrador shelf iceberg population.
2. Historical SLAR Iceberg Data Base Creation, Labrador Sea, 1978 to 1980 (Intera Environmental Consultants Ltd., 1982). Film records of 97 AES SLAR flights through the Grand Banks-Labrador Shelf area (south of 60°N) over the period of 1978-1980 were scrutinized to identify the locations and, when possible, the dimensions and type of surrounding ice environment for all imaged icebergs. Emphasis was placed on the use of the SLAR instrument in its 100 km range setting, again severely limiting both the completeness of iceberg detection and the resolution of iceberg dimensions and surrounding ice type.
3. SLAR/SAR Image Analysis, East Coast Labrador and Newfoundland (Perchanok et al., 1982). This Petro-Canada Resources study reviewed the same data covered in the above-cited (Intera) work together with additional analyses of the 1981 SLAR record and the inclusion of a small amount of sea-ice data obtained from flights of the Canada Centre for Remote Sensing (CCRS) SAR instrument. Much of the emphasis was placed on locating ice type boundaries, ice edges and

ice floe dimensions and shapes. Iceberg position data were compiled in terms of densities of icebergs/ $10^4\text{km}^2$ . On the basis of these data, it was proposed that the highest iceberg density region on the Labrador Shelf tends to shift southward and in an offshore direction as the season progresses from January to May. Again the temporal coverage and the deficiencies of the 100 km range for iceberg detection preclude quantitative use of these results.

4. Project Iceberg Statistics (Martec, 1982). This work reviewed iceberg positional and dimensional data collected over the period 1971-1980 at 23 different offshore drilling locations in the Labrador Sea and on the Grand Banks. Although the data potentially contain information directly relevant to year-to-year and regional differences in iceberg velocities and numbers, the more or less complete absence of standardization in the data-taking procedures and the highly localized spatial and temporal coverage of each data set greatly limits the usefulness of the results.
5. Iceberg density distributions were obtained during 1975-1978 for the eastern Davis Strait region (Greenland Technical Organization, 1979) (Figure 6). The data were recorded during oil drilling operations and apply to the May through October period only. They indicate high iceberg concentrations in the Disko Bay region, and in a region south of Godthaab. In the latter case, the observed icebergs were presumably transported from east Greenland source regions via the East and West Greenland currents.

Overall, it is apparent that present knowledge of the wintertime spatial distribution of icebergs in southern Baffin Bay, Davis Strait and the Labrador Sea is not adequate to provide quantitative measures of interannual variability in the source region. The need for areal densities of mobile icebergs (icebergs/unit area) together with corresponding data on iceberg size are of course essential to a complete understanding of the downstream variations in iceberg numbers.

## 2.2 ADVECTION

Wind and current are the two main forces which move icebergs south towards the Grand Banks. They are inter-related, as the wind also contributes to the surface water circulation.

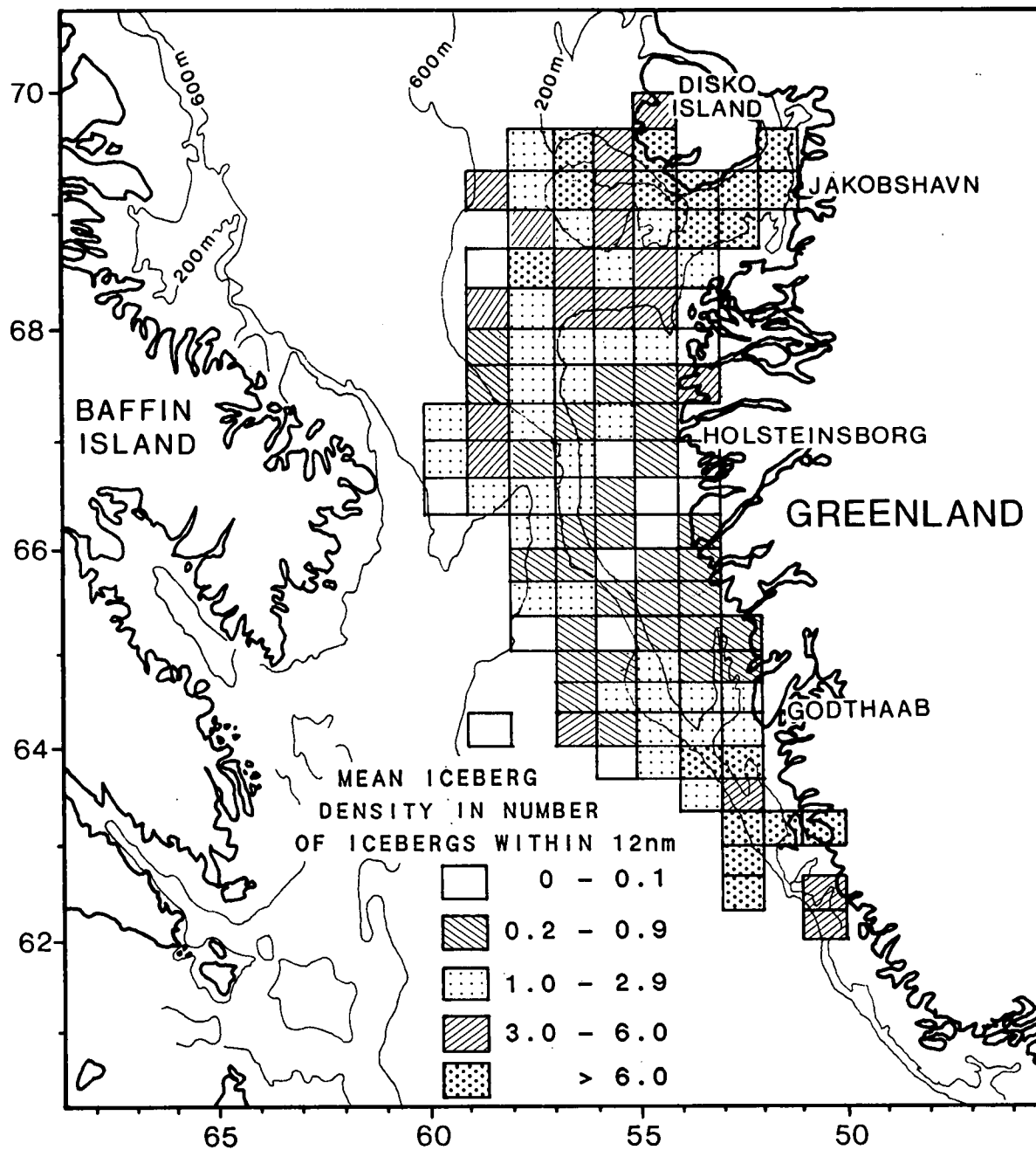


Figure 6: Mean iceberg density distribution, May through October, 1975-1978 (from Greenland Tech. Org., 1979).

### 2.2.1 CURRENT FORCING

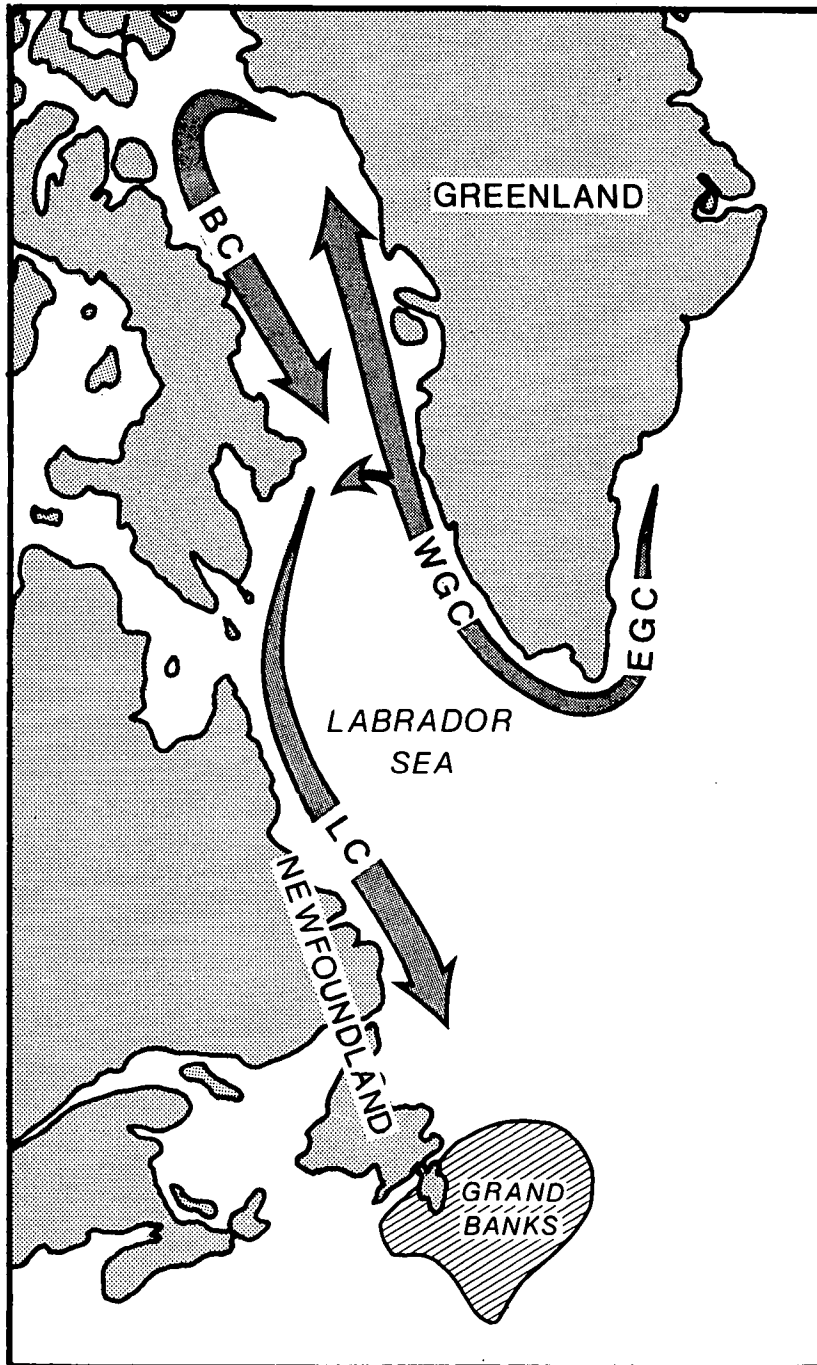
The main factor responsible for the southerly advection of icebergs is the Baffin-Labrador Current system (Figure 7). Icebergs produced along the Greenland coast are fed into this current feature via the East and West Greenland currents. The main core of the Baffin-Labrador Current is located over the continental slope and shelf break and has speeds of typically 20 to 40 km/day. Off Labrador, a second current branch is centered over the marginal trough which lies inshore of a series of shallow banks. The banks, spanning most of the length of the Labrador coastline, are separated from one another by deeper water, referred to as saddles.

The current follows the slope bathymetry with occasional diversions into re-entrant flow patterns over the continental shelves of Baffin Island and Labrador (Fissel and Lemon, 1982). The latter flow features have been most frequently observed in the trajectories of surface drifters which often move shoreward along the northern sides of a saddle and eventually exit eastward along the opposite, southern side of the saddle (Birch and Fissel, 1984).

The Baffin-Labrador Current consists primarily of Arctic Water which is colder and less saline than Labrador Sea Water. The colder temperatures help preserve the icebergs, particularly during late-winter and spring when ice concentrations are greatest. This factor contributes to the April-June seasonal peak in the numbers of icebergs crossing 48°N.

The circulation of the Baffin-Labrador Current has been extensively studied during the summer (Smith 1931; Fissel and Lemon, 1982; Petrie and Anderson 1983). However much less is known of the winter circulation. Long-term current meter data obtained by Lazier (1982) have generally been confined to considerable measurement depths of 150 m or more (to avoid ice damage) and may not be representative of the surface circulation. Lagrangian drift data from two buoys and one iceberg during January-April 1981 off Labrador (Birch, Fissel and Marko, 1983) indicated that the main flow was apparently over the slope region, but high speeds (up to 80 km/day) were also observed over Nain Bank. During summer, the currents on the banks are generally weak and variable (Fissel and Lemon, 1982). Symonds (pers. comm.) has been studying winter ice drift off Labrador but the data have yet to be fully analyzed.





BC - BAFFIN CURRENT  
LC - LABRADOR CURRENT  
WGC - WEST GREENLAND CURRENT  
EGC - EAST GREENLAND CURRENT

Figure 7: The main current patterns responsible for the southerly flux of icebergs.

Ice velocity data, obtained from NOAA satellite imagery as part of this study, compared well with the velocity of a nearby satellite-tracked iceberg in Davis Strait. This suggests that satellite-observed ice velocities could be used to estimate the motion of icebergs.

### 2.2.2 WIND FORCING

Iceberg motion is also affected by direct wind forcing. The direct response to the wind depends on factors such as surface roughness, geometry and exposed area. Rule-of-thumb estimates for the response of icebergs to wind forcing typically range from 1 to 3% of the wind speed.

During winter and spring, the winds in the Davis Strait/Labrador Sea region are mainly from the north-northwest (Figure 8). Data from coastal stations are generally unreliable due to topographic effects. Offshore measurements of extended duration are limited to the Ocean Weather Station (OWS) Bravo located in the central Labrador Sea. Continuous direct measurements are available for this site from 1945 to 1972.

In winter, the atmospheric pressure field is dominated by the Icelandic Low which is located near the southern tip of Greenland. During winter, a series of low pressure cyclones move into this region from the southwest. Their termination in this region, after arriving at near-peak intensity (hence the phrase "Icelandic graveyard"), results in the net atmospheric depression. The cyclonic flow about this low pressure cell produces the strong north-northwesterly winds which drive the icebergs south during the winter-spring period.

### 2.2.3 DIRECT MEASUREMENTS OF ICEBERG ADVECTION

The earliest indications of ice and iceberg velocities came from the drift of vessels which had (inadvertently) become trapped in the ice (Figure 9). The rates of southerly drift, for the Baffin Bay/Davis Strait region, were on the order of 5 to 20 km/day.

In the late 1970's, satellite tracking allowed the direct measurement of iceberg velocity. The early data of Brooks (1977) and Robe and Maier (1979) showed that iceberg velocities were consistent with the known summer current circulation patterns. The tendency of icebergs to follow the continental slope and shoreward intrusions at inlets and saddles was observed.

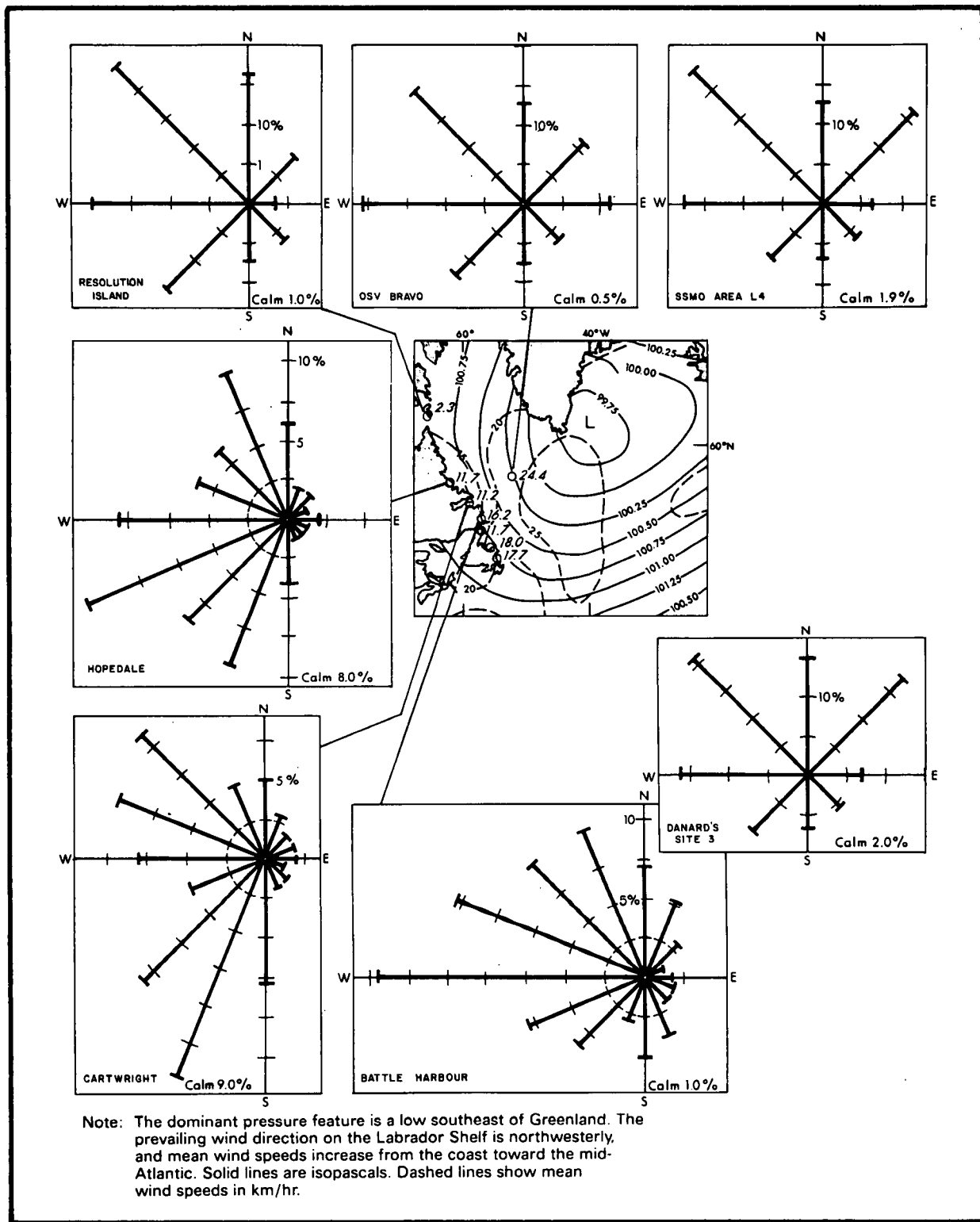


Figure 8: Mean sea-level pressure and winds for January (Meserve, 1974 after Petro-Canada, 1982).

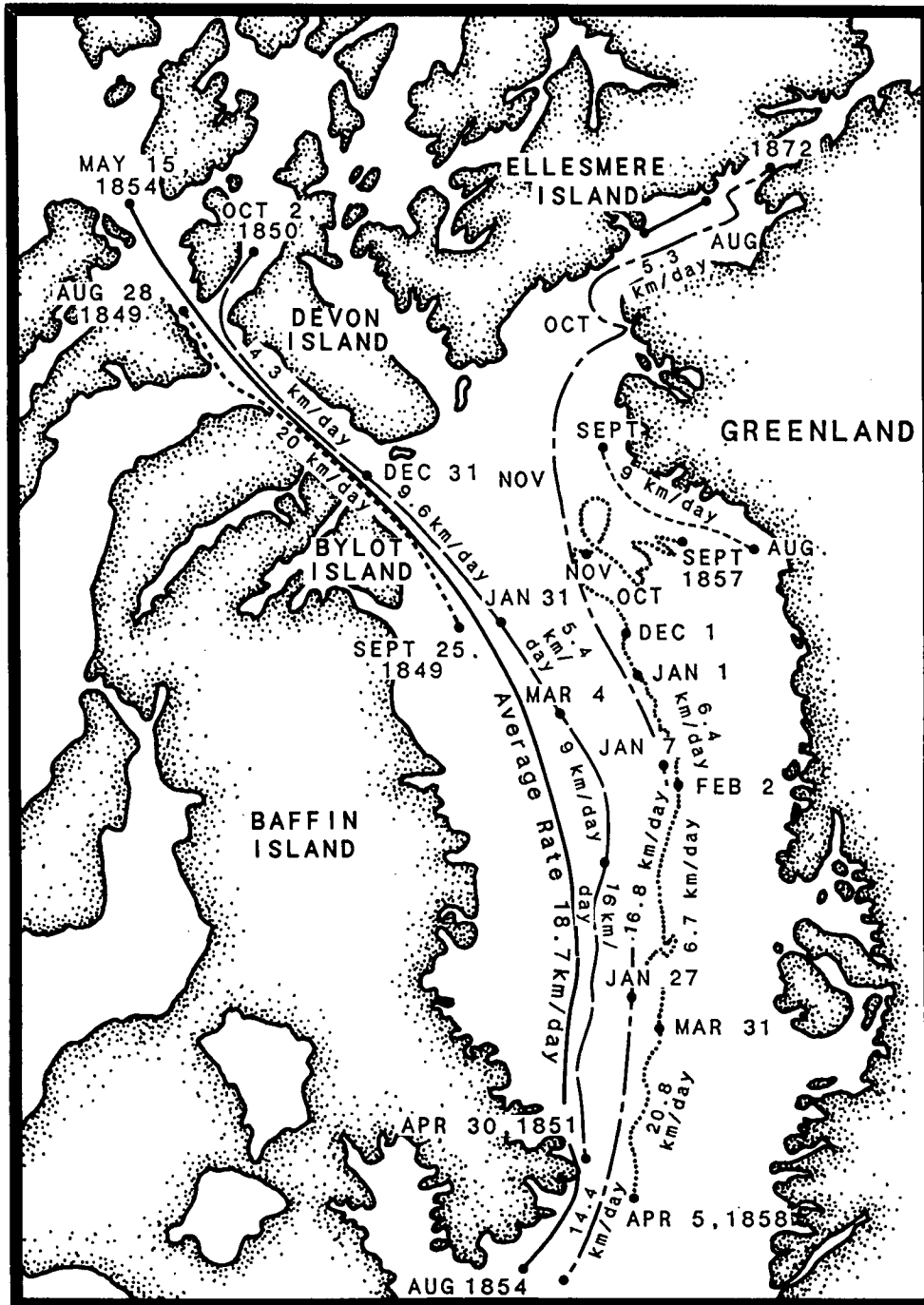


Figure 9: Tracks of several ice beset vessels and the Polaris floe party (Smith, 1931). Average speeds are shown for major segments of each track.

Icebergs were tracked during oil drilling operations in east Davis Strait from 1975 to 1978 (Greenland Technical Organization, 1979). The overall circulation pattern illustrated that "direct route" icebergs often follow westward across Davis Strait (Figure 10). Icebergs from both east and west Greenland waters, moving directly across Davis Strait, may contribute more than the oft-quoted 10% of the total number reaching the Grand Banks.

A study of 21 iceberg trajectories, covering the 1978-1980 period, suggested that shoreward excursions due to bathymetric steering could result in long periods of immobilization due to groundings and entrapment by landfast ice (Marko, Birch and Wilson, 1982). Icebergs that avoided the shelf region during the August-November period of clearing and landfast ice regrowth could sustain net southerly drift velocities on the order of 10 km/day. The broad, shallow shelf off southeastern Baffin Island appears to be a particularly likely area for grounding, as is the nearshore region southeast of Hopedale, where icebergs which have followed the marginal trough find themselves in increasingly shallow waters.

These periods of immobilization increase the travel time from the Melville Bay region, from the optimal 150 to 200 days, to typically 3 years. Icebergs which reach the Grand Banks during the March-June peak period, would generally have been in the Davis Strait region the preceding December-January.

### 2.3 DETERIORATION AND LOSS

The deterioration and loss of iceberg mass has been attributed to the following major mechanisms (Job, 1978):

1. Melting at the sub-aerial surface induced by warm air convection and solar radiation.
2. Convection processes, associated with: differential iceberg-water velocities occurring at the submerged water surfaces; buoyancy-induced flow along the sides and bottom portion of the submerged iceberg surface; and by wallowing or overturning.
3. Calving of icebergs due to: waterline erosion leading to fracturing of the resultant overhang; differential melting along cracks, faults or inhomogeneous inclusions; and subsurface calving due to upthrust on underwater shelves.

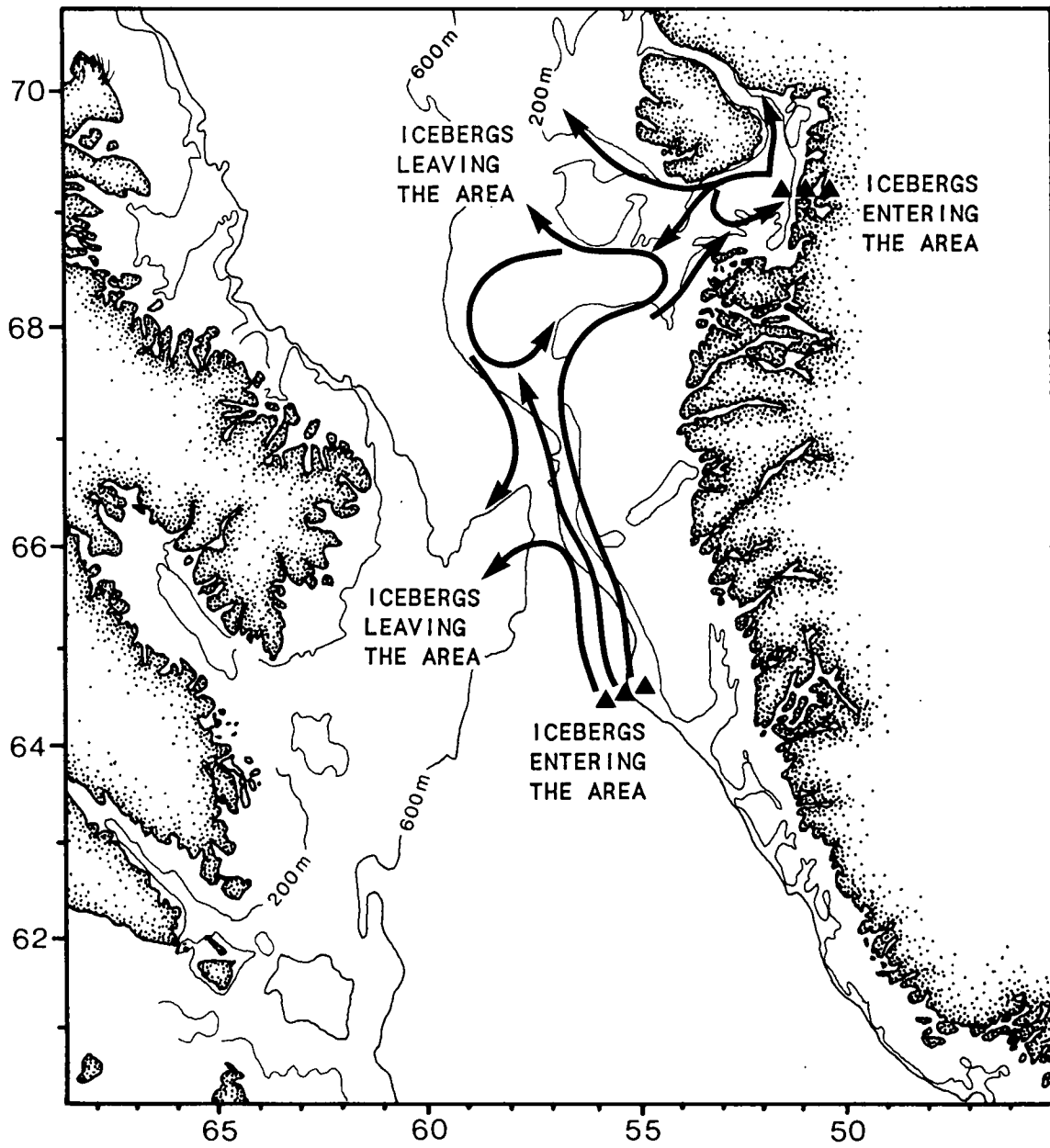


Figure 10: Large-scale patterns of iceberg drift in eastern Davis Strait, based on summer observations during 1975 through 1978 (from Greenland Tech. Org., 1979).

4. Fracturing of ice due to thermal stresses induced by wallowing or overturning in warm waters.

White, Spaulding and Gominho (1980) have examined mechanisms 1, 2 and 3 in some detail. The contributions of convection due to wallowing or overturning was judged to be insignificant because of the very short fraction of an iceberg's lifetime which is spent in this state. On the other hand, the neglect of deterioration due to subsurface calving and thermal stresses, while understandable in terms of the stochastic, shape-dependent nature of the fracture process, represents a serious gap in the characterization of both the overall loss of iceberg mass and, more particularly, in the time dependence of iceberg numbers. Difficulties in these respects arise from the apparently common (Diemand and Lever, 1986) occurrences of so-called major calving events in which a given iceberg breaks into two or more pieces, each of which is large enough to be considered an iceberg. It is clear that both the size and the sign (+) of changes in the areal iceberg concentrations, as a function of time, are determined by the magnitudes of the melting, convection and calving of small pieces relative to the iceberg multiplication rate attributable to subsurface calving and fracturing by thermal stresses.

The White, Spaulding and Gominho (1980) study concluded that wave erosion was the primary cause of iceberg deterioration due both to high melt rates in the vicinity of the waterline and the subsequent small-scale calving of undercut ice slabs. Theoretical estimates of the daily volume loss per unit length per unit difference in the ice and water temperatures are given in Figure 11.

Lesser but still substantial contributions to the melt process were associated with forced- and buoyancy induced-convective effects. The order of magnitude of these processes was estimated to be 5-20 cm/day/°C and 2 cm/day/°C respectively at the submerged surface. The only other treated melt mechanism of significance was the effect of solar insolation on the sub-aerial surface which produced typical melt values of 4 cm/day and 5 cm/day in winter and summer respectively.

These results have been applied by El Tahan, Venkatesh and El Tahan (1984) to interpret experimental data on the deterioration of a small number of icebergs (3). It is hard to judge the accuracy of the achieved understandings on such a small number of icebergs. The problem is compounded by the minimal information on underwater shape and dimension data and the lack of detailed current and temperature information. The cited experimental data, all obtained on icebergs of roughly 0.5

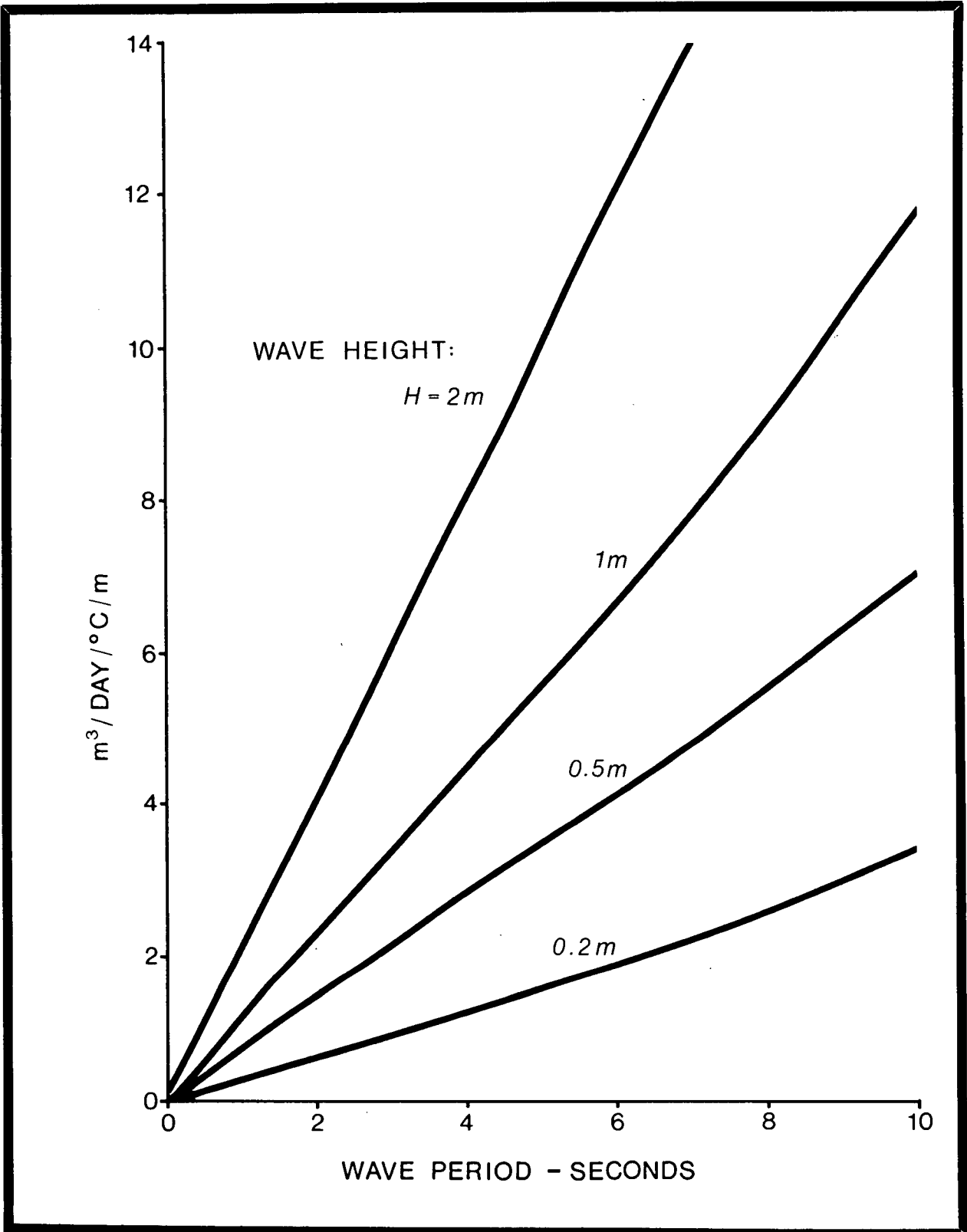


Figure 11: Theoretical strip-volume waterline melting rate due to wave erosion.



million tonnes in size, indicated daily percentage volume losses of 1.4, 2.5 and 11.6 for the April-May, May-June and September observations respectively. The large September loss rate was attributed primarily to high sea-state values. The inferred dependences on water temperature, sea state and other parameters suggests that detailed applications of even this limited contribution to changes in iceberg numbers would require a level of characterization of the oceanic environment which is presently unattainable. The additional absence of a capability for predicting the probabilities for major calving events precludes, at present, a first principles approach to characterizing the effects of deterioration on the numerical distribution of icebergs.

### 3. PREVIOUS APPROACHES TO ICEBERG SEVERITY MODELLING

The basic pattern followed in many previous efforts to predict iceberg severity was set by the early observation (Meinardus, 1904; Mecking, 1906) of a relationship between iceberg numbers off Newfoundland in the spring and preceding atmospheric pressure distributions over the North Atlantic and adjoining areas. After the accumulation of an improved record of iceberg counts and oceanographic and meteorological data, Smith (1931) used this idea to choose environmental parameters suitable for multiple regression testing against the severity record. It was hoped that the results of this testing would yield a statistically demonstrable relationship between the seasonal iceberg counts and the values of one or more atmospherically-related parameters as measured, or averaged, over some preceding period.

Smith faced two major problems in this work:

1. The lack of any certainty that an apparently complex, multi-phased process such as the creation, transport, deterioration and disappearance of icebergs over trajectories many thousands of kilometres in length, could be usefully treated in terms of a finite number of easily measureable parameters.
2. The quality of the dependent variable data base, i.e. the count of icebergs located to the south of 48°N, was highly suspect.

In the first instance, Smith was guided by the physical reasoning that the outflow of Arctic Ocean air west of Greenland and a corresponding inflow east of Greenland would coincide with a northwest wind orientation over areas upstream of Newfoundland. Such winds were favourable to southeasterly iceberg transport and hence to high severity. He further assumed such air flows to be associated with respectively high and low values of the atmospheric pressure gradients between Ivigtut, Greenland and Belle Isle, Newfoundland and between Stykkisholm and Bergen, Norway respectively. These gradients, along with several other quantities, were thus selected as suitable parameters for testing against the severity record.

The second cited problem was assumed to be the principal reason for the deviation of the severity probability distribution from the Gaussian or normal form. Smith's conclusion that "the iceberg values failed to follow the requirements of a variable; that is the greatest number of deviations did not fall

proportionately near the mean average", led to his arrangement of "the years in conformity with the shape of a probability curve and then from a transformation curve to obtain fresh relative values of the icebergs". This process resulted in a new scale of iceberg severity which ranged from 0 to 10 and which allowed the corresponding values for the years 1880-1929 to be normally distributed. Smith's procedure in making these "corrections" was not published. Other, more recent information suggests that the observed deviation of the iceberg probability distribution from the Gaussian form are not unexpected, given an iceberg population in the "near extinction" portion of its travel path. In this respect, it is useful to note some relatively recent results obtained by Ebbesmeyer, Okubo and Helseth (1980) in their statistical analyses of (1) the IIP iceberg count data and (2) the average monthly iceberg fluxes across successive lines of latitude over the period 1963-1969 computed by Anderson (1971) (Table 2). These authors concluded that the flux at any given latitude could be expressed as a sum of two terms: one linearly proportional to latitude; and the other representing a random fluctuation about a mean value. Additionally, arguments were presented suggesting that the overall probability distributions of the annual iceberg numbers were of the exponential form at a latitude of 48°N. This form is characteristic of a forward diffusive flow in its so-called extinction region, associated here with the final melting and disappearance of the icebergs. The difference relative to distributions for areas progressively more upstream is illustrated in Figure 12. The distribution in the source or near production areas is approximately Gaussian and centered at a relatively large value of the mean population. The experimental data for iceberg counts off Newfoundland (Figure 13, Figure 14) are consistent with an experimental probability distribution of the form:

$$p(N) = \frac{1}{\bar{N}} e^{-N/\bar{N}}$$

where  $\bar{N}$  is the long-term mean of the iceberg count at 48°N.

Smith's tests showed that, by far, the strongest correlations relative to iceberg severity ( $r = +0.86$ ) were achieved with the amount of pack ice present off Newfoundland in the February to May period. Nevertheless, Smith's subsequent development of predictive models ignored linkages to sea ice extent, possibly because of the impracticalities involved, at that time, in obtaining sea ice data, and in view of the negligible advance warning provided by a February to May averaged parameter.

**Table 2:** Monthly average fluxes of icebergs across each latitude from Newfoundland to Cape Dyer.

<b>Flux Across</b>	<b>Jan</b>	<b>Feb</b>	<b>Mar</b>	<b>Apr</b>	<b>May</b>	<b>June</b>	<b>July</b>	<b>Aug</b>	<b>Sept</b>	<b>Oct</b>	<b>Nov</b>	<b>Dec</b>	<b>Total</b>
67N	134	118	147	143	155	156	165	161	128	123	128	139	1697
66N	134	117	150	137	153	154	165	154	120	110	117	139	1651
65N	134	117	142	140	152	153	163	154	126	102	104	137	1624
64N	134	117	141	138	149	152	161	153	113	99	97	130	1584
63N	134	117	139	137	147	149	157	146	107	95	91	123	1542
62N	107	95	139	135	145	134	124	84	61	53	57	93	1227
61N	106	95	134	135	145	138	122	86	60	49	49	87	1206
60N	103	95	128	131	144	142	124	87	51	40	40	74	1159
59N	97	94	122	130	142	141	129	90	53	26	36	59	1119
58N	87	92	115	129	139	140	135	95	62	21	26	43	1084
57N	73	88	112	128	132	137	127	99	56	20	16	31	1019
56N	49	77	112	112	133	134	122	106	68	28	10	19	966
55N	31	59	99	105	126	130	120	118	75	35	11	10	909
54N	17	39	82	98	116	118	91	81	49	32	15	6	744
53N	12	30	73	93	111	107	64	54	33	23	11	2	613
52N	9	23	62	89	106	102	42	34	22	14	9	0	512
51N	4	14	40	76	86	67	37	11	2	5	5	0	347
50N	3	8	35	66	75	32	22	5	1	2	3	0	263
49N	2	5	25	53	67	29	15	1	0	0	0	0	197
48N	0	5	18	46	57	23	8	0	0	0	0	0	157
48N 1963-69 AVERAGE*	0	1	19	74	47	24	4	1	1	0	0	0	171

\*Reported by International Ice Patrol.

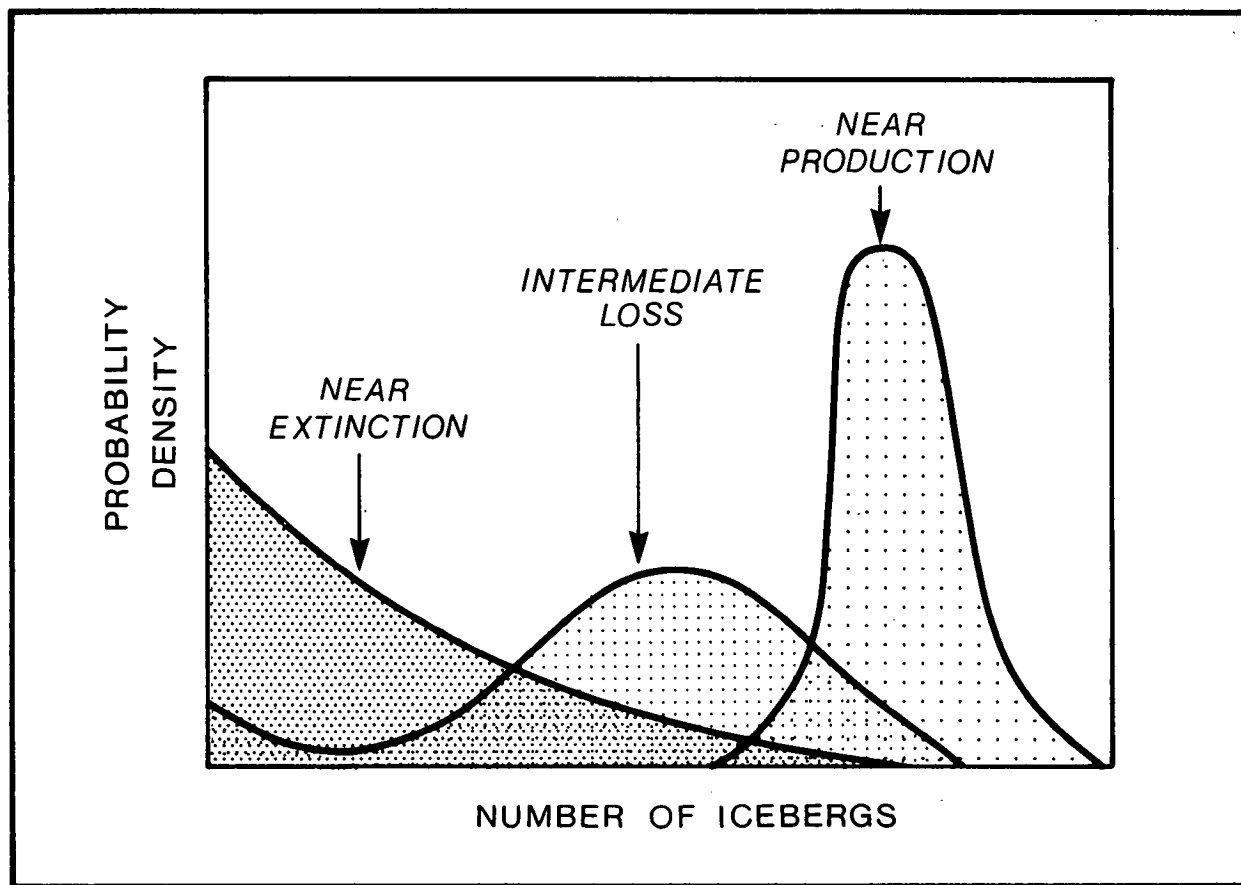


Figure 12: The nature of the probability density function for icebergs from the source region to the area of final extinction (from Ebbesmeyer, Okubo and Helseth, 1980; after Chandrasekhar, 1943).

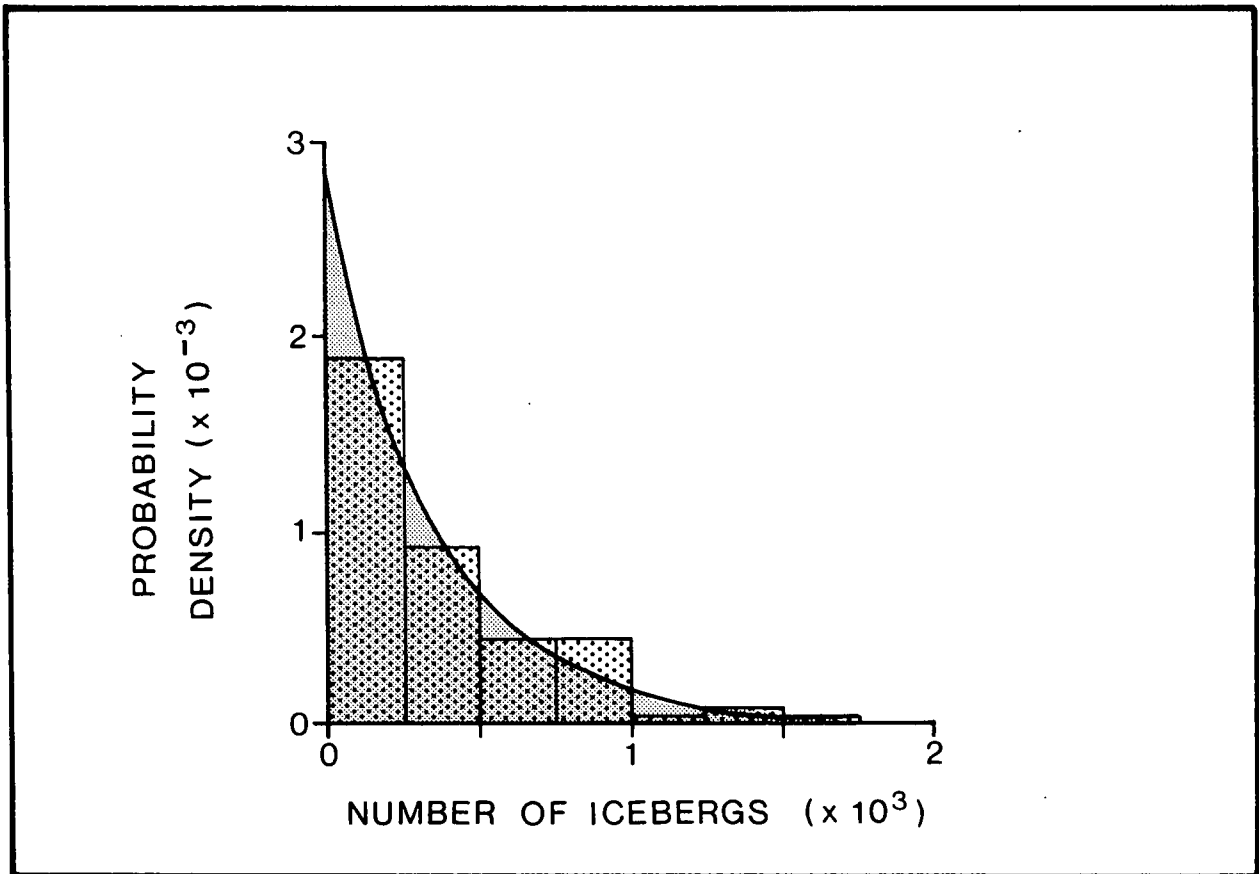


Figure 13: Probability density of the annual number of icebergs passing south of 48°N (grouped on 250 iceberg classes) (from Ebbesmeyer, Okubo and Helseth, 1980).

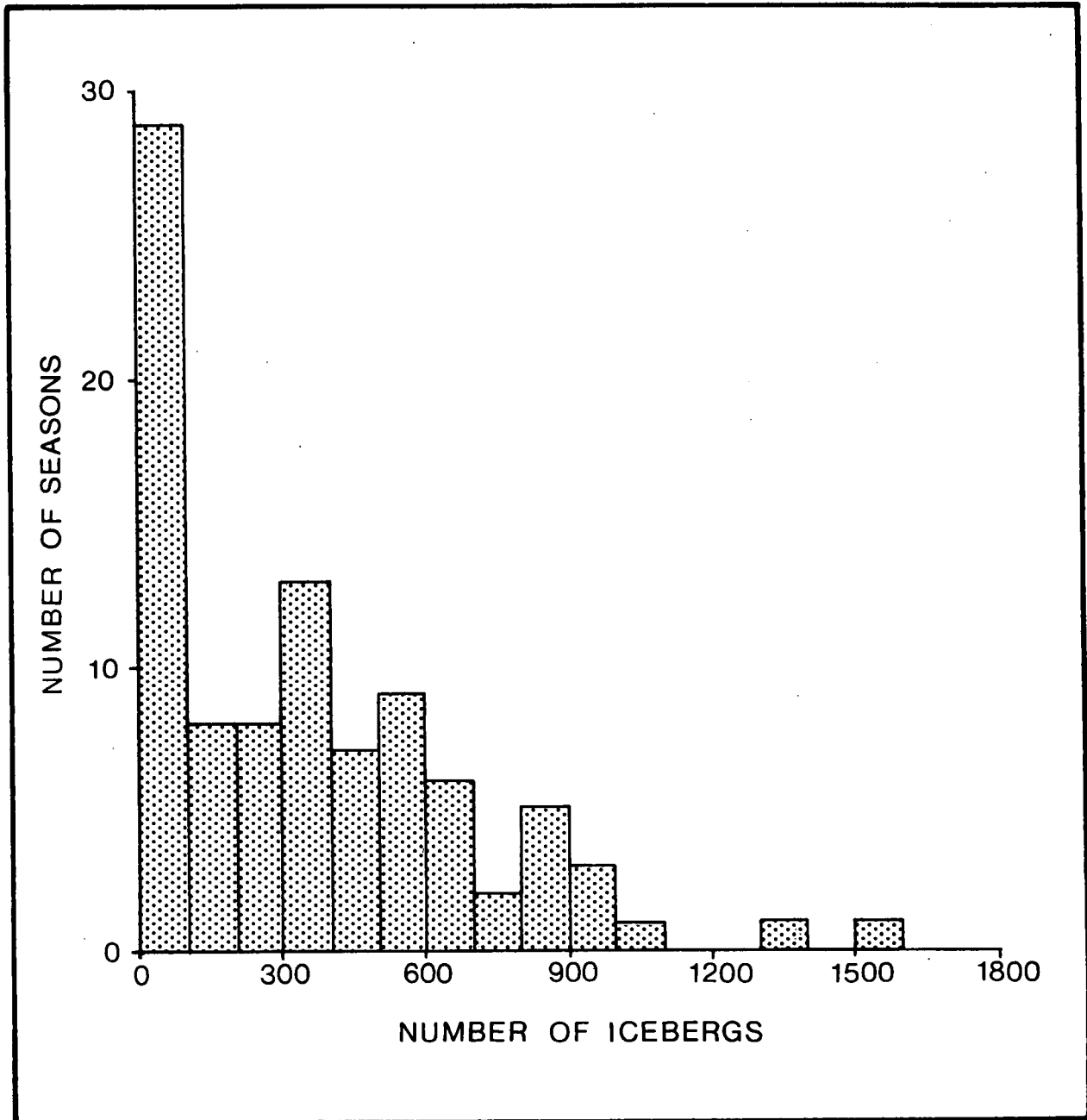


Figure 14: Histogram showing the number of seasons (1880 to 1972) having a given number of icebergs (from Murty and Bolduc, 1975).

Instead, an approximately optimized relationship was derived which retained some connection to the assumed role of northwest winds in forcing the southward iceberg transport. The resulting relationship was written as:

$$N = -0.016(6\Delta P_{IB} + \Delta P_S) - 0.12 \Delta P_{SB} + 4.8$$

where N is the iceberg count as expressed on Smith's 0 to 10 unit scale and:

$\Delta P_{IB}$  = Atmospheric pressure difference (mb), Ivigtut minus Belle Isle, December to March preceding the iceberg season.

$\Delta P_{SB}$  = Atmospheric pressure difference (mb), Stykkisholm minus Bergen in October to January.

$\Delta P_S$  = The pressure anomaly at Stykkisholm in October to March.

The average pressure gradients and anomalies used in the regression were in all cases weighted to favor those months which had the highest correlation coefficient relative to the iceberg count. In this way, Smith claimed separate correlations of -0.58 and -0.62 with the ( $\Delta P_{IB} + \Delta P_S$ ) and the  $\Delta P_{SB}$  parameters respectively. Tests of this expression against data from 1926-1930 (Table 3) showed generally good performance for 4 of the years for which the observed numbers were reasonably close to normal (1926, 1927, 1928 and 1930).

**Table 3:** Predicted and observed iceberg severity for the years 1926-1930 (Smith, 1931).

Year	Predicted	Observed
1926	150, below normal	345, below normal
1927	386, normal	390, normal
1928	500, above normal	515, above normal
1929	350, below normal	1300 (est.), far above normal
1930	520, above normal	475, above normal



On the other hand, it failed miserably in its most critical role, namely to forecast far above normal or severe seasons (1929). This discrepancy is not surprising in view of the large differences between the extent of the tails of the observed exponential iceberg- and the Gaussian independent parameter-distributions. Nevertheless, the basic ideas underlying Smith's approach have had continuing influence on the development of severity prediction methodology.

Subsequent work by Schell (1940, 1950, 1952, 1962) was particularly significant in maintaining the prominence of both the detail and philosophy of Smith's work. Schell's contributions utilized the additional iceberg count data of the post-1926 period to explore possibilities for modifications and/or additions to the Smith relationship which would achieve higher correlations with the experimental count record. It incorporated Groissmayr's (1939) suggestion that the preceding air temperatures over the North Atlantic and elsewhere could have a causative role and considered the possibility suggested by Walker (1947) that the statistics of the studied process were not stationary in time.

The principal defects of Smith's work were left largely uncorrected, including the use of the transformed 0 to 10 severity scale. Comparisons with separate segments of the overall unreliable 1880-1949 severity records were noted to show a poor correlation (0.08) relative to the Stykkisholm-Bergen pressure difference in the period 1915-1949. This result was judged to be indicative of the reduced importance of the Arctic air inflow as a causative factor and was attributed to unspecified but marked changes in the circulation of the northeastern North Atlantic Ocean. At the same time, correlations between 0.23 and 0.64 were noted between the annual counts and the December through March temperatures at St. John's, Bermuda and Uppsala in all three studied subintervals, 1880-1949, 1880-1914 and 1915-1949. On this basis, Schell proposed a new relationship:

$$N = -0.12\Delta P_{IB} - 0.31\Delta T_{SJ} - 0.19\Delta T_B + 0.17\Delta T_U$$

where  $\Delta T_{SJ}$ ,  $\Delta T_B$  and  $\Delta T_U$  represent the deviations from the long term average December to March temperatures at St. John's, Bermuda and Uppsala, respectively. A correlation of 0.53 was attributed to the relationship for the 1927-1949 period. Separate comparisons against 1927-1951 data gave an  $r = +0.8$  correlation. Although it is again difficult to interpret the significance of such a result, it is important to note that in the 5 years having the most extreme values of the 10 unit

severity index (magnitudes  $\geq 4.2$ ), the average prediction error was 3.3 units, again suggesting that this modification has the fundamental weakness of the original Smith approach, namely an inability to forecast the occurrences of extreme events. Later simplifications of the Schell formula to a simple two term form (Schell, 1962; Corkum, 1971) did not substantially affect this inadequacy.

A particularly notable exception to the reliance on the basic Ivigtut-Belle Isle pressure relationship was advanced by Post in 1956. He disagreed with the basic premise that no one cause could be cited in explaining the observed variability in severity. Moreover, he proposed that fluctuations in the Gulf Stream System provided such a cause and attempted to derive a predictive technique from causative variables of this System. While, at least, his technique differed from earlier efforts by working with the raw, untransformed severity data, it retained the same basic premise that any addition to a linear regression relationship which produced a positive change in the magnitude of the correlation could be taken as evidence of an actual physical contribution to the observed variability. Statistics were used to support the hypothesis that the interannual changes in iceberg numbers could be explained in terms of:

1. Positive and negative anomalies in surface water temperatures in the Straits of Florida, because of their association with weaker and stronger flows respectively in the Gulf Stream and the circumstance that such flow changes will, 3 months later, result in larger and smaller numbers of icebergs, again respectively, entering the Grand Banks region.
2. Associated changes in the strength of the Labrador Current due to the weakening or strengthening of the Gulf Stream, as denoted by the positive or negative temperature anomalies. These changes occur after a delay of 3 years (associated with the time needed for changes to work their way through the interrelated Irminger and Baffin Current System). As a result, a positive correlation was obtained between the Straits of Florida temperature anomaly and the 3-year subsequent iceberg severity.

Arguments were mounted by Post for the existence of each mechanism through a maximization of correlation coefficients as a function of the time delay between the severity and temperature measurements. A predictive scheme was derived based on the pair of temperature measurements in the Straits of Florida 3 months

and 3 years prior to the iceberg season. An impressive looking observed-predicted curve (Figure 15) was then produced in proof of the proposed mechanism.

A very detailed criticism of the Post work was given by Kinsman (1957) as a classic illustration of misleading and unproductive applications of statistical analysis. Major interpretive errors, cited by Kinsman, included misplotting and misclassification of data, unrepresentative water temperature measurements in the Straits of Florida and the use of other Florida temperature data in 19% of the years studied (in spite of the fact that the standard deviation between the temperatures of the 2 locations was comparable to the Straits of Florida standard deviation). Overall however, Kinsman was most critical of the assumption that the identification of parameters and time lags capable of giving high ( $r = +0.94$ ) correlations could be taken as a confirmation of the existence of the two linkages in the absence of any other physical evidence for such relationships. To illustrate his point that short-run comparisons can be misleading, Kinsman presented a comparable degree of hindcast matching of the 1942-1951 iceberg record (Figure 16), as well as limited predictive success. This relationship used the number of commas on each page of Post's article as the independent variability-determining parameter! Although, there has been only one further attempt (Murty and Bolduc, 1975) to apply Post's hypotheses to the severity prediction problem, it is important to note that Kinsman's criticism of the fundamentals of the correlation maximization approach apply to both the preceding work of Smith (1931) and Schell (1940, 1948, 1952) and to later efforts by Schell (1962) and Corkum (1971).

Similarly negative conclusions on multi-variate analysis, relative to pressure gradient and temperature parameters, were also obtained in the study of Murty and Bolduc (1975). However, these authors allowed that "these parameters determine the severity to some extent (up to 50% of the variance explained), the physics of the problem is not understood well enough to make accurate quantitative predictions at present".

The only serious attempts to achieve further understanding of the physical processes underlying severity variability were, until recently, carried out by the IIP. The results of this work is presented in the IIP's annual reviews of each iceberg season in terms of the preceding winter's pressure and temperature parameters. These explanations often had to rely on poorly documented pre-season iceberg counts in source areas and on estimated average values for the strength and direction of mean cross-flow wind components during the winter and spring season.

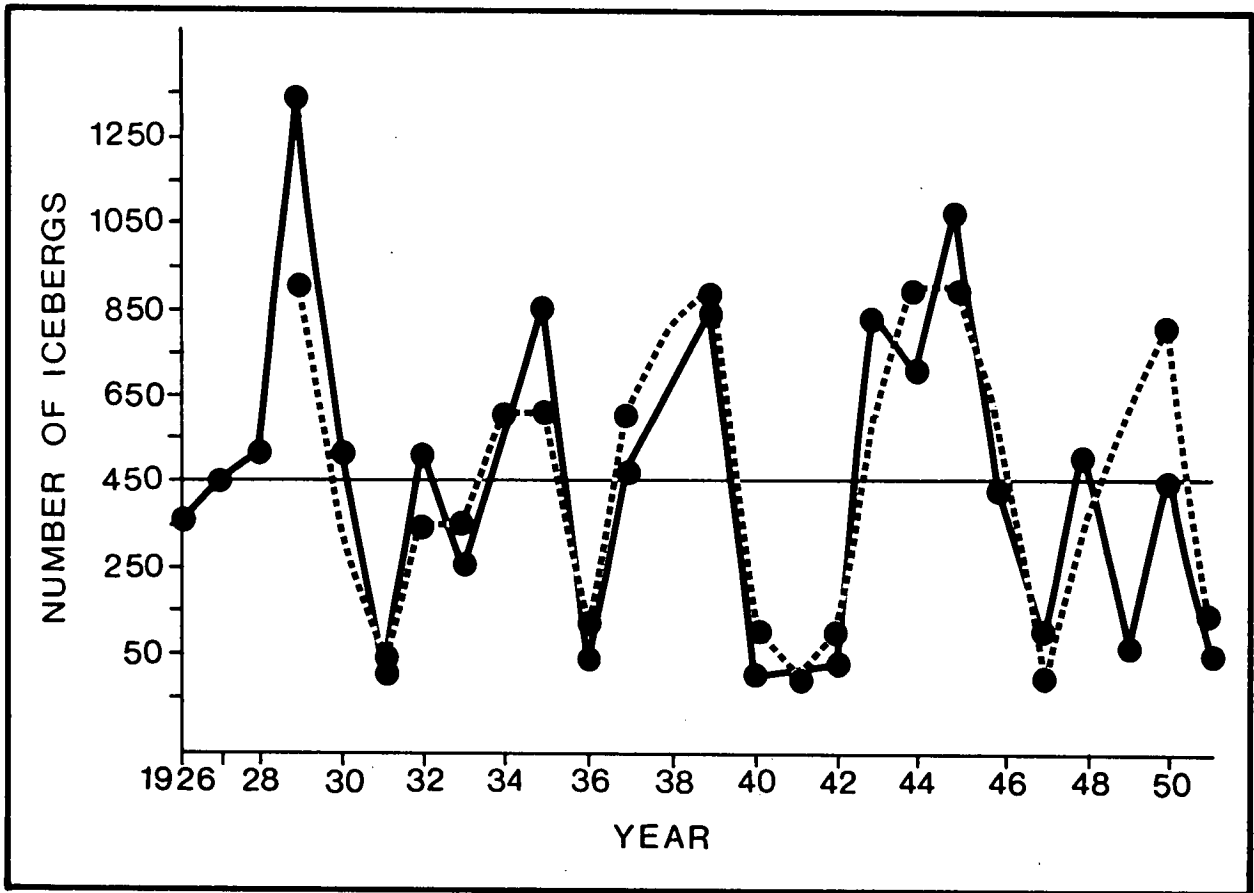


Figure 15: Observed (solid) and computed (dashed) iceberg counts passing 48°N (from Post, 1956).

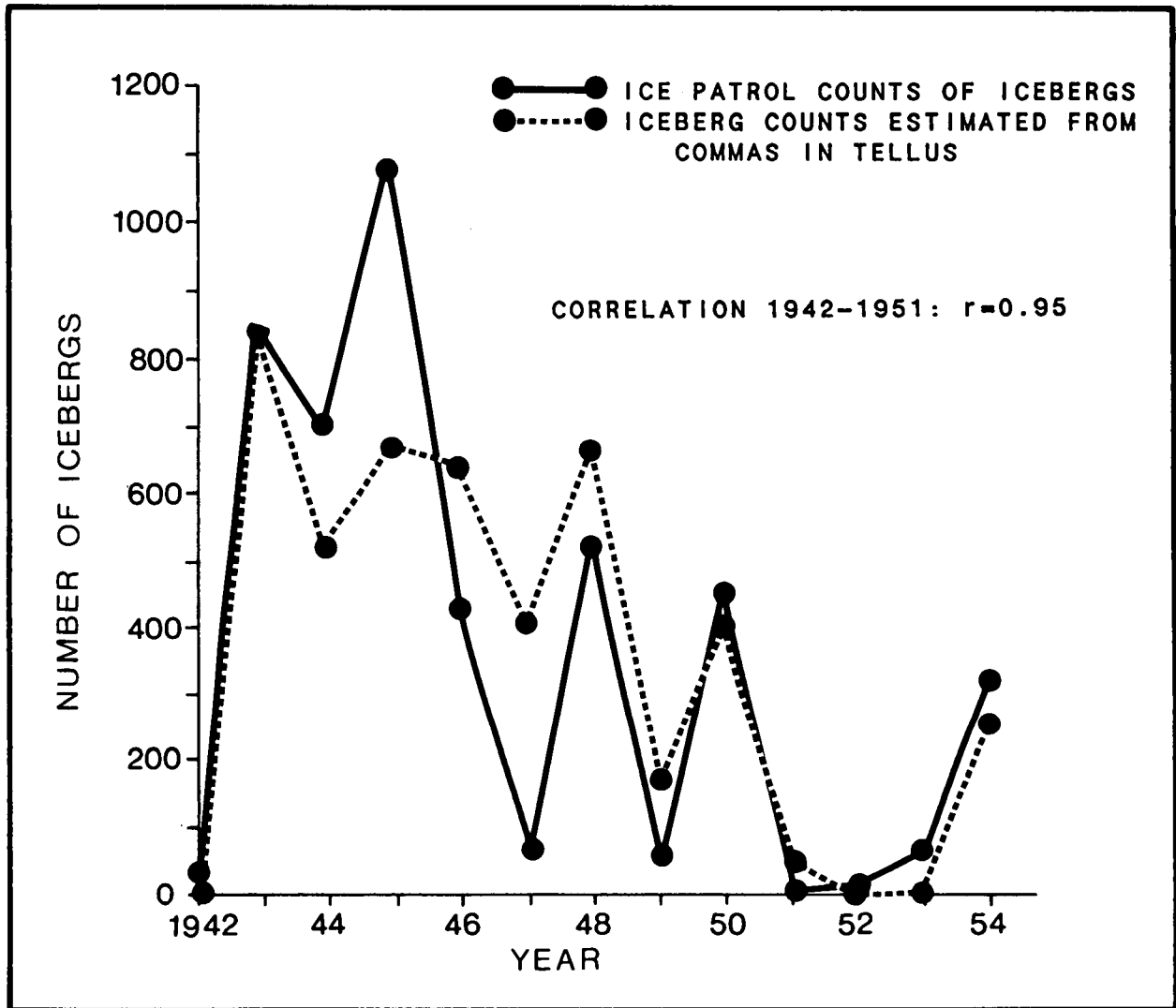


Figure 16: Observed (solid) and computed (dashed) iceberg counts based on a correlation of the number of commas in Tellus (from Kinsman, 1957).

The difficulties involved in achieving such explanations, consistent with meteorological forecasting capabilities, eventually led to the abandonment of the IIP serverity prediction program.

#### 4. NEW APPROACHES TO SEVERITY PREDICTIONS

##### 4.1 INTRODUCTION

###### Planned Approach

Our original program to examine the feasibility of forecasting iceberg severity relied heavily on the previously described (see Figure 3) representation of variability in terms of three causative factors (source area distributions, advection and deterioration of icebergs) and a severity resultant. This approach allowed the possibility of obtaining a physical understanding of the underlying processes by using relatively new, high-quality data sets to characterize three of the indicated entities. These characterizations would then be used to deduce the origin of iceberg severity variability through consistency arguments. In particular, it was anticipated that detailed, same-year characterizations of the pre-season iceberg distributions in source areas, the spatially- and temporally-dependent iceberg advection fields, and the seasonal total iceberg count south of 48°N would allow deduction of the corresponding deterioration and loss rates.

Applications of this type of analysis to several annual data sets held the promise of offering critical information on the nature and extent of the interannual variability in each of three causative factors. Such results would ideally form a good starting point for both determining the feasibility of the method and for choosing optimal approaches to severity forecasting.

It was our impression that good iceberg count data sets were available for characterizing both the pre-season source factor and the total severity count. These data were presumed to have been obtained from the recent, since 1978, introduction of comprehensive SLAR (side-looking airborne radar) capabilities into the surveillance programs maintained by Atmospheric Environmental Services (AES), Canada and the U.S. Coast Guard.

Data sources for the annual advection fields were identified in terms of the archives of hardcopy NOAA satellite imagery maintained by AES, Ice Forecasting Branch, for the post-1978 period. Review of these archives suggested that characterization of the sea-ice fields of motion was possible from sequences of images recorded at intervals of 1 to 3 days. The conversion of these sea-ice fields of motion directly into iceberg equivalents was justified in terms of calculations (Canpolar Consultants Ltd., 1985) showing that the total forces needed to crush the typical mid-winter pack ice surrounding each iceberg were orders

of magnitude greater than the corresponding total of the atmospheric and oceanic forces acting on such icebergs. As a result, except perhaps in areas of thin ice or shallow water, icebergs can be assumed to move with the adjoining ice fields. Sea-ice motion data, then, could be used to characterize iceberg advection.

Further confirmation of the use of sea-ice velocities as a measure of iceberg motion was obtained from the measured sea-ice velocity of two large floes adjacent to the positions reported for a satellite tracked iceberg-mounted beacon, #1994 on February 22-23, 1981. The average velocity of the two floes over the period 13:24Z, February 22 to 13:01Z, February 23 was 12.3 km/day at 220°. The velocity of the iceberg beacon was measured over the interval 13:43Z, February 22 to 23:22Z, February 23, giving a mean velocity of 12.7 km/day at 209°, in agreement, within the estimated experimental error of 4 km/day, with the sea-ice velocity.

Nevertheless, although satellite images were acquired, assembled and to some extent processed for the December to March periods of 1980-1981, 1981-1982, 1982-1983, and 1984-1985, it soon became clear that the critical iceberg count data were not sufficiently complete to allow the envisaged detailed analysis. The AES survey products, whether in raw or processed form, were found to provide less than 50% nominal coverage of potential source areas and moreover, did not allow separate recognition of those icebergs which were immobilized in landfast ice. In most instances, such icebergs were not likely to contribute to the wintertime southward iceberg flux. Additional uncertainties were associated with the completeness of the survey counts within each individual 1/2° latitude X 1° longitude grid square. Likewise, discrepancies were noted between the more recent IIP total count values and the iceberg counts maintained at individual exploratory drillships. These defects in the assumed data bases precluded their use in drawing conclusions regarding the individual components of Figure 3.

#### Actual Approach

In view of these circumstances, adherence to a physically-based evaluation program required some modification of our original approach. The chosen modification utilized a rationalized severity record in conjunction with corresponding annual data sets for several environmental parameters, each of which could be expected to bear some physically demonstrable relationship to each other and to the processes or forces which are believed to determine the numbers of icebergs appearing south



of 48°N. A key additional requirement in this approach was that the parameter data sets had to be of quality and duration sufficient to allow the drawing of meaningful inferences.

In the following subsections, we shall describe and, as much as possible, justify our particular choices of parameters and the methods used to obtain corresponding representations of their interannual variability and that of a rationalized severity parameter (Section 4.2 and 4.3). Emphasis will be placed on using the full duration of each parameter data set to resolve their individual weaknesses in order to allow an accurate as possible description of the annual iceberg environments. Actual comparison of the parameter and severity data sets in potential hindcast and forecast schemes are presented below.

## **4.2 PHYSICAL PARAMETERS**

### **4.2.1 SEA-ICE EXTENT**

Initial surveys of the 1980-1985 NOAA satellite imagery suggested the existence of a reasonably close relationship between winter sea-ice extent and the number of icebergs observed south of 48°N during the following spring and summer. As mentioned above, such a relationship had been previously noted by Smith (1931) with respect to the Newfoundland pack ice. A physical link between southern iceberg numbers and large upstream ice extents is to be expected if the latter can be taken as indications of larger than normal ice advection rates, in the absence of corresponding reductions in the number of icebergs per unit area of sea-ice.

Unfortunately, because of the typically late (February) arrival of ice in the vicinity of Newfoundland, Smith's observations, even if followed up on, would have been unlikely to give much advance notice of seasonal iceberg severity levels. On the other hand, because of the north to south progression of the ice front, clearly a lengthening of the forecast time was possible if a similarly close correspondence could be found to exist between iceberg severity and ice extension in more northern, upstream areas.

Initially, the correspondence of annual iceberg severity relative to ice extent in more northerly areas was examined for the months of November through April. The strongest correlation was found to be associated with the ice extent in the Davis Strait area as indicated in Figure 17. Similarly, the largest correlations over the potential November-January prediction period were obtained in the month of January.

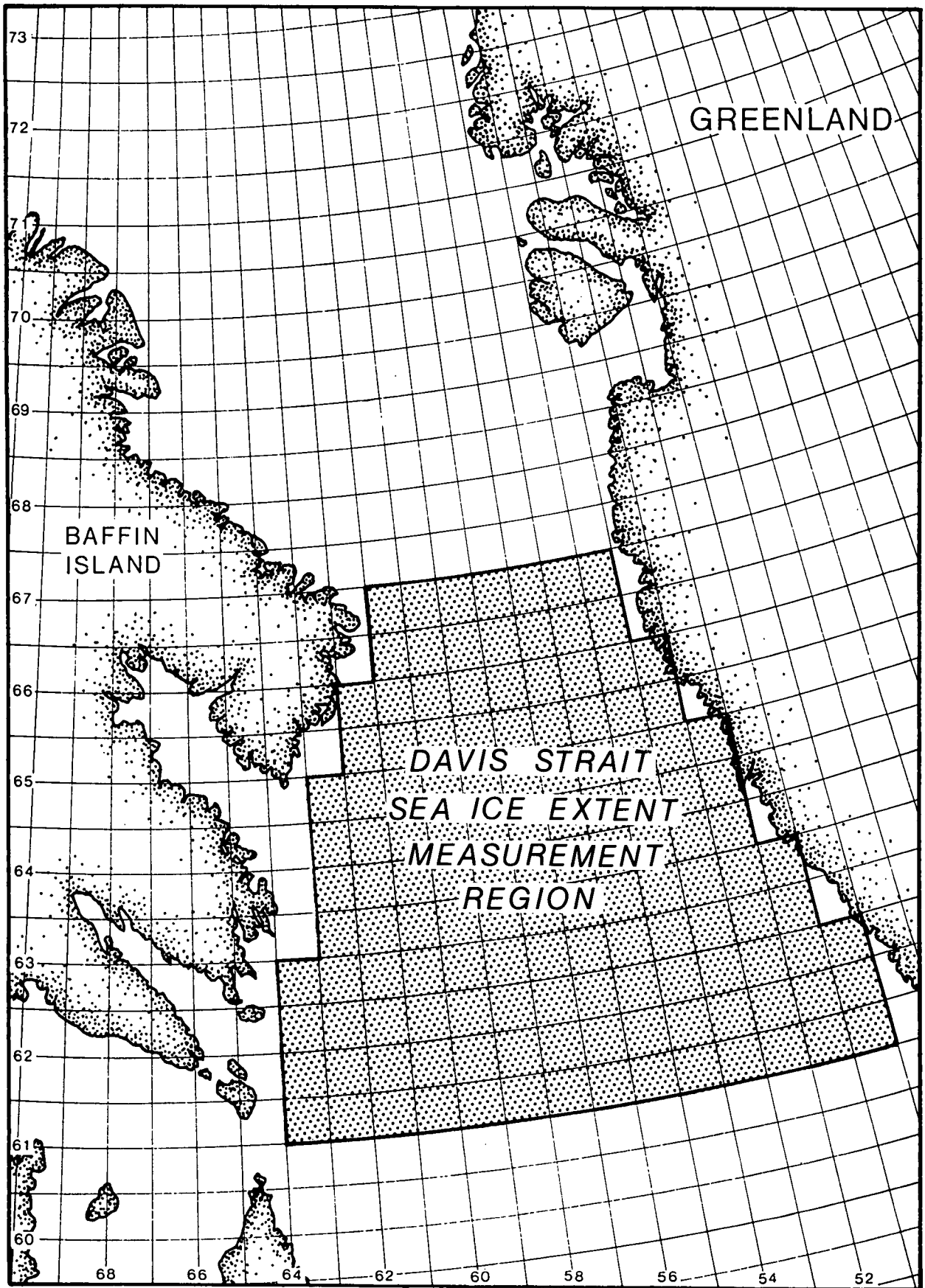


Figure 17: Area of Davis Strait used for ice extent measurements.

Sea-ice extent values were extracted from the data sources indicated in Table 4 using, whenever possible, the largest extent observed during January and definition of the pack edge as the boundary between 3/10 and 4/10 coverage. The values for the sea-ice extent, along with other parameters discussed later in this Section are provided in Table 5.

Data for the 1972-1985 period were particularly reliable and complete because of the ease with which ice edge positions could be determined from NOAA satellite imagery. Ice extent measurements for this period were obtained from planimeter measurements of charts produced from sources 1 and 3 of Table 4. Earlier data were taken from the monthly ice concentration compilations produced by Walsh (1979) (source 5), based on a review and rationalization of all corresponding Danish, British,

**Table 4:** Sources of sea-ice extent data.

- 
1. AES Canada weekly and bimonthly ice charts 1970-1985.
  2. U.S. Naval Oceanographic Office Reports of the Arctic Ice Observing and Forecasting Program 1953-1971.
  3. U.S. Fleet Weather Facility, Eastern Arctic Sea Ice Analyses 1972-1985.
  4. Danish Meteorological Institute Ice Conditions in the Greenland Waters 1960-1968.
  5. A summary of much of the above data for the period 1953-1977 on a 60 n.mi. X 60 n.mi. grid scale by Walsh (1979).
- 

United States and Canadian data. For the earlier (pre-1972) data, areal extents were determined simply by counting the grid squares in the measurement area which had concentrations equal to or greater than 4/10. This procedure gave good agreement with our planimeter measurements for the common (1972-1977) period of overlap. According to Walsh (1979), data quality were particularly poor in the earliest 1953-1960 period when observational capabilities were primitive. Moreover, the distinctly lower values of sea-ice extent reported by Walsh for the 1953-1966 period were increased by 35% to bring the mean

**Table 5:** Tabulation of annual iceberg severity counts and other parameters which may be related to iceberg severity.

Year	# of Bergs	Davis Strait Ice Area (Jan)	ENSO Rating	Frobisher Bay Temperature		Wind Anomaly (Dec-Feb)	Bravo Wind		Frobisher Bay $\Delta H$	
				(Dec)	(Jan)		(Jan)	(Mar)	(Dec)	(Jan)
				$^{\circ}\text{C}$	$^{\circ}\text{C}$	Pa	$10^4$ km		mbar	mbar
1940	5		2							
1941	10		4							
1942	25		0							
1943	830		2							
1944	695		2							
1945	1075		0							
1946	420		1		-30.6					
1947	60		0	-20.8	-24.5					
1948	520		1	-15.5	-27.3					
1949	20		0	-23.9	-28.5					
1950	445		0	N/A	-32.6	.140	25	7		
1951	10		2	-14.5	-29.9	-.020	28	19		2638
1952	20		0	-24.9	-28.5	.015	17	-8	2629	2618
1953	50	0.82	3	-15.9	-27.9	-.035	18	18	2717	2626
1954	310	0.55	0	-29.8	-30.8	.032	13	16	2588	2619
1955	60	0.55	0	-22.3	-22.3	-.050	1	-19	2642	2683
1956	75	0.66	0	-16.2	-25.5	-.035	26	6	2714	2639
1957	925	1.00	4	-27.1	-33.8	.090	44	-10	2599	2580
1958	1	0.93	4	-20.7	-21.8	-.115	11	-11	2673	2684
1959	685	1.05	0	-17.9	-18.7	.015	17	5	2710	2713
1960	260	0.82	0	-19.5	-21.4	-.050	24	-20	2681	2681
1961	105	0.77	0	-22.1	-29.1	.100	46	8	2671	2648
1962	115	0.77	0	-15.4	-26.6	.005	12	-7	2744	2643
1963	20	0.55	1	-20.3	-20.6	-.090	3	7	2681	2671
1964	370	0.93	0	-19.8	-26.8	.010	24	4	2686	2659
1965	70	0.72	3	-19.2	-27.3	-.030	5	-21	2675	2639
1966	1	0.77	0	-21.6	-24.1	.015	25	-33	2668	2679
1967	435	0.93	0	-20.9	-23.4	.030	34	26	2655	2685
1968	215	0.94	0	-19.5	-27.4	-.035	5	13	2681	2634
1969	50	0.41	2	-18.9	-19.7	-.095	4	-9	2703	2725
1970	75	0.74	0	-20.3	-24.2	-.055	0	4	2672	2682
1971	65	0.78	0	-23.1	-22.3	.005	16	-8	2660	2677
1972	1540	1.02	4	-29.9	-32.4	.070	33	27	2596	2587
1973	840	0.81	4	-28.5	-29.1	.130			2640	2639
1974	1390	0.77	0	-22.8	-30.7	.050			2658	2616
1975	100	1.09	1	-27.8	-29.6	.050			2609	2608
1976	145	0.62	3	-22.6	-25.3	.015			2647	2652
1977	15	0.38	0	-22.1	-16.2	-.075			2674	2708
1978	75	0.83	0	-22.8	-30.7	.025			2663	2628
1979	152	0.30	0	-15.0	-21.6	.000			2769	2702
1980	24	0.77	0	-23.5	-20.4	.025			2676	2719
1981	63	0.61	0	-22.4	-21.1	.0				
1982	188	0.51	4	-16.8	-18.8	N/A				
1983	1352	1.44	4	-27.6	-33.9	.066				
1984	2000	1.49	1	-26.1	-33.3	.0				
1985	1500	1.24	1							

coverage for this period into agreement with the subsequent mean value. This procedure was discussed with Dr. Walsh who believed such a correction could be justified because of the transition, in 1966-1967 from primary reliance on British to North American sources and notations.

The extent data, normalized to 61,000 n.mi<sup>2</sup>, satisfied an overall approximately Gaussian probability distribution (Figure 18) for the 1953-1985 study period. Separate breakdowns of the lower- and higher-quality 1953-1971 and 1972-1985 data indicate that the latter period was characterized by an exceptionally widespread distribution. The degree to which this difference, relative to the 1953-1971 results, is attributable to observational changes will have to be estimated from other parameter records (see Section 4.2.2). Clearly, the range of variability in the January sea-ice extent is huge, corresponding to a 4 fold difference between the observed minimum and maximum values.

The correspondence between the annual normalized ice extent and the raw iceberg severity count is evident in the plot of Figure 19. Comparisons are presented separately for sea-ice data obtained from the 1953-1971 and the 1972-1985 periods of lower and higher accuracy measurements, respectively. It is our impression (See Section 4.3) that the relative reliabilities of the ice extent data for the two periods are similarly reflected in the corresponding iceberg count results. In both plotted data sets, large iceberg counts (i.e. > 600) always occurred for years in which the areal extent of Davis Strait sea-ice exceeded the mean value (i.e. the sea-ice extent normalized by the mean was  $\geq 1.0$ ). Likewise, ice extents less than 0.87 were never observed to be associated with high iceberg counts (in excess of 300). In spite of the undoubted uncertainties, these data would appear to hold some promise for the use of sea-ice extent as a severity forecast tool.

#### 4.2.2 AIR TEMPERATURE

Air temperature in eastern Canadian marine and coastal locations was included as a parameter because of both the presence of several relatively long and reliable temperature records and the well-established relationships between this parameter with other parameters (ice extent, wind speed and direction) also considered in this study. In general, it is expected that low temperatures in such areas would tend to be associated with strong northwest winds and with large sea-ice

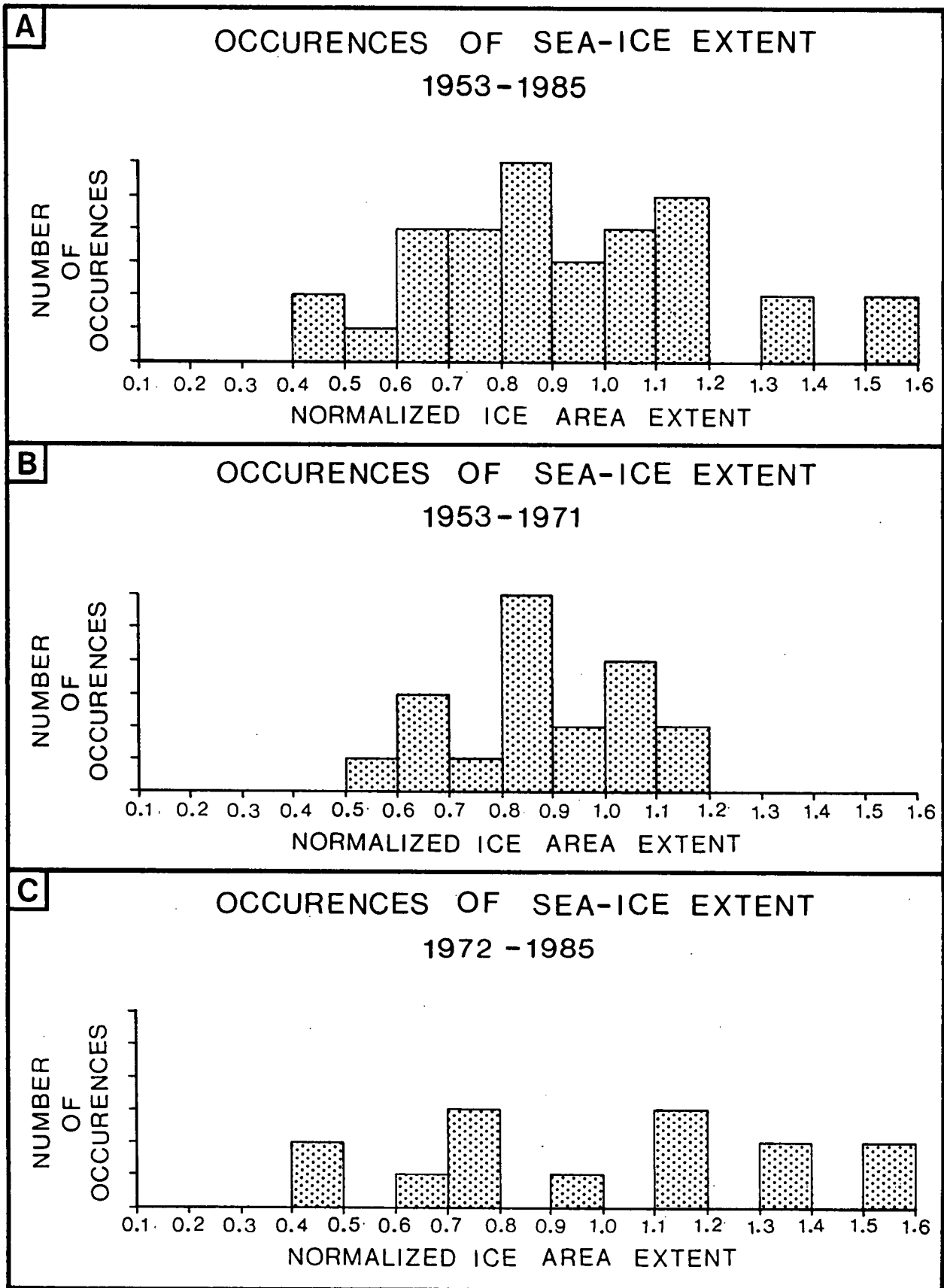


Figure 18: Sea-ice extent data, normalized to 61,000 nautical miles squared for a) the entire record 1953-1985; b) the period of lower quality data, 1953-1971; and c) the period of higher quality data, 1972-1985.

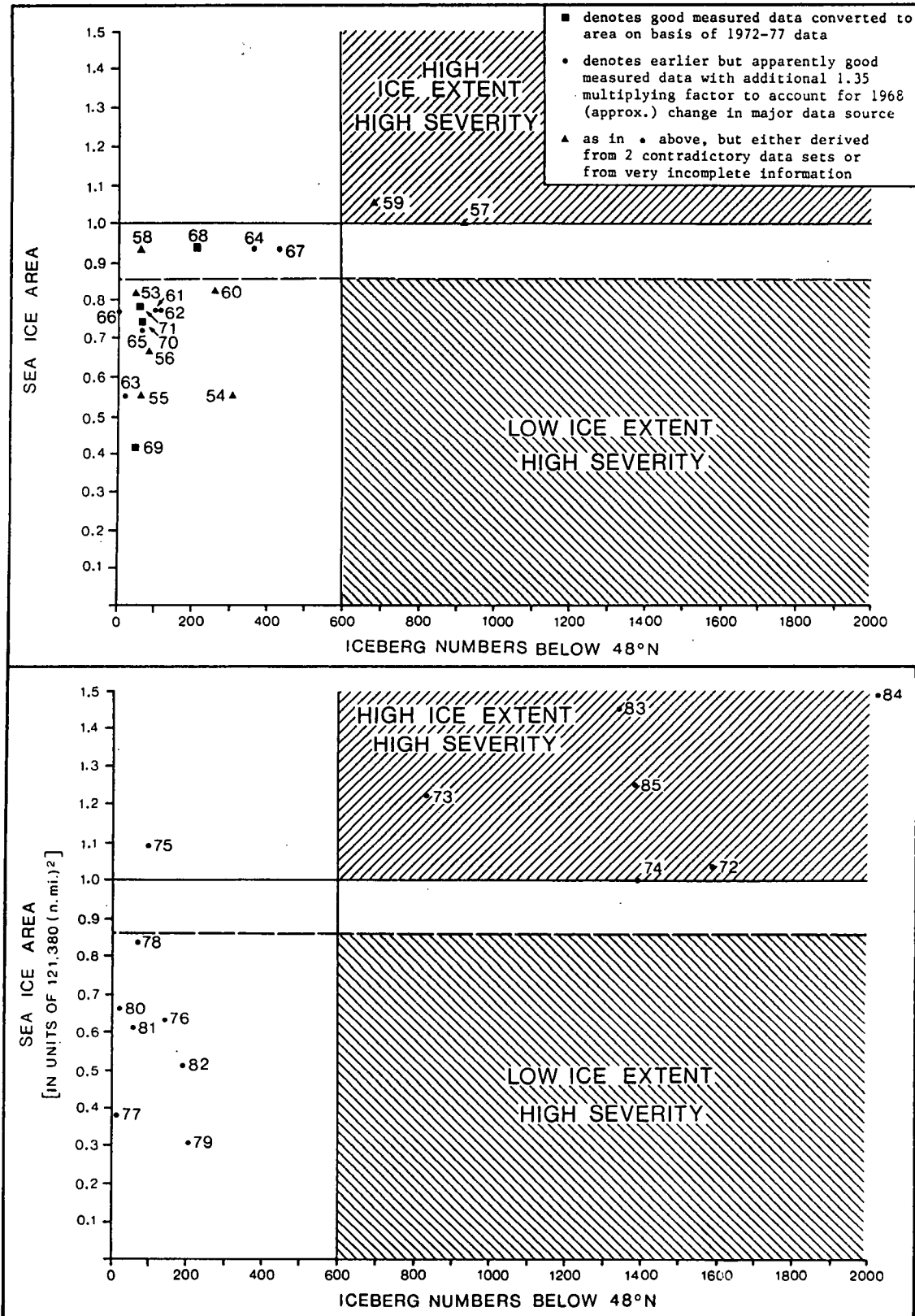


Figure 19: Scatter plot of both early low quality (upper) and later higher quality (lower) data on the reported numbers of icebergs passing south of 48°N as functions of the corresponding spatial extents of the January sea-ice cover in Davis Strait. Accompanying each data point is a 2-digit number representing the year. The experimental data points corresponding to high severity, i.e. numbers greater than 600 and hence to the right of the drawn vertical boundary, all have normalized ice extents  $\geq 1.0$ . The absence or presence of high severity entries for intermediate sea-ice extents depends on the precise specification of the high/intermediate extent boundary. No such ambiguity exists with respect to the data points associated with the low,  $< 0.87$ , sea-ice extent regime. High iceberg severity was never observed to follow such conditions.

extents which both tend to reduce the moderating influence of the relatively warm, open-water surface lying to the east of the offshore ice pack.

Temperature data consisting of monthly mean values were obtained for the four coastal stations operated by AES, Canada for the periods indicated in Table 6. The greater length of these records allows some extensions (relative to the sea-ice data base) of comparisons with the iceberg severity record back to the 1940 decade. Additional estimates of temperatures, possibly less influenced by the effects of local topography, were obtained as the monthly values of the separation  $\Delta H$ , in metres between the 1000 mb and 700 mb atmospheric pressure contours. These values were derived for the marine gridpoint centred on 65°N, 60°W to the east of Frobisher Bay. Values of the separation  $\Delta H$ , proportional to the corresponding air temperatures, were computed by the U.S. Navy Fleet Weather Center and were made available to us by Mr. Laurie Davidson of Seaconsult Ltd. for the 1951-1980 period.

**Table 6:** AES, Canada temperature data and periods of coverage.

---

St. John's	1942-1984
Goose Bay	1941-1984
Frobisher Bay	1946-1984
Cape Dyer	1959-1984

---

Comparisons of the coastal temperature data sets with the severity data indicated that the best degrees of correspondence for the mid-winter months relative to the raw severity record was achieved with the Frobisher Bay data for January. Plots of these data against iceberg numbers, as in Figure 20a, offer obvious opportunities for associations between low temperatures and high severities; and high temperatures and low severities which are similar to, but not as consistent as those noted above between sea-ice extent and severity. A similar plot of the 700-1000 mb separations (Figure 20b) shows similar characteristics.

Plots of the probability distributions for the Frobisher Bay January temperatures and the corresponding 700-1000 mb separations are presented in Figures 21 and 22. Much of the relatively small differences between the two overall distributions is attributable to the slightly different periods covered by the two plots. The separate plots of the early and



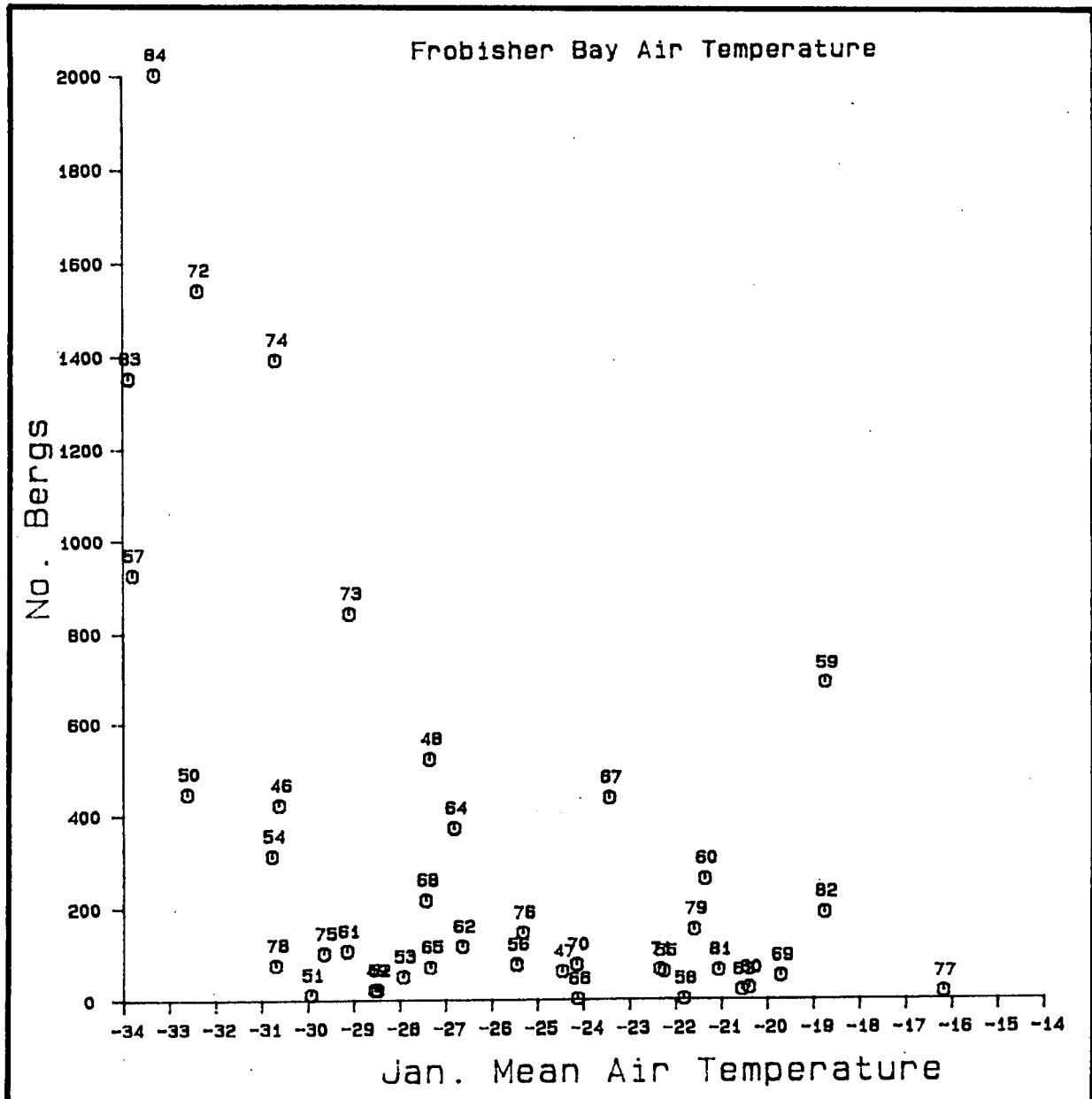


Figure 20: a) January air temperatures at Frobisher Bay versus yearly iceberg count. Accompanying each data point is a 2-digit number representing the year.

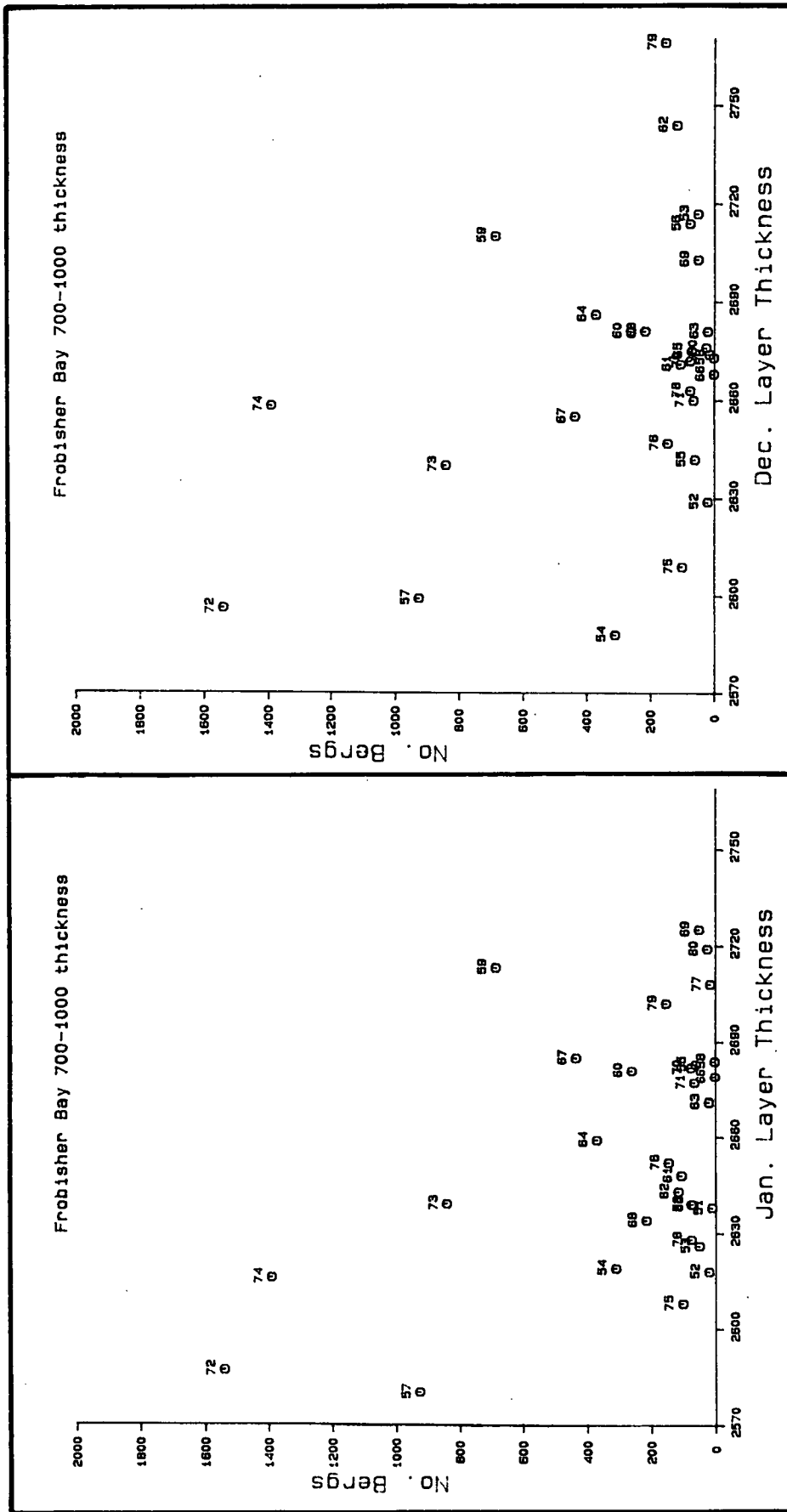


Figure 20: b) 700-1000 mb separations, at 65°N, 60°W for December and January, versus the yearly iceberg count. Accompanying each data point is a 2-digit number representing the year.

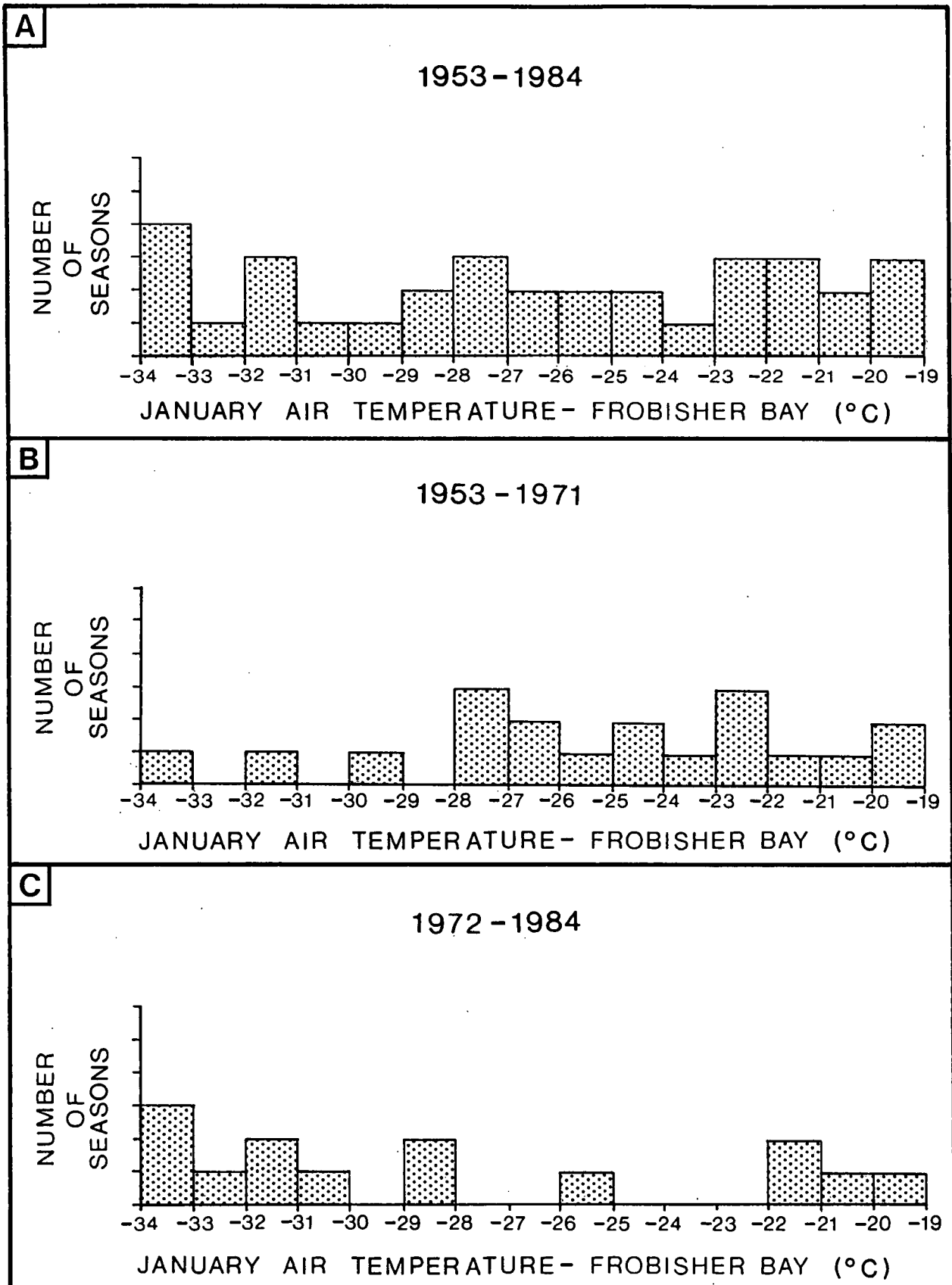


Figure 21: Probability distributions of Frobisher Bay air temperatures (January).

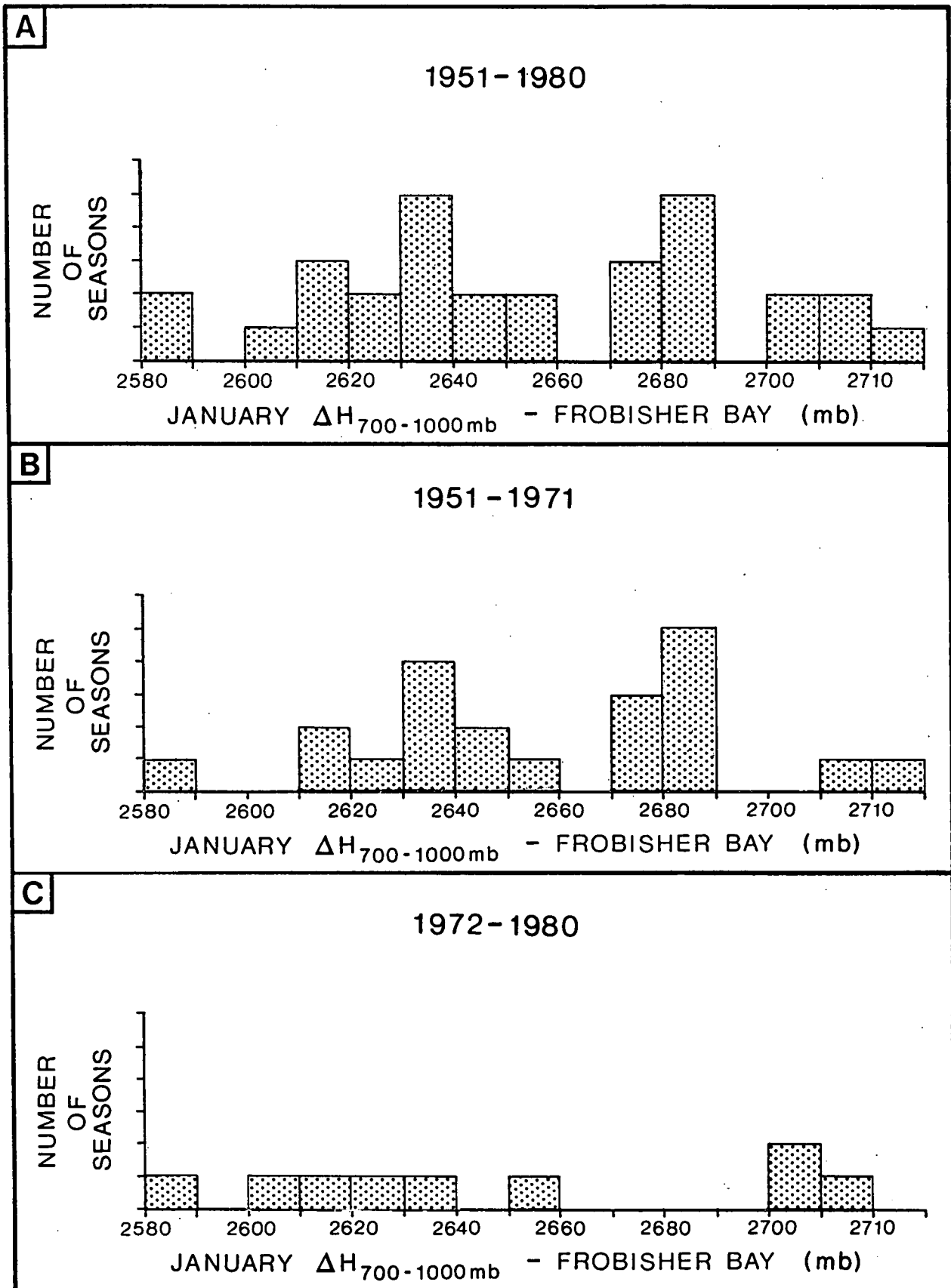


Figure 22: Probability distributions of 700-1000 mb separations, January.

later data for both parameters (T and  $\Delta H$ ) show the broader, more uniform distributions of the post 1971 data which were previously noted in the sea-ice extent distributions (Figure 18). Because the early air temperature data are considered more reliable than the corresponding sea-ice extent estimates, the general correspondence between ice area and air temperature (see for example, Figure 23) suggests that the apparently broader distribution of the 1972-1985 sea-ice extent values is not an artifact of the improved observational capability. Instead, the large observed range in sea-ice extent likely represents either a genuine climatic change or a large but not statistically significant fluctuation of the sampled distribution.

A comparison of the January sea-ice extent with air temperatures measured in the previous month (December) (Figure 24) exhibits much more scatter than was apparent in the January-January plot of Figure 23. This result suggests that the large ice extents of January were not the result of low December temperatures. The relative importance of advection and local ice growth in changing ice extent (i.e. are temperatures low because of large ice extent or are ice extents large because temperatures are low?) is an important issue. It would appear that, while these results cannot be considered conclusive, they suggest ice growth is either a strong function of advection rates or is closely related to the immediately preceding air temperature values.

#### 4.2.3 WATER LEVEL

Long term measurements of water level were examined in order to explore the possibility that interannual changes in current-patterns, -speeds and possibly grounded iceberg refloatation rates were causative factors in severity variability. All monthly mean water level data at St. John's, Nain (Labrador) and Frobisher Bay were obtained from Marine Environmental Data Services for the periods 1958-1983, 1963-1973, 1965 and 1972, respectively. Initial examinations indicated negligible correspondence between these records and the corresponding iceberg severities. Large gaps in the data records precluded a proper analysis however, and further plans for processing and analysis of the data were abandoned.

#### 4.2.4 WIND FORCING

The intense winds experienced in winter and early spring over the Labrador Sea and Davis Strait represent, along with ocean currents, the principal physical mechanisms driving iceberg

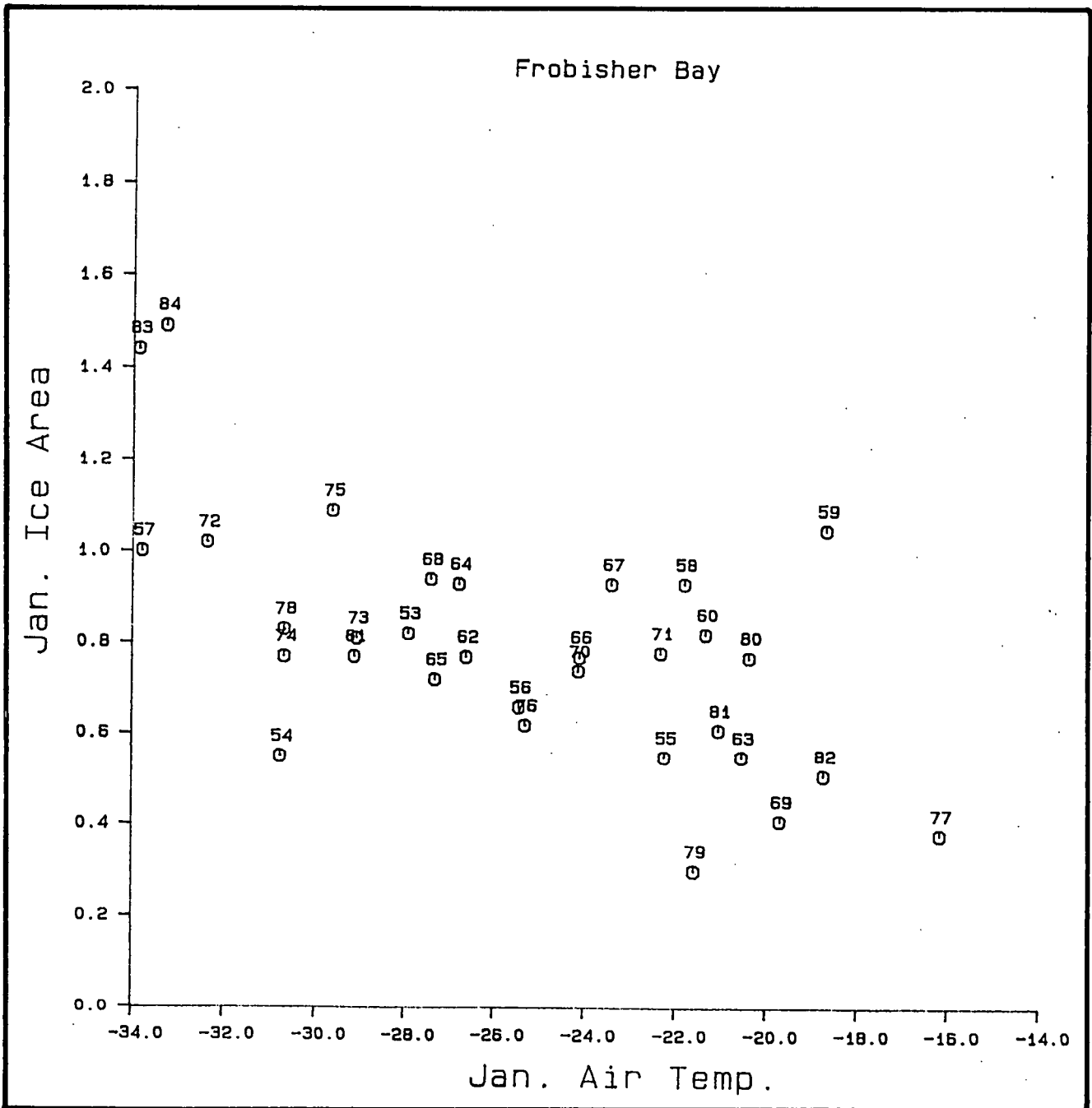


Figure 23: Frobisher Bay air temperature versus offshore sea-ice extent, January. Accompanying each data point is a 2-digit number representing the year.

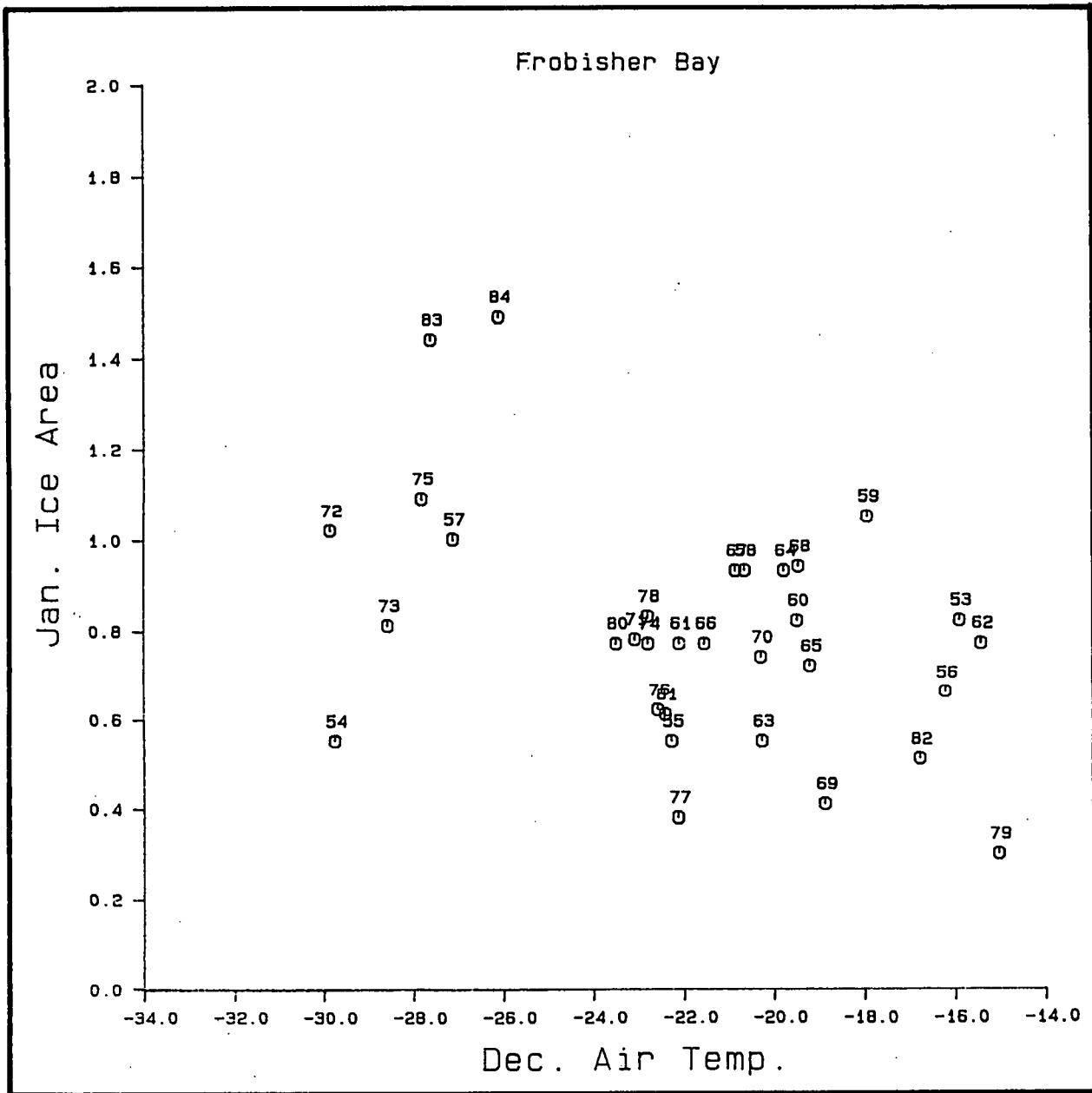


Figure 24: Frobisher Bay air temperature (December) versus the sea-ice extent in January. Accompanying each data point is a 2-digit number representing the year.

movement (Section 2.2). For this reason, indices of wind patterns available over many years were assembled and compared with iceberg severity.

The first major set of wind data used in this study was the anomaly of the seasonal wind stress values, computed from atmospheric pressure distributions, over 5° latitude by 5° longitude grids (Thompson and Hazen, 1983). The anomaly, i.e. the deviation, from the long term mean wind stress, used for our purposes, was calculated for a latitude-longitude grid square located midway along the Labrador coast (55-60°N; 55-60°W), over the seasonal period December to February. Seasonal wind stress anomaly values, for both the longshore and cross-shore directional components were obtained for the 31-year period, from 1950 to 1980. Wind stress anomaly values were also estimated from monthly mean pressure charts for 1983 and 1984 at the same location and time of year.

Comparisons of the the wind stress anomaly data with iceberg counts (Figure 25) indicates a favourable correspondence for the longshore wind stress component. There was no discernible correspondence of iceberg severity with the cross-shore component of wind stress anomaly. In most years of high iceberg severity (1957, 1972-74, and 1983), the winds had a stronger-than-normal contribution from alongshore northwesterly winds, favouring southeastward advection along the Labrador coastline. However, in some years of high iceberg severity (1959, 1984), the alongshore wind stress was not abnormally favourable to southward advection of icebergs. Moreover, in other years of large positive wind stress anomalies (e.g. 1961, 1975), iceberg severity was low. This suggests additional factors, such as the supply of icebergs, play an important role. In general, the correlation of iceberg severity to wind stress was lower than that found for sea-ice severity or air temperatures in Davis Strait.

The absence of any correspondence between cross-shore winds with iceberg severity was somewhat puzzling. Simple physical reasoning suggests that strong winds having a component directed perpendicular to the Labrador Current could have a considerable effect on iceberg advection. For example, winds blowing to the northeast could, over a few days, move icebergs out of the main southeastward flow of the Labrador Current. The icebergs displaced northeastwards would move into the deep abyssal waters of the central Labrador Sea, where currents, and hence iceberg advection rates, are expected to be reduced considerably. Similarly, a southwest (onshore) displacement could lead to loss of icebergs due to grounding or landfast ice entrapment. The



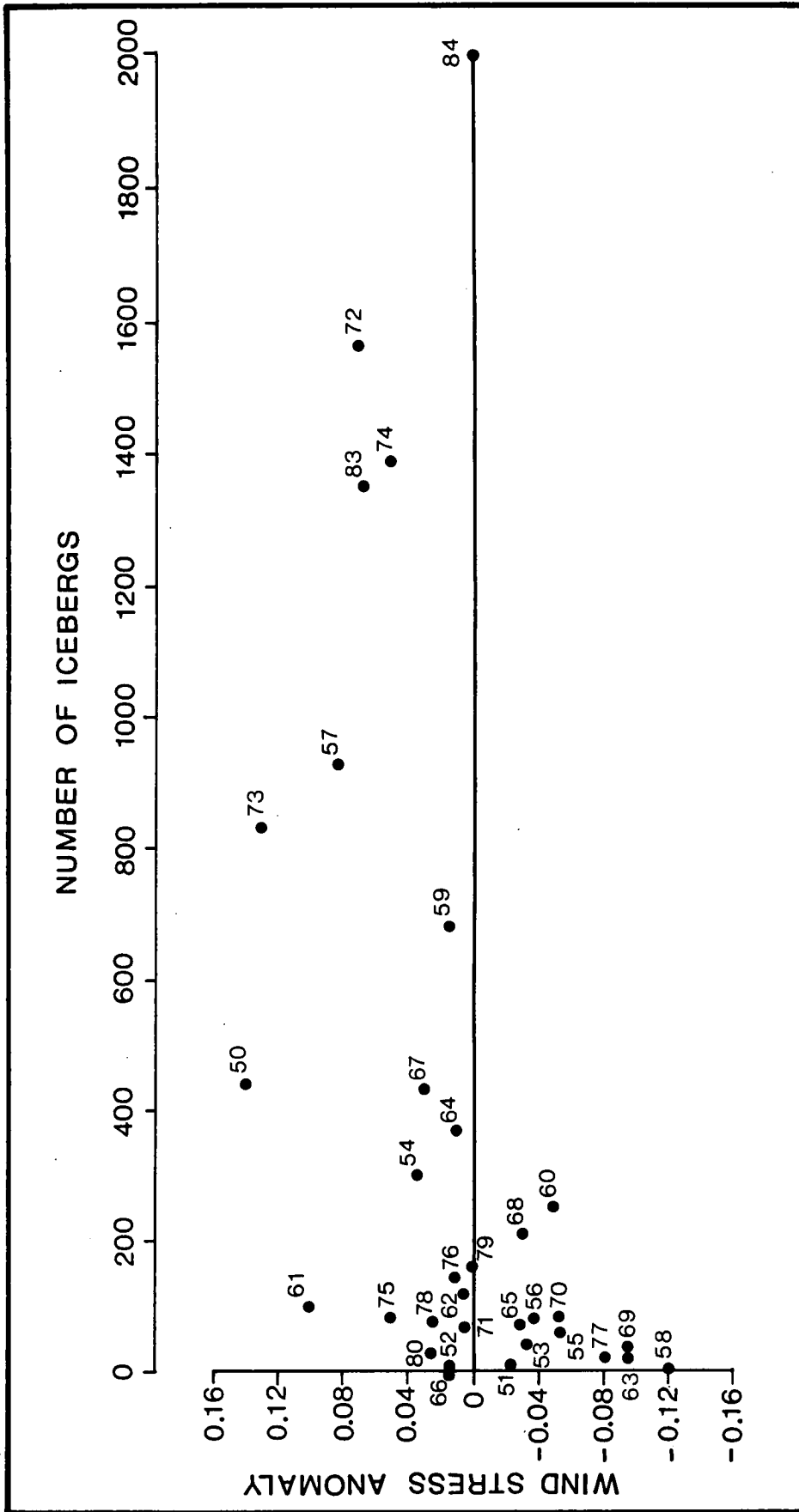


Figure 25: Anomaly in the longshore component of the winter (Dec.-Feb.) wind stress, computed for offshore Labrador ( $57^{\circ}\text{N}$ ,  $58^{\circ}\text{W}$ ), plotted versus the yearly number of icebergs crossing  $48^{\circ}\text{N}$ . Positive anomalies represent an above-normal wind stress from the northwest. Accompanying each data point is a 2-digit number representing the year.

effect of such lateral displacements on iceberg position could be of greater importance to net iceberg advection rates than the effect of variations in the alongshore wind component scale.

To further examine the cross-shore component of wind forcing, the 3-hourly wind observations from Ocean Weather Station (OWS) Bravo were acquired and analyzed. OWS Bravo was located at  $56.5^{\circ}\text{N}$ ,  $51^{\circ}\text{W}$ , approximately 450 km from the Labrador coastline. This site is well offshore of the main pathway of southward moving icebergs. However, direct wind measurements obtained at OWS Bravo are not strongly influenced by topographic effects as is the case for coastal Labrador measurement sites. Usable data were available from OWS Bravo over a 23-year period, 1950 to 1972. The 3-hourly data were first used to compute daily mean wind velocity vectors. From these data, the mean components of the wind over the 3-month period, January to March inclusive, were computed. The seasonal wind vectors were represented as components directed along the southeast-northwest direction (i.e. assisting/retarding iceberg advection) and along the northeast-southwest (i.e. directing icebergs offshore or onshore). The correspondence between seasonal wind components and iceberg severity, as displayed in Figure 26, are consistent with the comparisons of iceberg severity to wind stress anomalies, described above. Iceberg severity exhibited a tendency to increase with the southeasterly-directed wind component, while there was no correspondence evident between iceberg severity and the across-shore component of the OWS Bravo winds.

To further examine the role of cross-current wind forcing on shorter, synoptic time scales, progressive vector diagrams of the cumulative displacement of the wind (wind run) were computed and plotted for the December to May period of each year (Figure 27). From these plots, wind "events" of possible relevance to iceberg advection were catalogued. The wind events were defined as continuous displacements over individual directional sectors. The minimum displacement for a given event was chosen as 10,000 km of wind run, corresponding to a hypothetical iceberg displacement of 100-200 km, assuming iceberg movements respond as 1-2% of the wind speed.

From the tabulation of major wind "events" (Table 7) observed at OWS Bravo, only 7 of the 23 years (1950, 1953, 1963, 1965, 1966, 1968 and 1970) had one or more event that would result in major offshore (A) displacements. The onshore-directed wind events (C) numbered 6, consisting of the years 1958, 1959, 1960, 1962, 1965 and 1969. Neither set of years exhibiting strong on- or offshore directed wind events appears to correspond to consistently reduced numbers of icebergs reaching southern

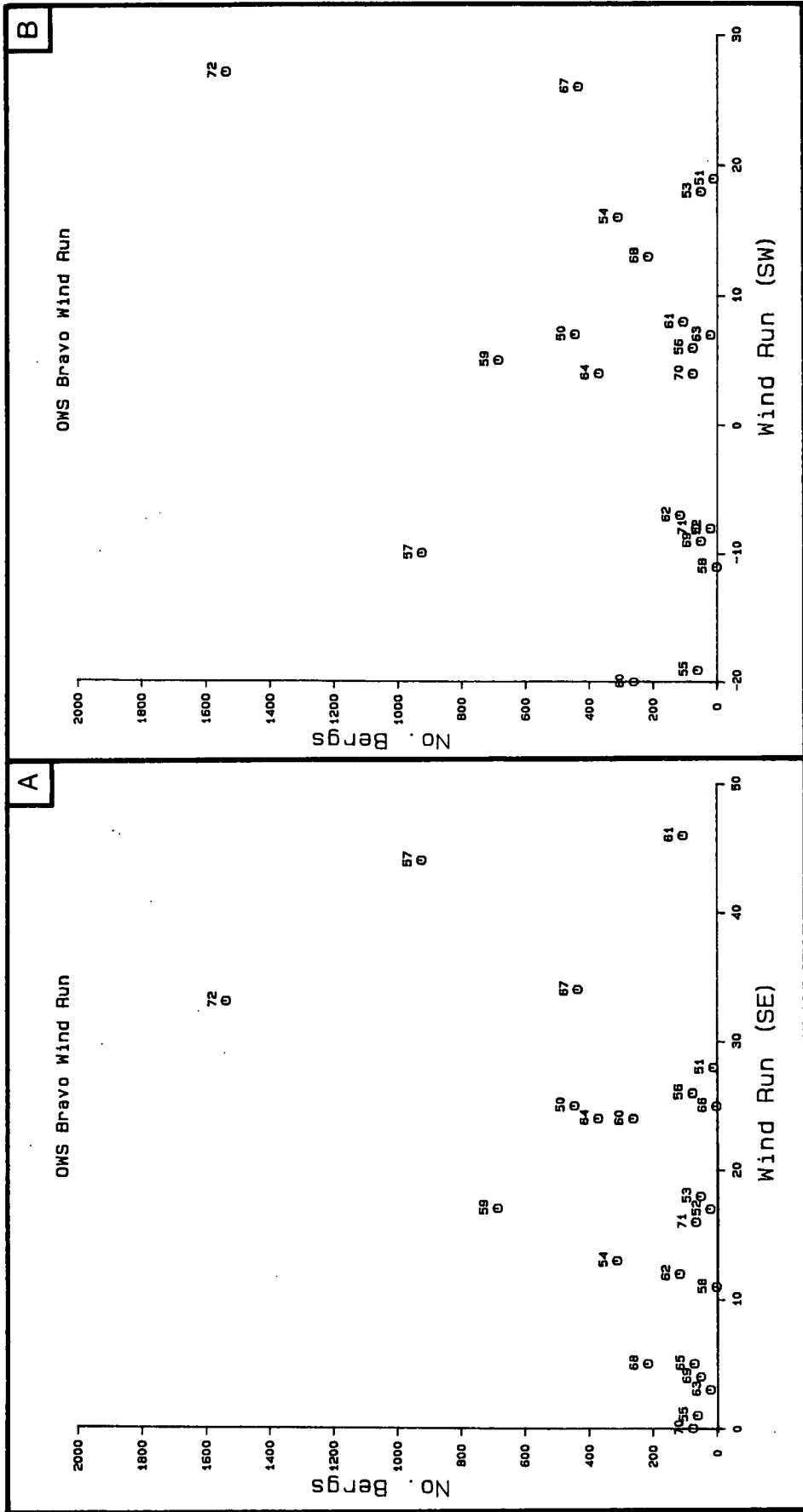


Figure 26: January-March wind run ( $\times 10^3$  km), computed from OWS Bravo data, versus iceberg counts for a) alongshore and b) cross-shore.

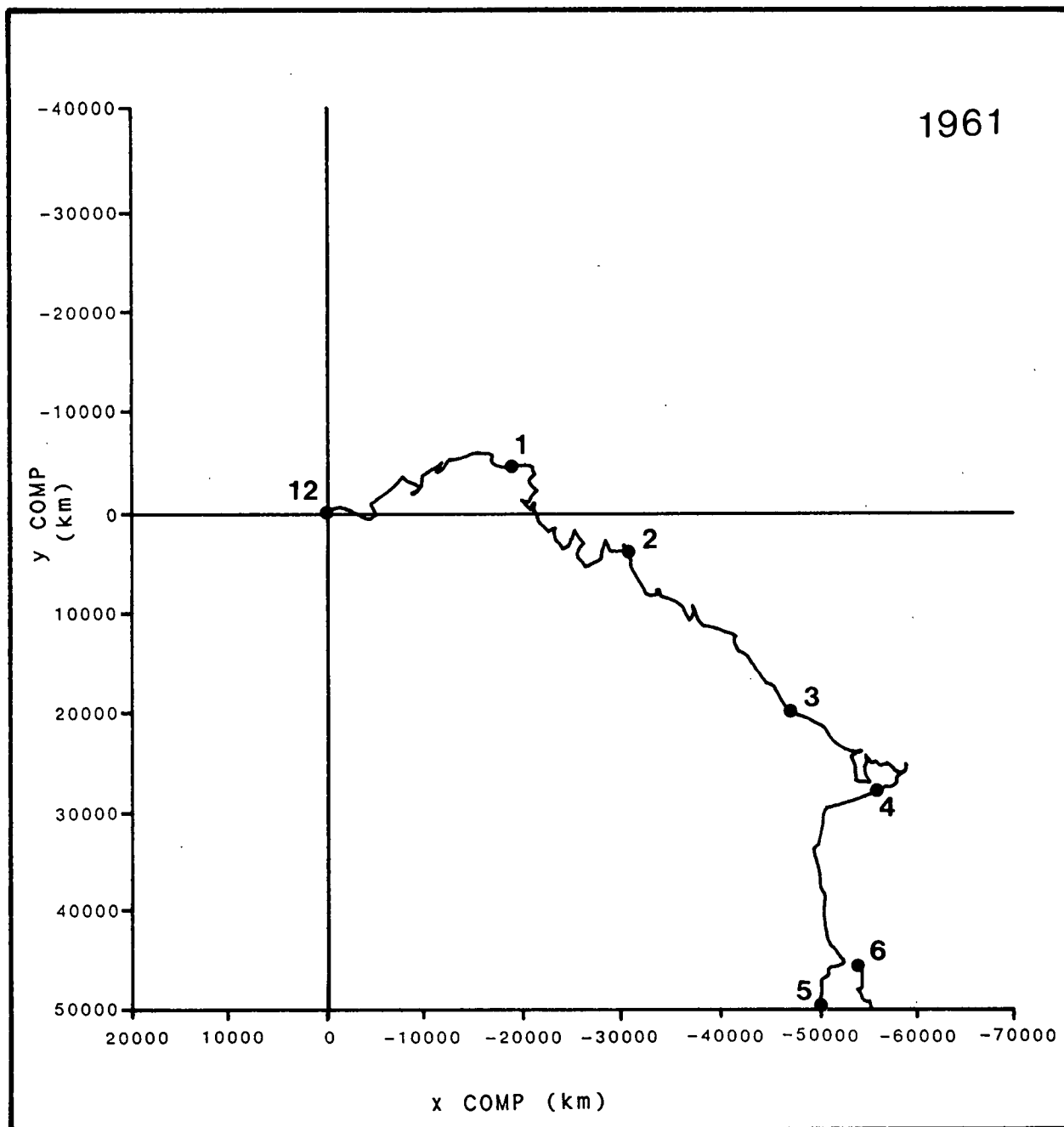


Figure 27: Example of wind-run progressive vector diagrams used to determine cumulative iceberg displacements. The numbers accompanying the dots are month indicators. Assuming a 1-2% iceberg-to-wind response, a wind run of 10,000 km would correspond to an iceberg displacement of 100 to 200 km.

**Table 7:** Tabulation of wind "events" observed at OWS Bravo from December to May, inclusive, 1950 to 1972. The results are expressed as nnX, where nn is the wind run during the event in thousands of km and X is the category for the direction sector. A key to the directional sectors, X, is provided below the tabulated values.

Year	Dec	Jan	Feb	Mar	Apr	May
1950	17A		26B	9B		
1951			13B	12B		
1952	27B			21B		
1953			8A	22B		
1954	15B			15B	15B	
1955	15B				15B	
1956		8B		8B		
1957	57B					
1958			18C		27B	
1959		12C		18B		
1960	20B		12C	28B		
1961			48B			30B
1962	14C			30C	10B	
1963			14A	14B		14A
1964			15B	16B		15B
1965	10A			28C		14C
1966	10A	22B				
1967				33B		10B
1968		9A	15D	12B		
1969	13B	9D	11D	11B	10B	10C
1970		13B	17A			
1971	11B		16B			
1972	12B	12B	37B	18B		

Direction Ranges:

Hypothetical Effect on Iceberg Advection:

- |    |          |                                                                                                                           |
|----|----------|---------------------------------------------------------------------------------------------------------------------------|
| A. | 0 - 70°  | Offshore displacement beyond strong shelf edge currents.                                                                  |
| B. | 100-190° | Favourable to southeastward advection.                                                                                    |
| C. | 230-280° | Onshore displacement resulting in delays due to possible grounding or impediment to motion due to sea-ice concentrations. |
| D. | 310-360° | Retardation of southeastward advection.                                                                                   |

latitudes. Thus, the hypothesis that wind events cause reductions in iceberg severity through removal of icebergs from the major current regimes appears to be either invalid or the effect is not detectable using OWS Bravo winds.

#### 4.2.5 LARGE SCALE ATMOSPHERIC PROCESSES

In Subsections 4.2.1-4.2.4, we have described and justified our extraction and compilation of data on specific, well-defined environmental parameters which, arguably could be directly related to observed variations in the number of icebergs moving south of 48°N. Two kinds of relationship were hypothesized:

1. Indicative, whereby the values of parameters such as sea-ice extent and air temperature can be expected to give early and unambiguous evidence of the seasonal forcing trend and hence, of the forthcoming severity levels.
2. Causative, whereby parameters such as the wind stress anomaly or along-flow windage can be expected to influence iceberg severity through direct and indirect (through an ocean current intermediary) forcing.

A third type of parameter may also be advantageous for a physical-based evaluation of the feasibility of severity prediction. Ideally, this type of parameter would represent the status of the global atmospheric-oceanic system. It is this system, with its myriad of complex linkages, which is fundamentally responsible for the observed interannual changes in the causative and indicative parameters and, of course, for the variations in iceberg severity.

The identification of such a global parameter, of necessity, requires the examination of the somewhat suspect raw severity record (Figure 4) in conjunction with data and present understandings of world climatic changes. Following a very brief summary of the observed trends in both the overall northern hemisphere climate and the iceberg severity, we introduce a candidate for such a parameter, the El Nino Southern Oscillation (ENSO) phenomenon. Numerous world-wide climatic changes have been previously attributed to ENSO. Our treatment, while certainly speculative, tries to demonstrate both hard evidence for the necessary changes in the causative parameters and for the linkage or teleconnections whereby atmospheric changes are communicated over thousands of miles to impact upon the northeastern corner of North America.

### Long Term Variability

The record of annual numbers of icebergs reaching 48°N (Figure 4) exhibits a very rough periodicity on the order of 10 years, as judged from the separation in time of two or more closely spaced "pulses" of large annual severities.

Any global factor fundamentally responsible for the observed variability would thus have its own scale of temporal variation equal to approximately one decade. Its influence on the iceberg severity would have to be exerted through the Baffin and Labrador currents and the northerly winter winds which are believed to provide the main driving forces for the southward iceberg movements. These winds are associated with counter-clockwise flows of air around the Icelandic Low which appears south of Greenland in the mean winter atmospheric pressure distribution. This feature is, in fact, normally associated with a series of cyclones which pass through this region.

Interpretations of the changes which have occurred in the positions and intensities of the Icelandic Low must be made in the presence of often poorly-understood and -documented trends in the climatic data. The initial 1880 to 1940 portion of the severity record coincided with a gradual warming of the northern hemisphere. Subsequent data purportedly indicated a later establishment of a distinct cooling period (Figure 28). January temperatures in Greenland were reported (Putnins, 1970) to be consistent with the cooling trend. On the other hand, climatic data obtained over Baffin Island (Bradley, 1973) were not consistent with the latter hypothesis.

The raw iceberg count record does indicate that a change in its periodicity occurred sometime around 1950. Although one must be very careful in drawing any conclusions from this highly effort- and technology-dependent record, it would appear that cyclic behaviour occurred with periodicities of approximately 7 years and 13 years for the pre- and post-1950 years, respectively.

The apparent reversal of temperature trends during the 1940's was accompanied by a long-term change in the strength of the Icelandic Low (Dickson, et al., 1975; Schell, Corkum and Sabbagh, 1975). Mean winter (December-February) sea-level pressures increased by 8 mb from 1900-1939 to 1956-1965, and by another 2-4 mb from 1956-1965 to 1966-1970 (Figure 29). This effect is also evident in the reduction in the pressure gradient measured across the Labrador Sea, beginning in approximately 1930 (Figure 30). Such changes tended to reduce the strength of the

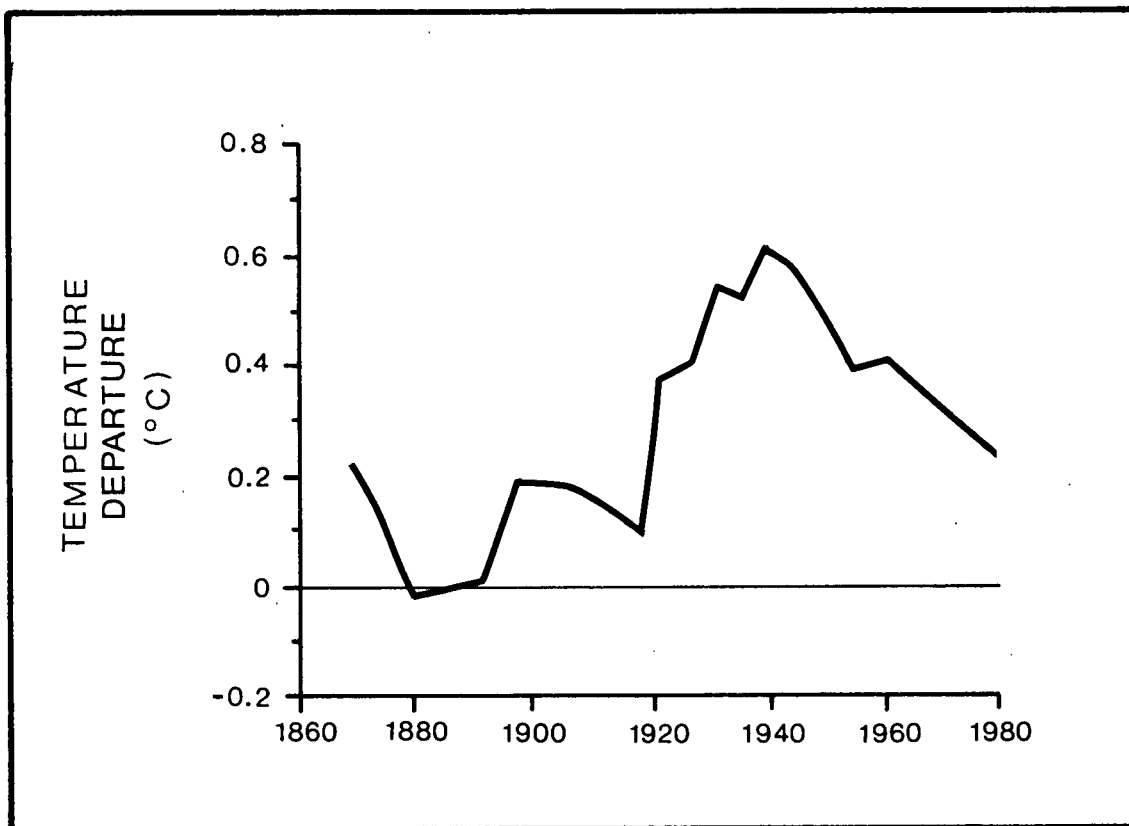


Figure 28: Deviation of northern hemisphere mean air temperature from mid-1880 values (after Mitchell, 1963).



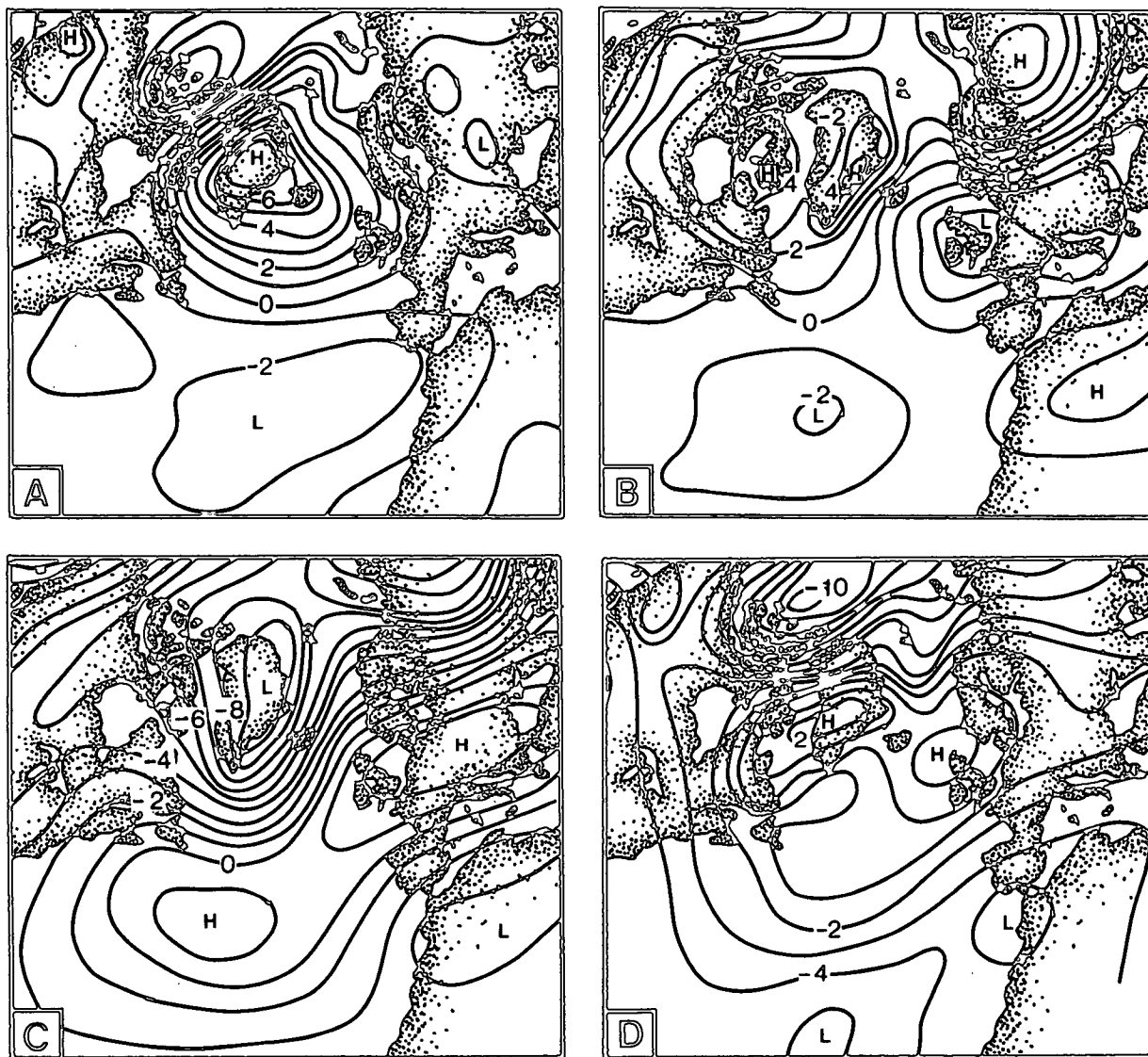


Figure 29: Change of mean winter (Dec.-Feb.) sea-level air pressures (mbar) between the periods: a) 1900-39 and 1956-65; b) 1956-65 and 1966-70; c) 1966-70 and 1971-74; and d) 1900-39 and 1971-74 (from Dickson et al., 1975).

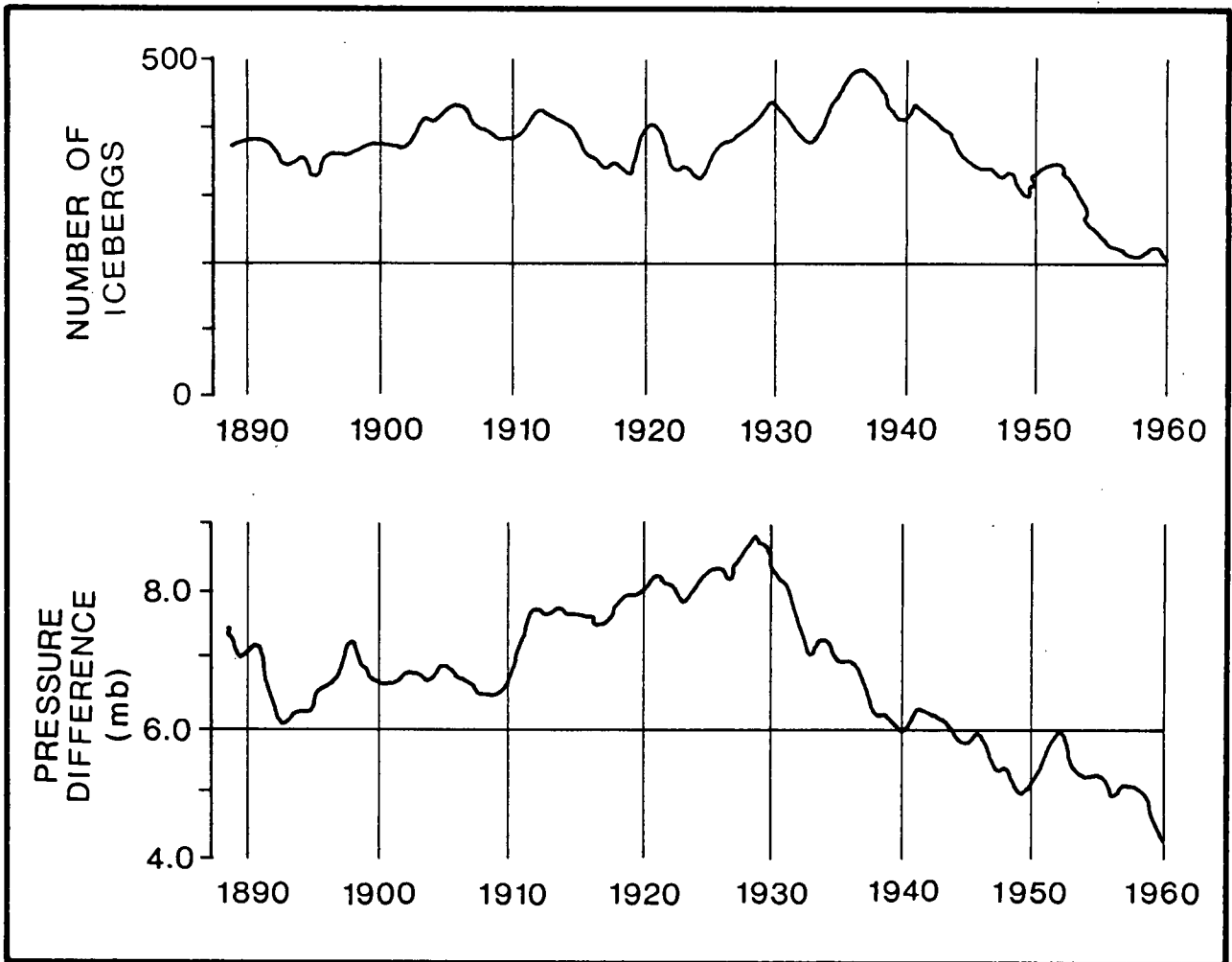


Figure 30: 19-year running average of iceberg counts, March-July (upper), and (lower) 19-year average of December-March Belle Isle (Nfld.) minus Ivigtut (Greenland) pressure difference (after Morgan, 1974).

northerly winter winds after about 1940. Coincidentally, the severity of northern European winters have increased since the 1950's largely due to the increase in northerly air flow caused by elevated air pressures over Greenland. The reduced northerly air flow over the Labrador Sea region in winter coincided with a large-scale net reduction in the number of icebergs reaching the Grand Banks. The average dropped from 427 per year during 1900-1950 to 196 per year for the 1951-1970 period. During 1971-1974, the Icelandic Low intensified (Figure 29c), together with the number of icebergs crossing 48°N (averaging 1273 per year for the 1972-1974 seasons).

### Intermediate Term Variability and the El Nino Connection

El Nino events are associated in the public mind with large changes in the surface water temperatures and anchovy catches off the Peruvian and Ecuadorian coastlines. They are known to occur on a typical time scale of 2 to 10 years, with particularly strong events appearing every 7 to 15 years. Years associated with such strong events have been indicated by the arrowhead symbols along the time axis of Figure 4. The coincidence, of strong events and the commencement of peaks in the iceberg counts is striking, particularly since about 1950. In order to understand how an El Nino-type event, generally associated with the Pacific Ocean, can influence icebergs off Labrador, we must briefly review relevant portions of the current understanding of large-scale atmospheric and ocean-atmosphere interactions. We will begin with an examination of periodic climatic oscillations in the North Atlantic.

### A North Atlantic Oscillation

The sea-level air pressures associated with the Icelandic Low have been found to be negatively correlated with North Atlantic pressures in a broad east-west belt centred near 40°N (Figure 31). This pattern has been noted by Defant (1924), Walker and Bliss (1932) and Kutzbach (1970). Walker and Bliss believed that the patterns of both sea-level pressure and temperature were due to an oscillation between the low and high pressure cells. They termed this the North Atlantic Oscillation (NAO). The strength of the oscillation has been indexed primarily in terms of the noted mean surface pressure and/or temperatures changes.

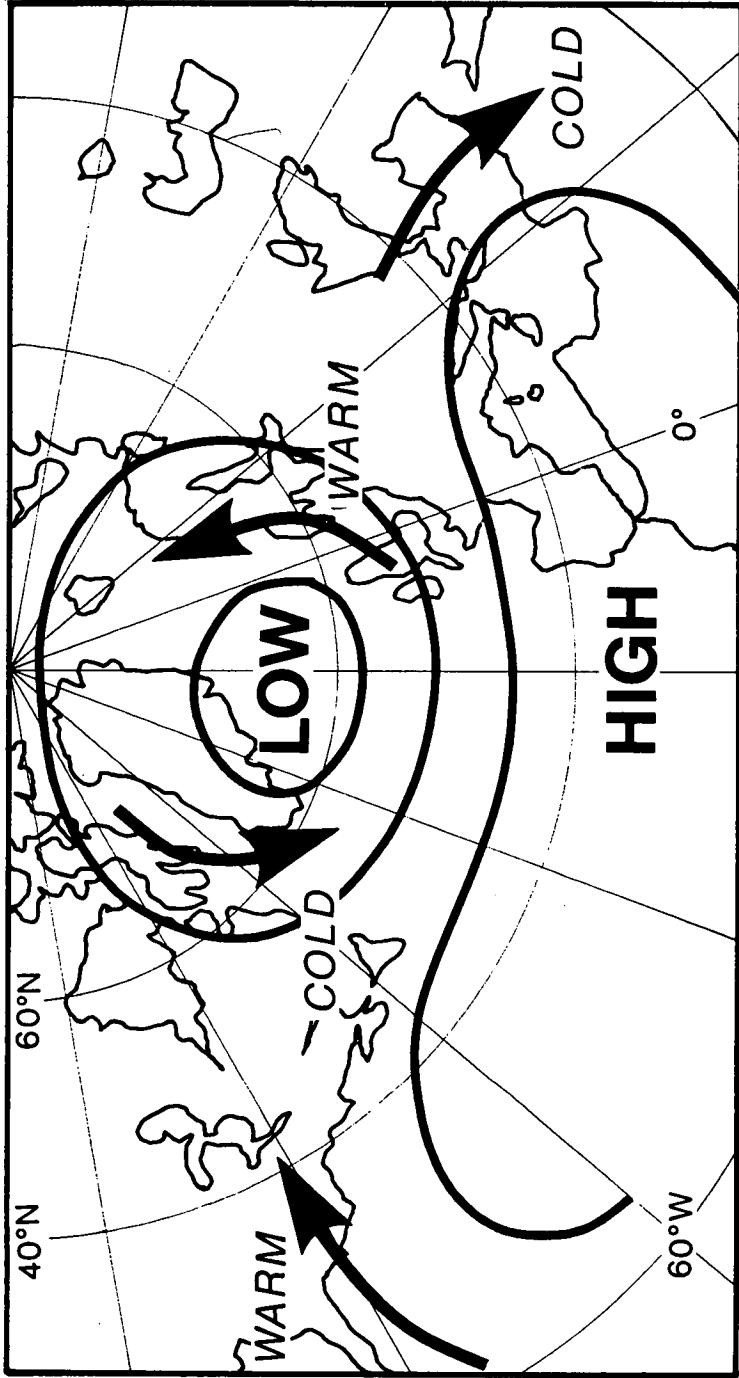


Figure 31: Schematic representation of the North Atlantic Oscillation (after Wallace and Gutzler, 1981).

Rogers (1984) recently carried out such an indexing using the winter pressure difference between the Azores and Iceland. A spectral analysis of the normalized record for the 1900-1983 period resulted in a peak period centred at 7.3 years. This value is intermediate to the 6.5 and 13-year periodicities noted in the yearly number of icebergs reaching the Grand Banks during the periods 1900-1950 and 1950-1983, respectively.

### The El Nino Southern Oscillation (ENSO)

Walker (1924) thoroughly documented a much larger atmospheric oscillation in the southern hemisphere. This Southern Oscillation (SO) was apparently first recognized by Hildebrandsson (1897). El Nino, characterized by anomalously warm water off the coasts of Ecuador and Peru, and the Southern Oscillation are closely linked. A broader term El Nino Southern Oscillation (ENSO) is generally used to describe this complex ocean-atmosphere interaction process.

As noted above, our interest in the Southern Oscillation stems from the fact that strong ENSO events (indicated on the time axis of Figure 4) have coincided with the arrival of the last three major cycles, or peaks, in the time series of iceberg counts. Before going any further in considering the interrelatedness of ENSO, the NAO and the interannual variability of the number of icebergs reaching the Grand Banks, it will be worthwhile to provide a brief overview of present understandings of the ENSO phenomenon.

Walker's own summary (1928) described ENSO as "a swaying of pressure on a big scale backwards and forwards between the Pacific and Indian Oceans". The pressure oscillation is associated with accompanying large-scale shifts in atmospheric mass. Figure 32 shows the regions of the globe directly involved in the Southern Oscillation. Pressures at Port Darwin and Santiago are almost exactly out of phase. As the pressures associated with the South Pacific High increase, those in the area of the Indonesian Low decrease, and vice versa. The pressures are oscillatory with the Southern Oscillation pressure index (Santiago minus Port Darwin) for the period 1882-1973 having a maximum coherence for a time lag of 2.8-3.5 years (Julian and Chervin, 1978).

Ordinarily, pressures associated with the South Pacific High are elevated and easterly tradewinds drive equatorial surface waters towards the west. The offshore flow leads to upwelling of cold, nutrient-rich water along the coastlines of Ecuador and Peru. In most years, during January through March, upwelling

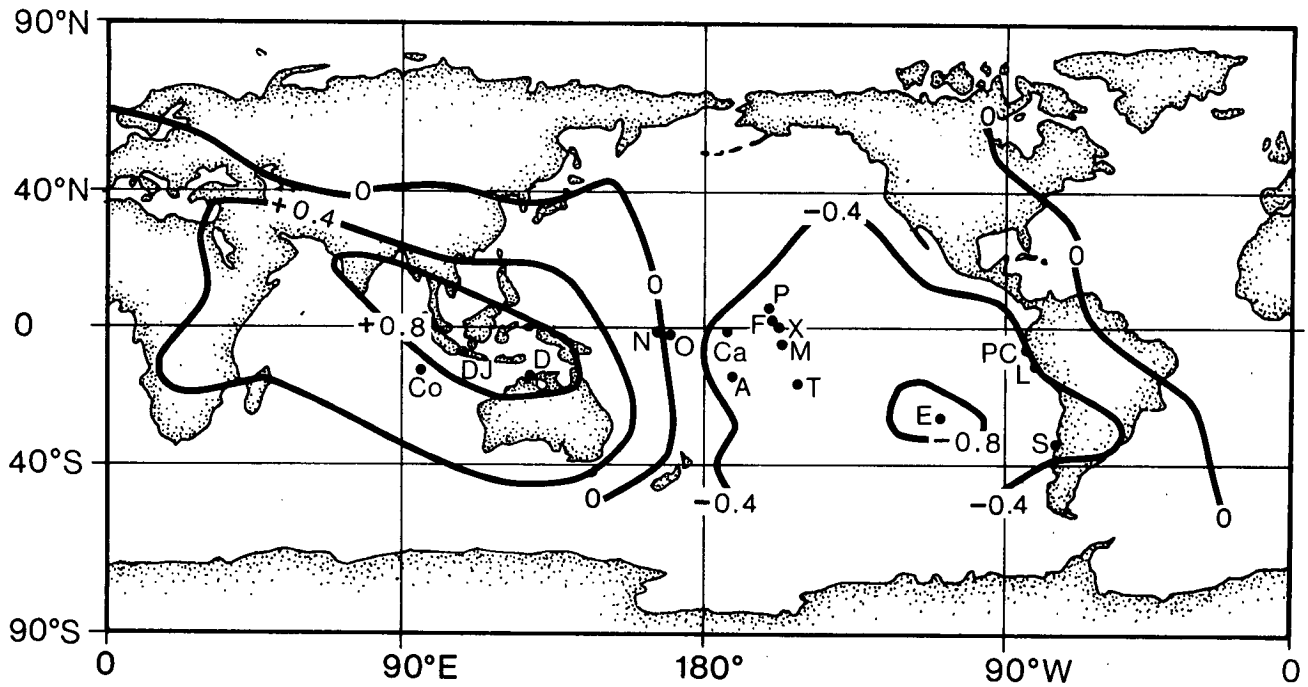


Figure 32: Schematic map showing isopleths of correlation of monthly mean station pressure with that of Djakarta, Indonesia (DJ). Other localities shown are Cocos Island (CO), Port Darwin (D), Nauru (N), Ocean Island (O), Palmyra (P), Christmas Island (X), Fanning (F), Malden Island (M), Apia, Samoa (A), Tahiti (T), Easter Island (E), Puerto Chicama (PC), Lima (L) and Santiago (S). (from Julian and Chervin, 1978 after Berlage, 1966).

ceases and a warm branch of the Equatorial Countercurrent sets southward along the coast of Ecuador and Peru. The arrival of the warm water marks the end of the local anchovy fishing season. Since this occurs near Christmas, the term El Nino or Christ Child, evolved.

It is now known that El Nino is only one manifestation of the ocean-atmosphere interaction process associated with the Southern Oscillation. During an ENSO event, the Southern Pacific High weakens (the SO index falls), as do the tradewinds in the western half of the equatorial Pacific. Water levels rise in the eastern Pacific and a strong sea-surface temperature (SST) anomaly develops in the equatorial Pacific. The Australian-Indonesian region receives abnormally low amounts of precipitation, whereas the eastern tropical Pacific experiences heavier rainfall.

Individual ENSO events exhibit considerable differences in the pattern of development. Generally, the easterly tradewinds build up prior to the event and then relax. And usually the SST anomaly first appears in the eastern equatorial Pacific and spreads westward. The strong 1982-1983 ENSO event, however, was not preceded by a build up of strong easterlies, and the SST anomaly spread from west to east (Quinn and Zopf, 1984; Thomson, 1984).

The start of an ENSO event is generally evident during October-November when the associated Walker cell shifts eastward and the tradewinds in the western Pacific begin to weaken. At about this time the pressures associated with the South Pacific High also start to fall. As the event progresses, the SST anomaly develops, generally reaching a peak during April-June of the El Nino year. Often a secondary peak in the SST anomaly will occur around the end of the El Nino year. This is then followed by a rapid decline in SST, reaching a minimum between May and August of the year following the El Nino event. About 12 to 18 months after the beginning of the ENSO, the upwelling and strong easterly tradewinds reappear, generally in the eastern tropical Pacific first, and expanding westward.

Walker's work demonstrated global-scale coherence of the atmospheric pressure patterns in the southern hemisphere. Later analyses concerning the relationship between the SO and sea-level pressure distributions in the northern hemisphere were carried out by Bjerknes, (1966), Namias, (1976) and Trenberth and Paolino (1981). Van Loon and Madden (1981) correlated pressure at Darwin with northern hemisphere pressure for four periods covering 1899-1977. They found that the Southern Oscillation was well

correlated with alternations extending from the Pacific, across North America, and ending over the western Atlantic Ocean. This pattern, termed a teleconnection, is known as the Pacific-North America Pattern.

It was noted by Horel and Wallace (1981) that high equatorial Pacific sea surface temperatures tend to be accompanied by below normal heights of the upper tropospheric geopotential height anomaly (i.e. lower atmospheric pressure) in the North Pacific and southeastern United States and above normal heights over western Canada. Theoretical work on Rossby wave propagation has provided a model of these teleconnections (Opsteegh and Van Den Dool, 1980; Hoskins and Karoly, 1981; Webster, 1981).

Others have addressed the possible association between the SO and NAO. Walker presumed no connection, while Berlage and De Boer (1960) suggested that from 1931 to 1938 the SO was weak and the NAO actually forced an oscillation in the equatorial Pacific. Later, from 1949 to 1957 Berlage and De Boer (1960) suggested that a strengthened SO dominated world weather, even in the Atlantic. Berlage (1966) found that Djakarta pressures were correlated with pressures in the area of the Icelandic Low. Van Loon and Madden (1981) found that teleconnection patterns differing from the Pacific/North America pattern were unstable and moreover, that the ability of the SO to influence the North Atlantic circulation is determined by the strength of the Oscillation index. Weak SO indices will not allow the propagation of effects into the North Atlantic. Recently, Barnett (1985) analyzed sea-level pressures (SLP) using complex empirical orthogonal functions and concluded that the NAO and a large-scale SLP signal, associated with the SO, were unrelated. Barnett's results were based on the 1951-1980 period, and used monthly-averaged, low-passed data.

In spite of the apparent lack of convincing evidence in favour of an ENSO-NAO connection, the coincidence of strong ENSO events (ratings of 4 on a 1-4 scale, as per Quinn, et al., (1978) and Rasmusson, (1984); see Table 8) with large southerly fluxes of icebergs (Figure 4) suggests that strong ENSO events may have influenced atmospheric-oceanic conditions in the large areas traversed by icebergs from Davis Strait to Newfoundland during the 1950-1985 period. Moderate and weak ENSO events, (i.e. ratings of 1-3) did not exhibit such influence. Figure 33 illustrates the winter (December-February) surface air pressure anomalies for the years 1957, 1972 and 1983. These are the years in which a strong ENSO event coincided with the start of a peak cycle in the time series of yearly iceberg counts. In each case,



**Table 8:** Year of onset of El Niño type events, 1725-1983, as classified according to event intensity by Eguiguren (1894), Quinn et al. (1978) and Rasmusson (1984). Numbers refer to event intensity: 1, very weak; 2, weak; 3, moderate; and 4, strong (events below intensity 3 were not accepted prior to 1841 when pressure data became available; unbracketed intensities pre-1891 are by Eguiguren (1894)).

Year	Event Intensity	Key to Source	Year	Event Intensity	Key to Source	Year	Event Intensity	Key to Source	Year	Event Intensity	Key to Source
1726	(3)	G	1852	2	B,PC	1896	(3)	PI,R	1943	(2)	G,T,R
1728	(4)	A,G	1854	2	B	1899	(4)	D,PI,R	1944	(2)	PI,T
1763	(4)	A	1855	(2)	PC	1900	(3)	PI,R	1946	(1)	PI,R
1770	(4)	A	1857	2	B,PC	1902	(3)	PI,R	1948	(1)	PI,T,R
1791	4	A,B	1862	2	B	1905	(3)	PI,R	1951	(2)	G,PI,T
1803	2	B	1864	4	A,B,PI	1911	(4)	F,E,PI	1953	(3)	G,E,T
1804	4	B	1866	2	B	1912	(3)	F,PI	1957	(4)	G,L,PI
1814	4	B	1868	1	B,C,PI	1914	(3)	G,PI,R	1958	(4)	G,L,PI
1817	3	B	1871	4	A,B,C	1917	(2)	H	1963	(1)	PI,R
1819	3	B	1873	(2)	PI	1918	(4)	C,D,PI	1965	(3)	M,PI,T
1821	3	B	1875	1	B,PC	1919	(3)	D,PI,R	1969	(2)	PI,T,R
1824	3	B	1877	4	A,B,PI	1923	(2)	H,PI	1972	(4)	N,O,PI
1828	4	A,B	1878	4	A,B,PI	1925	(4)	D,E,PI	1973	(4)	N,O,T
1829	1	B	1880	2	B,PI	1926	(4)	I,PI,T	1975	(1)	P,PI,T
1832	3	B	1884	4	A,B,PI	1929	(3)	G,I,PI	1976	(3)	Q,PI,T
1837	3	B	1885	(4)	PI	1930	(3)	G,PI,T	1982	(4)?*	S
1844	3	B,PC	1887	2	B,PI	1932	(2)	E,I,J	1983	(4)	S
1845	4	B,C,PC	1888	2	B,PI	1939	(3)	E,J,T	1984	(1)	X
1846	2	B,PC	1889	1	B,PI	1940	(2)	C,PI,T	1985	(1)	X
1850	2	B,PC	1891	(4)	D,E,PI	1941	(4)	E,K,T			

Key	Source	Key	Source	Key	Source
A	Frijlinck (1925)	H	Lavalle (1917,1924)	O	Caviedes (1975)
B	Eguiguren (1894)	I	Shepard (1930,1933)	P	Wyrtki et al. (1976)
C	Hutchinson (1950)	J	Mears (1944)	Q	Quinn (1976)
D	Murphy (1923,1926)	K	Lobell (1942)	R	Rainfall (equatorial and/or Peruvian)
E	Sears (1954)	L	Wooster (1960)	T	Sea-surface temperature off Peru
F	Forbes (1914)	M	Guillen (1967)	PC	Pressure component of Southern Oscillation index
C	Schweigger (1961)	N	Idyll (1973)	PI	Southern Oscillation pressure index
		S	Rasmusson (1982, 1983)	X	Estimated by authors

\*1982 was the start of the 1982-1983 event which actually occurred in spring 1983. Therefore we believe the 1982 rating of 4 should actually be reduced.

the winter pressures have a negative anomaly in the area of the Icelandic Low, and a positive anomaly in the region of the Azores. Such perturbations of the NAO would result in increased northerly winds over the Labrador Sea region, making conditions more favourable for the southerly flux of icebergs.

Conversely, during three recent years, 1953, 1965 and 1976 having moderate ENSO ratings (3) (Quinn, et al., 1978), the NAO was affected in the opposite sense, with pressures in the region of the Icelandic Low increasing (Figure 34). The resulting anomalies in wind stress off Labrador would tend to reduce the southerly flux of icebergs. Similar patterns in the NAO have been found to be indicative of the amount of rainfall forthcoming in northeastern Brazil. Namias (1972) found that high levels of precipitation (the rainy season peaks in March-May) in northeastern Brazil were preceded by anomalous winter cyclonic activity (in the 200 mb geopotential field) in the region of Newfoundland-Greenland. Nobre, Moura and Norbe (1985) expanded on this and produced two atmospheric circulation deviation patterns typical of the winter conditions preceding either wet or dry seasons. The wet pattern is similar to that resulting from strong ENSO events (Figure 33) while the dry pattern represents the opposite phase of the NAO (Figure 34). Nobre, Moura and Norbe (1985) recognized the predictive potential of these atmospheric circulation patterns, which appear about 3 months prior to the period for which rainfall predictions are valuable.

The "wet" atmospheric pattern (Figure 33) results in increased southerly winds off the eastern United States which could increase the strength of the Gulf Stream. Post (1956) had suggested that a strengthened Gulf Stream could hinder the flux of icebergs onto the Banks. Although support for this hypothesis was found to be highly suspect (Section 3), the results here also imply that evidence for this phenomenon would be obscured by the effects of an intensified Icelandic Low.

The Pacific-North America or central Pacific to eastern North America (CPNA) teleconnection pattern extends from the Pacific, across North America to the eastern United States. Nobre, Moura and Norbe (1985) illustrated another global teleconnection pattern which originates near Indonesia, the other end of the SO, and extends across Siberia, terminating in the NAO (Figure 35). This teleconnection may represent the path by which strong ENSO events could affect the NAO. Such a possibility is speculative at this time. Inter-hemispheric teleconnections are

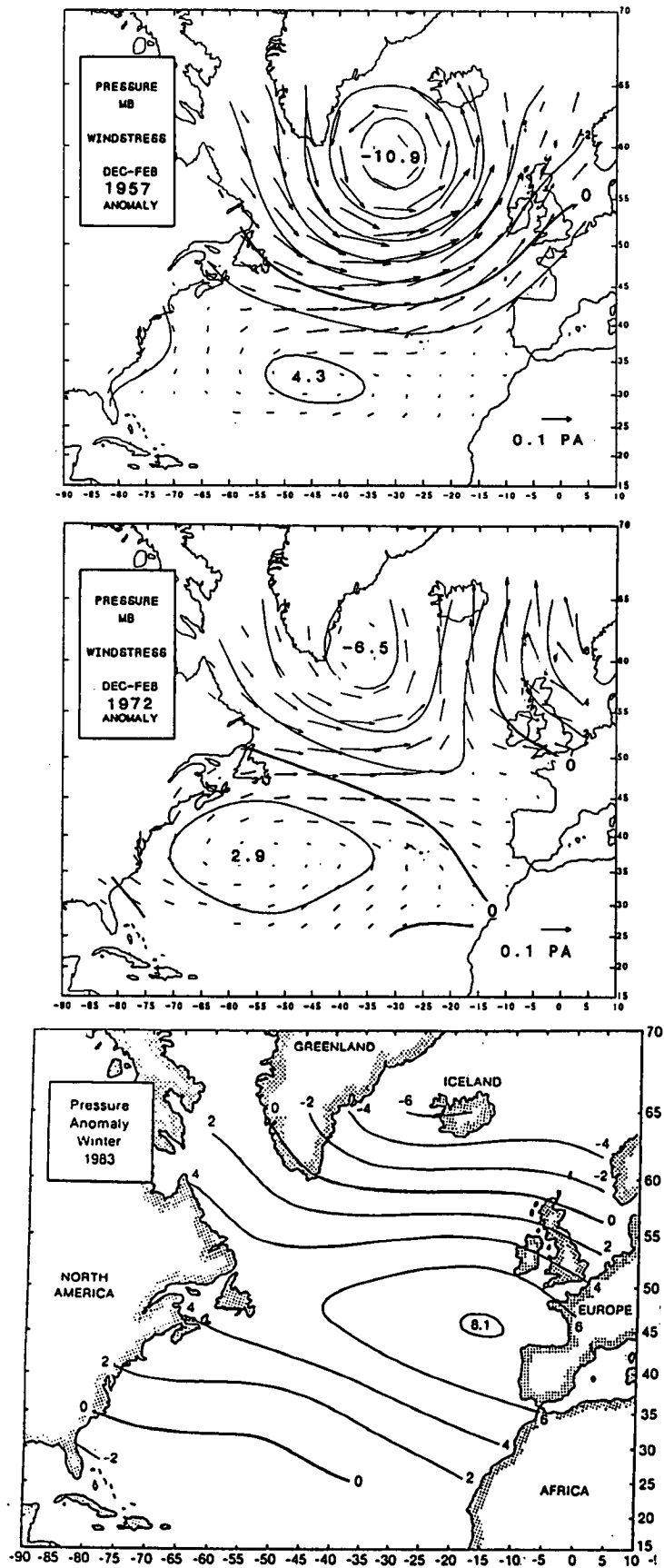


Figure 33: Winter wind stress anomaly patterns associated with years of strong ENSO events, 1957, 1972 and 1983 (data from Thompson and Hazen, 1983).

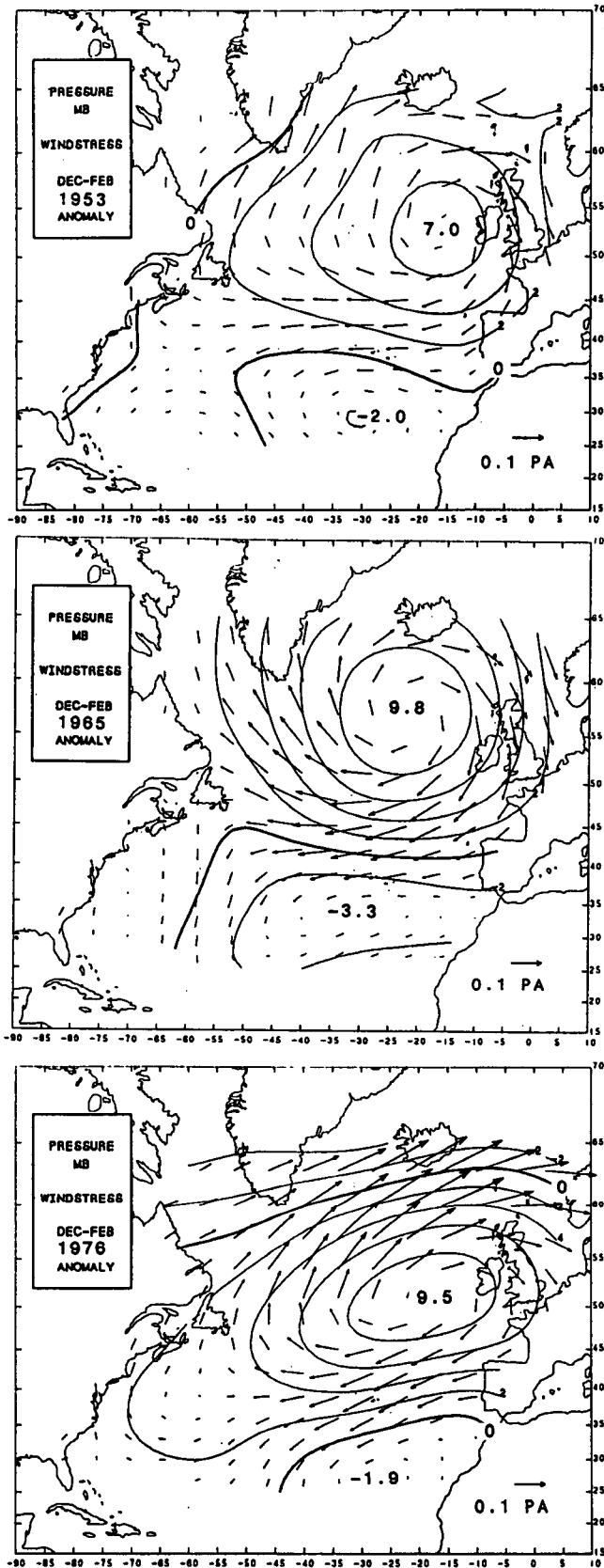


Figure 34: Three winter wind stress anomaly patterns (1953, 1965 and 1976) representative of years of moderate ENSO events (data from Thompson and Hazen, 1983).

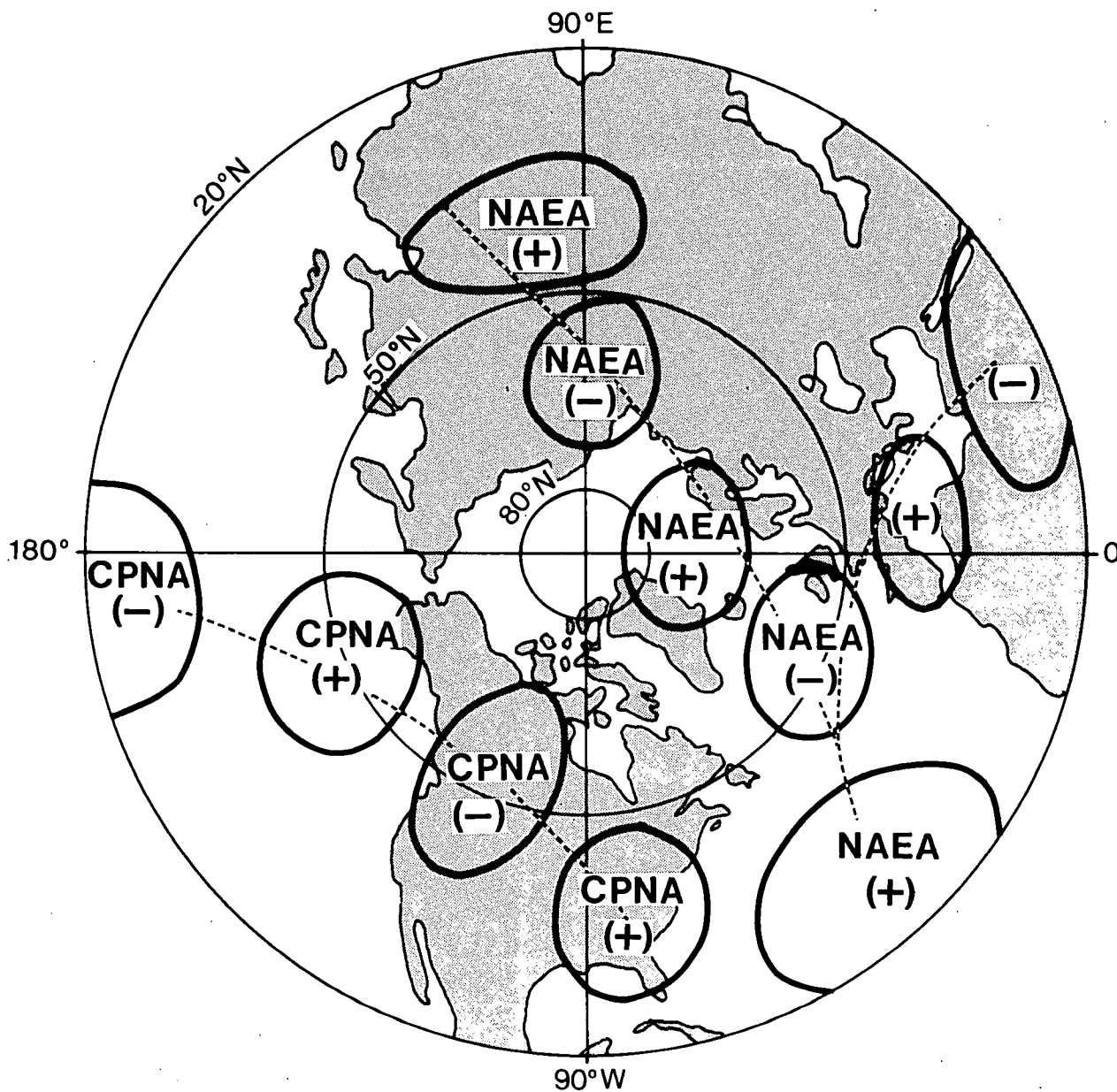


Figure 35: Northern-hemispheric teleconnection patterns; North Atlantic East Asia (NAEA) and Central Pacific-East North America (CPNA) (after Nobre, Moura and Norbe, 1985).

presently the subject of much research and hopefully more conclusive, quantitative descriptions of the involved phenomena will be forthcoming in the relatively near future.

### Possible Relationships Strong Between ENSO Events and Iceberg Severity

Our review of the physical evidence for a linkage between the ENSO phenomenon and the observed variations in southern iceberg numbers will be primarily focused on the post-1950 data. This period was chosen over earlier years because of (1) the greater reliability of the iceberg counts and (2) the differences in the periodicities exhibited in both iceberg severity and ENSO records of the earlier and later data records.

Since 1950, there have been three cycles of high yearly iceberg counts, with each cycle lasting about 3 years. The periods of high severity are 1957-1959, 1972-1974 and 1983-1985 (or longer). The yearly iceberg counts during each of these periods are an order of magnitude higher than in intervening years.

A strong ENSO event occurred during the first year of each cycle. The SST anomalies associated with ENSO events generally peak during April-June, and it is during the April-May period that generally about 60% of the yearly total number of icebergs move south of 48°N. In two of the three cycles, strong ENSO events occurred in two consecutive years.

If strong ENSO events do herald a severe iceberg season, such events would provide a valuable predictive tool since their occurrence is usually apparent during the previous fall as anomalous oceanographic and atmospheric conditions in the equatorial Pacific. Given that the ENSO is identified during the fall and its severity recognized by January or February, this would provide at least a 3-month lead time prediction of the severity of the following spring's iceberg conditions on the Grand Banks.

In two of the three cycles, two strong consecutive annual ENSO occurrences were each accompanied by correspondingly high iceberg counts (1958 is anomalous in that strong ENSO conditions were in effect but the Icelandic Low was weaker than normal and very few icebergs reached the Banks), followed by a third year of high severity. The effects of the strong ENSO events appear to have carried over into an additional third year. This circumstance may be related to the fact that ENSO events often have two SST anomaly peaks, the major one during April-June, and

a second near the end of the year. However, in the most recent cycle, this ENSO index pattern was not maintained. One of the strongest ENSO years on record was 1982-1983, but El Nino-like conditions did not persist more than the one year. Yet high iceberg counts, possibly the highest ever, continued not only for the 1983 season, but also for at least the next two seasons. The 1982-1983 event also had a double SST anomaly peak, but centred on January and May 1983, much closer together than normal. The fact that the 1982-1983 ENSO was anomalous in many respects may eventually help explain this deviation from the pattern established during the previous two cycles.

Although the studied 1950-1985 period is clearly too short to draw definitive conclusions on the nature of the possible ENSO-severity relationship, the following hypotheses appear to have some validity.

1. A strong ENSO event, occurring after a period of moderate, weak or non-ENSO years, appears to immediately precede the start of a multi-year cycle of severe spring iceberg conditions on the Grand Banks.
2. The length of any particular cycle is difficult to predict. Two strong ENSO events have occurred consecutively, followed by a third year of high iceberg counts. However, in the most recent cycle (1982-1985), one strong ENSO event was followed by two, and possibly more, years of high iceberg counts.

The strong ENSO events appear to have resulted in an intensification of the Icelandic Low, such that winter wind stresses over the Labrador Sea region were anomalously high. The increased north-northwesterly winds, accompanied by more extensive sea-ice than normal, resulted in an increased number of icebergs reaching the area of the Grand Banks. Although the mechanism of these large-scale atmospheric interactions, or teleconnections, is unclear, the evidence points to a possible link between strong ENSO events and an intensification of the Icelandic Low.

#### 4.3 RATIONALIZATION OF THE ICEBERG SEVERITY RECORD

In Section 3, we reviewed the defects of previous severity prediction formulae. One of the most serious flaws has been the absence of any consideration of the inherent "noisiness" of the severity "signal". More specifically, the evidence indicates that a significant portion of year-to-year variation in reported iceberg numbers was attributable to corresponding annual

differences in observation conditions, levels of effort and technology. The regression formulae derived from such data would not normally be expected to perform well in predicting future raw iceberg counts, measured with potentially different levels of effort, observation conditions and technology.

The present section is concerned with our own efforts to minimize the confusion introduced by such unwanted sources of variability into our investigations of the feasibility of severity prediction. An obvious means of effecting such precautions is equivalent to a coarsening or reduction in the resolution of the severity data so that inequalities between the resulting rationalized severity levels may safely be assumed, in most cases, to correspond to genuine differences in the annual number of icebergs moving south of 48°N.

In order to set appropriate levels of resolution, we reviewed the annual IIP iceberg summaries to obtain a rough idea of the relationship between the reported iceberg counts and the degree of concern expressed for marine safety. We also took note of recent estimates by IIP personnel that southern iceberg count values reported prior to the introduction of SLAR observing capabilities in the late 1970's were likely to have been underestimated by a factor on the order of two relative to values which would have been obtained with the newer technology.

This information, together with the raw severity probability distributions (Figures 13, 14 and 36), was used to devise a three level "rationalized" severity classification system. The three levels of this system were designated as:

1. Low, corresponding to raw severities equal to or less than 200 icebergs;
2. Intermediate, corresponding to raw severities greater than 200 but not greater than 600 icebergs; and
3. High, corresponding to raw severities greater than 600 icebergs.

We believe that this rationalization scheme (Figure 37), or its equivalent, is necessary to correctly portray the detectable, true interannual variability over the long periods of time (i.e. 1953-1985) needed for meaningful comparison with prediction schemes. It allows a rather clear-cut separation of the low and high categories since even a two-fold underestimate of raw iceberg numbers will not cause an incorrect assignment with regard to these two categories. Some ambiguity is retained in



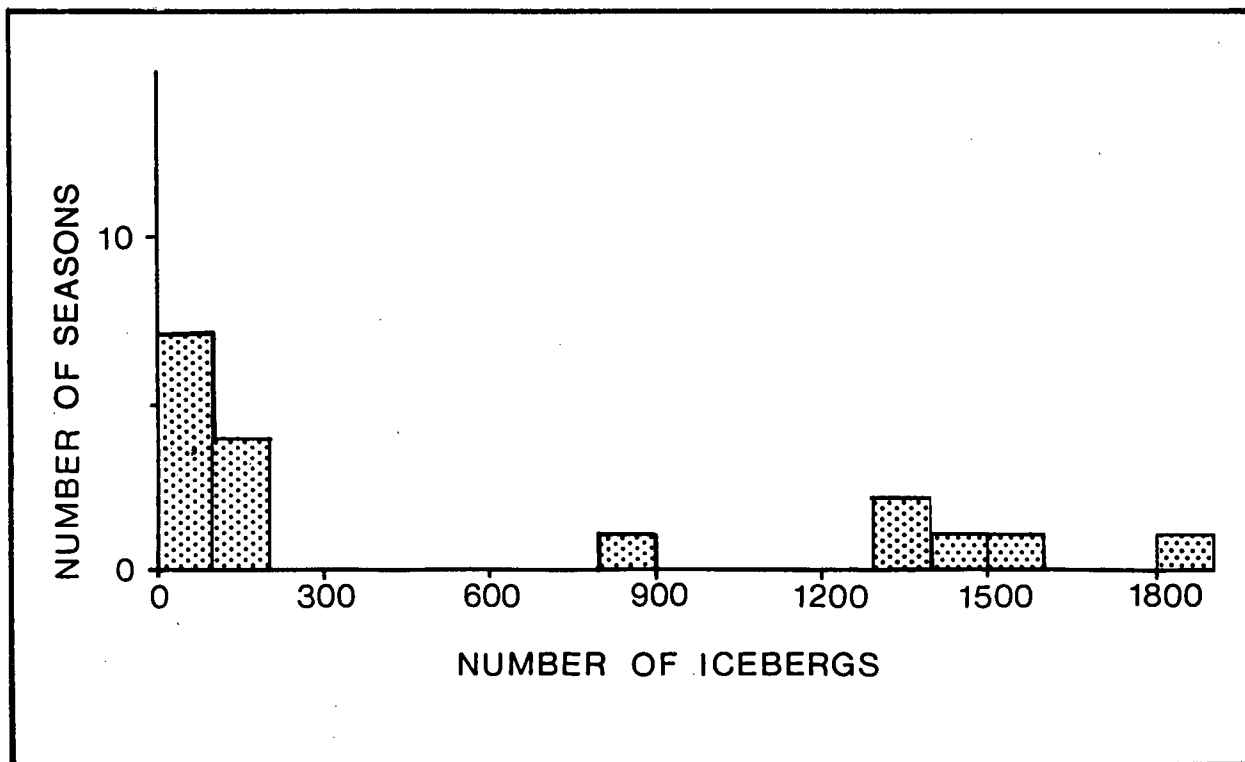


Figure 36: Probability distribution of iceberg counts, 1969-1985.

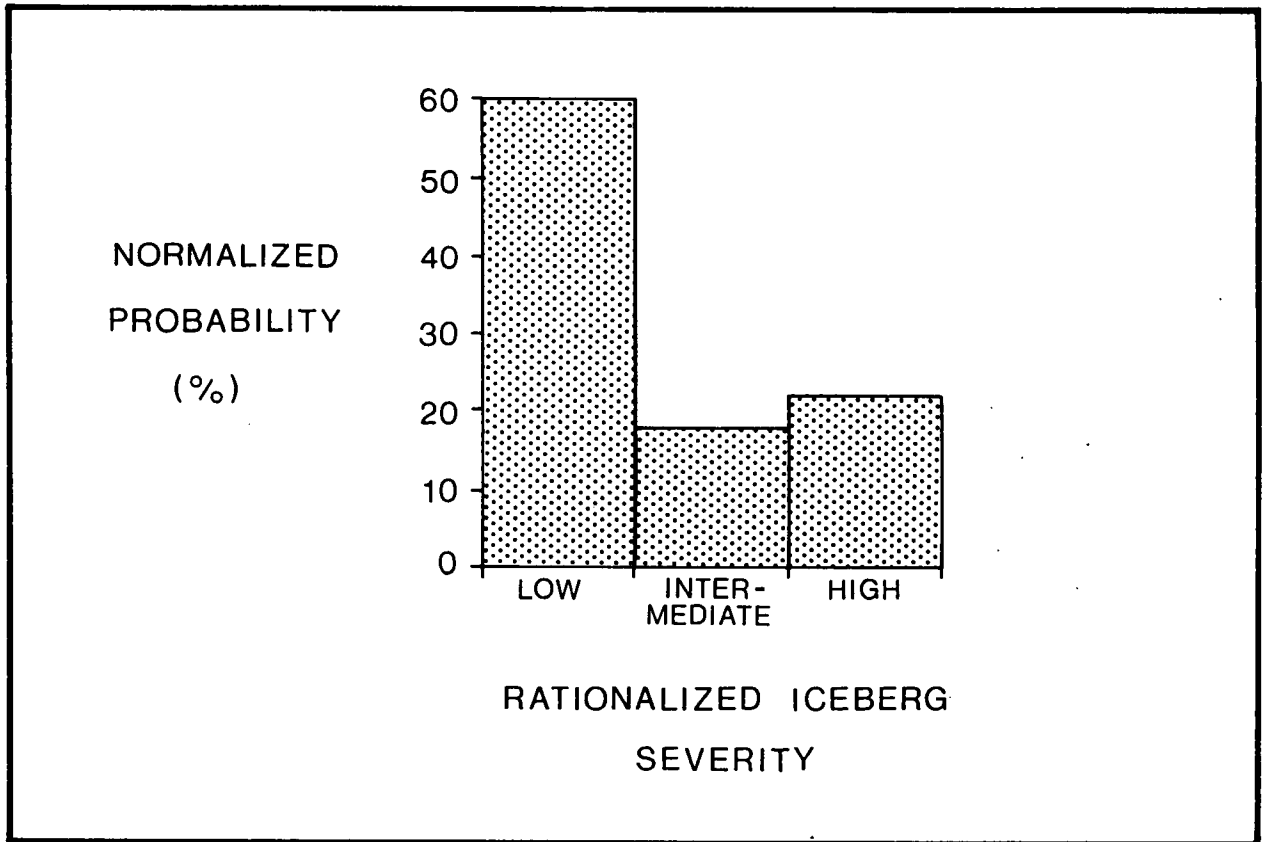


Figure 37: Normalized probability distribution for rationalized iceberg severity in the period 1953-1985.

intermediate severity assignments which can represent either truly intermediate levels of actual iceberg severity or could alternatively represent under- and over-estimated high- and low-severities, respectively.

It is interesting to note that intermediate levels of severity have not been observed since 1968 (See Figures 4 and 36). One possible interpretation of this fact was that the relatively higher quality of the post-1968 iceberg counts, relative to earlier portions of the post-war record, allowed the true bimodal (high or low) nature of the annual severity signal to be seen. Such an interpretation is now considered unlikely, because the bimodal distribution in the recent severity data record has direct counterparts in the probability distributions previously noted for recent portions (post-1971) of the sea-ice extent and air temperature parameter data records (Sections 4.2.1 and 4.2.2).

#### 4.4 SEVERITY PREDICTABILITY AND EVALUATION

Considerable evidence was presented in Section 4.2 to support the existence of three sets of measurable or calculable parameters which respectively:

- a) appear to exhibit a variability which correlates in a very direct way with iceberg numbers seen 3 to 6 months later south of 48°N;
- b) display variations in their average or net values over the mid to late winter periods which also correlate well with severity variability; and
- c) appear to exceed an identifiable minimum measure of strength immediately prior to all recently observed cycles of high iceberg severity.

These sets of parameters have been designated as:

- a) indicative - an earlier and more easily visible response to the mechanisms which determine the forthcoming level of severity;
- b) causative - a measure of the direct forcing acting on the icebergs during the period immediately preceding the iceberg season; and
- c) global - major changes in global atmospheric patterns which may be teleconnected into the iceberg infested region.

The individual member parameters of each of these sets are: sea-ice extent and air temperature; flow-parallel windage and stress anomalies; and the ENSO strength parameter, respectively.

Moreover, it is possible to propose a reasonably consistent picture of the variability mechanism in which the global shifts in pressure induce a strengthening of the cyclonic air and water circulations in Baffin Bay, Davis Strait and the Labrador Sea. This strengthening is first and most easily visible in January in the ice extents and air temperatures of the upstream Davis Strait region. By the end of February or March, its effects are also evident in the wind forcing parameters as accumulated or averaged since December and/or January. Finally, at the end of this chain of events, the effect of the initiating global event appears as a high value of the number of icebergs which arrive south of 48°N in the March-July period.

A more quantitative evaluation of the consistency of this picture with past physical events could be carried out by the derivation and hindcast testing of simple prediction modes for the use of each parameter relative to the rationalized historical iceberg severity record.

Our procedure for the derivation of the prediction rules, pertinent to all parameters except the ENSO strength index, was based upon a partitioning of the individual parameter probability distributions into three portions, each of which corresponds to the total fractional probability associated with a corresponding portion of the probability distributions as derived for the rationalized iceberg severity (Figure 37).

The boundaries of the high, intermediate and low iceberg severity regions of the distributions are given for each parameter in Table 9. The hindcast process then involves a classification of the raw annual prediction parameter values according to this partitioning. The iceberg severity predicted for each year is then given directly by the parameter classification.

Such a simple scheme is not readily applicable to the ENSO strength parameter. Nevertheless, we have included in Table 9 a brief description of tentative, ad hoc criteria to be used for generating predictions from this parameter. It was assumed, on the basis of the results discussed in Section 4.2.5, that the ENSO strength index is capable only of giving a binary prediction product in the form of a yes/no prediction for the occurrence of

a high iceberg severity. The absence of any consistent effects of lesser strength ENSO events on historical iceberg severities means that no distinctions could be made between the low and intermediate severity alternatives, i.e. low and intermediate severity levels. Our criteria should be considered speculative because of the readily apparent complexity of the proposed linkage and, as well, because of the relatively small number of strong ENSO events (5 since World War II) upon which our derivation of these criteria were based. The criteria assumed that high iceberg severities follow the occurrence (during the preceding fall and winter) of any strong ENSO event. Additionally, the successive occurrence of two annual strong ENSO events was assumed to produce, as well, a third year of high iceberg severity.

**Table 9:** The boundaries between the high, low and intermediate categories of each predictor assuming approximate equality between the total fractional probabilities associated with subportions of the corresponding parameter distributions and those associated with iceberg severity.

	<b>High</b>	<b>Intermediate</b>	<b>Low</b>
Sea-Ice Extent	>1.004	0.87 to 1.004	<0.87
Air Temperature	<-30.5°C	-25 to -30.5°C	>-25°C
Wind Stress Anomaly	>0.04 Pa	0.02 to 0.04 Pa	<0.02 Pa
Bravo Windage	>27x10 <sup>3</sup> km	20 to 27x10 <sup>3</sup> km	<20x10 <sup>3</sup> km
ENSO	preceded by strong event or within one year of two successive events	N.A.	high requirement not satisfied

The results of the hindcast comparisons are presented as: (1) time series representations of rationalized annual iceberg severities over the duration of the usable data records for each prediction parameter (Figure 38) and (2) statistical summaries of

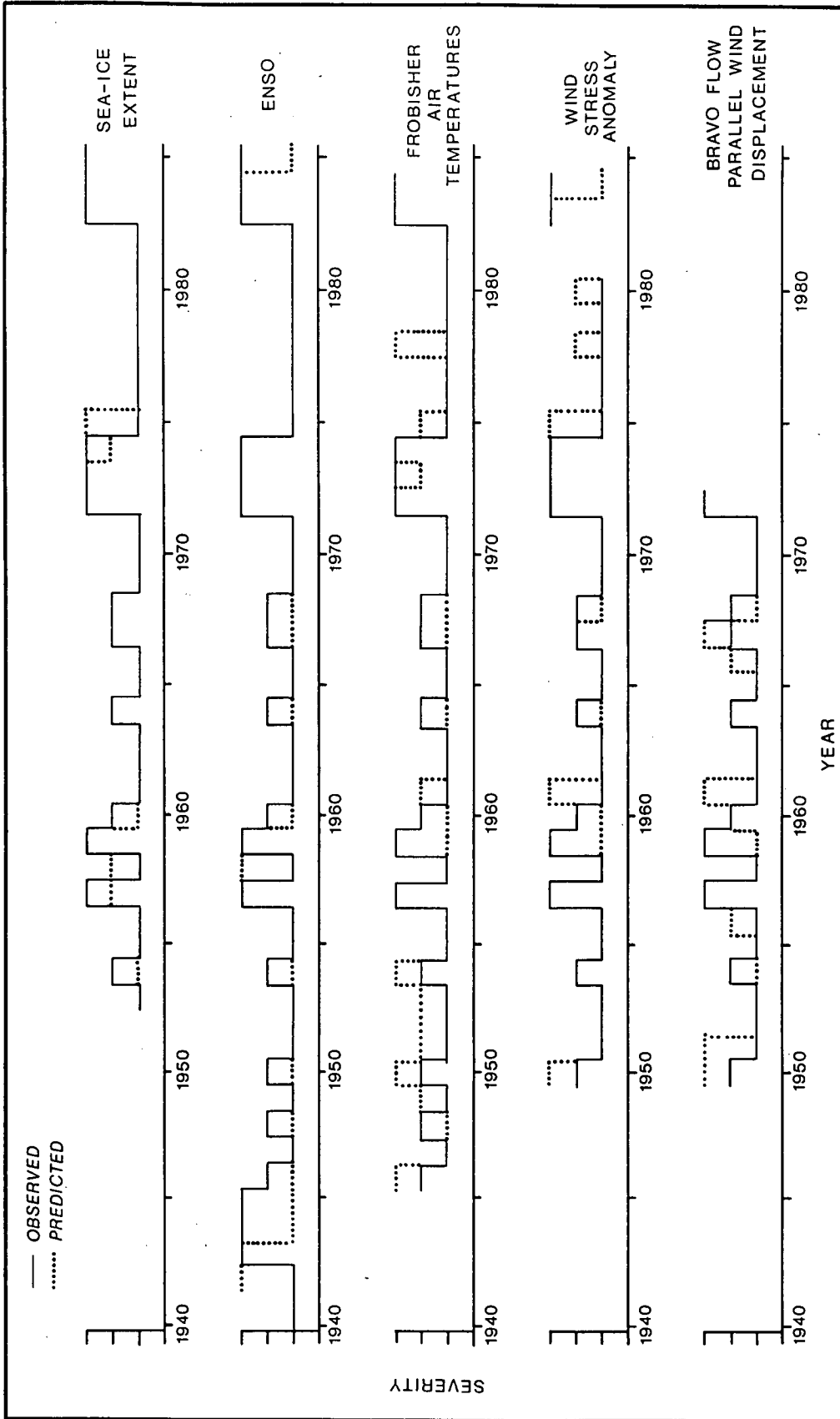


Figure 38: Predicted and observed severity levels (low, moderate or high) for the tested indicators. The dotted prediction curves are visible only when they differ from the observed 3-level severity value.

the differences between the predicted and actual iceberg severities (Table 10). The broken-line representations of the predicted or hindcast rationalized time series are visible only in those portions of the time record when their values differ from the solid line "observed" data.

In general, the correspondence of the predicted (hindcast) and observed curves is reasonably good for all parameters if errors of one level are judged to be tolerable. The statistics describing the performance of each parameter are given in Table 10 and indicate the overall superiority of the January sea-ice extent as a predictor parameter. The closely related Frobisher Bay air temperature parameter was particularly prone to one-level errors. The ENSO statistics are surprisingly good, considering the binary predictions obtained from the use of this parameter must be in error by one level in any year of intermediate iceberg severity. Its overall performance was approximately equivalent to that obtained with each of the two wind-related parameters which, strictly speaking, were not forecast parameters because of their inclusion of data from the February-March periods which could be coincident with the start of the iceberg season.

**Table 10:** Predictor statistics in terms of mean and standard errors (in levels) and percentage distribution of error magnitudes.

Predictor	Mean Error	Standard Deviation	% Correct	% Correct or One Level Error	% Two Level Error
Sea-Ice Extent	-0.03	0.53	82	97	3
ENSO	-0.22	0.75	72	89	11
Air Temperature	-0.08	0.83	56	95	5
Wind Stress Anomaly	0.0	0.97	70	88	12
Bravo Windage	0.17	1.24	61	87	13

It is important to note that the performance of the most promising predictor, sea-ice extent, may be further improved if the requirement on equality between the corresponding regions of the partitioned parameter- and iceberg severity-probability distributions is relaxed. Specifically, by allowing a more realistic boundary to be chosen for the high severity category, corresponding to normalized sea-ice extent = 1.00 (1.004, is within measurement error, identical to 1.00), the number of errors in the prediction curve is reduced to 4 out of the 33 represented years (Figure 39). In either case, the only two-level error in the hindcast prediction scheme occurred with respect to the 1975 severity. The sign of this discrepancy, corresponding to an over prediction of severity level, suggests the rather conservative predictive nature of the sea-ice extent noted previously in the scatterplots of raw count data (Figure 19). No instances of high severity were ever observed to follow low sea-ice extents. This result would appear to provide some assurance to the offshore industry that large drilling commitments in years of anticipated low severity would not be left at risk to a high iceberg influx.

It is important to note that 3 of the 4 errors made by the optimal January sea-ice extent predictor occurred during the years 1953 to 1960 when the deduced ice concentrations in Davis Strait (Walsh, 1979) were denoted by an "estimated" designation. This special designation was used to indicate that the quoted values required additional judgements to account for one or more of the following difficulties:

- a) discrepancies among values reported by two or more observers;
- b) the label "estimated" appended to the observer reported concentration values; and
- c) the absence of data which required the data base organizer to either extrapolate between the values reported for the preceding and following months (if available) or to substitute the long-term mean value.

After 1960, this notation did not appear in the January Davis Strait ice data and it is not an unlikely assumption that some or all of the pre-1961 errors were attributable to the suspect data source. Thus the performance of this predictor in its only valid test interval (1960-1985) is rather remarkable, corresponding to (depending on the precise criterion used for the high severity ice extent category boundary) one or two errors over the 25 year period.



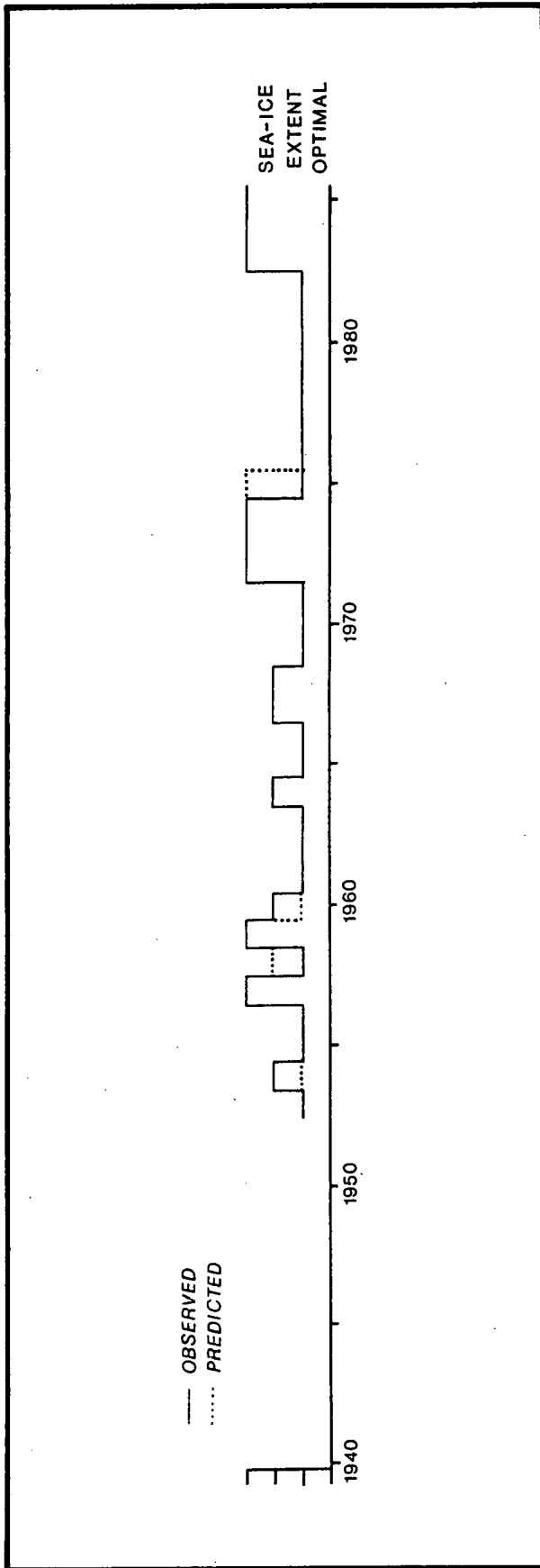


Figure 39: Predicted and observed severity levels for the sea-ice parameter, using optimized partitioning.

Nevertheless, the two-level over-estimate of the 1975 iceberg severity is a genuine error which is, moreover, common to all other tested predictors (Figure 38) with the exception of the ENSO strength parameter. Perplexity with regard to this particular year was also evident in the corresponding IIP annual report which noted the great strength of the recorded wintertime cross-flow atmospheric pressure gradients. The IIP report went to a great length to provide explanations for the failure of large iceberg numbers to arrive on the Grand Banks. Cited possibilities included smaller than "normal" numbers of icebergs between 62°N and 67°N in February and an onshore wind in April which drove many icebergs aground off Labrador. On the basis of the limited upstream coverage of the cited surveys, we do not believe that the evidence for a reduced iceberg supply can be accepted as definitive. Similarly, IIP suggestions of source reductions due to high sea states off West Greenland, two months of ice-free conditions in Baffin Bay and "the fact that the last three seasons had brought record numbers of icebergs to the Grand Banks" were highly speculative. The significance of the springtime cross-flow wind forcing mechanism would have to be judged from, for example, careful calculations of the cross-flow wind stress anomaly during the early portion of the iceberg season.

Thus, although the 1975 anomaly suggests a real need for additional characterization of iceberg source areas and late cross-flow forcing, it would appear that the January sea-ice extent in Davis Strait is a reliable and conservative predictor of iceberg severity within the limitations of the three level rationalized severity representation. We believe that such a representation is consistent with the true resolution of the raw severity data over the extended periods (i.e. 1953-1985) required for detailed testing of predictors. Improvements in survey accuracy may eventually allow upgrading to four or more levels in which case, a more precise evaluation of the ice-extent/iceberg number correspondence should be possible.

At this stage of development however, three level prediction does appear to be feasible using the sea-ice extent indicator in conjunction with the other parameters. The other parameters, while less reliable, are still surprisingly effective as predictors. The important point to note here is that taken together, tolerable to excellent performance of the entire set of predictors is consistent with a single consistent picture of iceberg severity variability. In this view, the southward iceberg flux is controlled by the strength of the mean cyclonic atmospheric circulation off the northeastern corner of North

America. Some evidence is available linking the strength of this system, and hence iceberg flux, to important large-scale shifts in global pressure patterns. Our results suggest that the best measure of forthcoming severities can be obtained from measurements of the sea-ice extent indicator supplemented by monitoring of the other physical parameters which appear to be associated with a casual chain linking a global source of variability and the severity end product.

## 5. CONCLUSIONS AND RECOMMENDATIONS

### 5.1 SUMMARY AND CONCLUSIONS

In the foregoing sections, the existence of physically understandable relationships between environmental parameters and subsequently observed iceberg severities has been demonstrated. Moreover, these relationships appear to be consistent with a reasonably well-established mechanism whereby the circulation of icebergs off Canada's eastern coastline is governed by oceanic and atmospheric forcing. Of particular importance in the variability process are shifts in the position and intensity of the cyclonic mean atmospheric pressure gyre (the Icelandic Low) which is normally positioned near southern Greenland. Correspondences were evident between the exponentially distributed "raw" severity values and Gaussian distributed variables, including: the areal extent of January sea-ice and January air temperatures in Davis Strait; and December-to-February and January-to-March measures of the coast-paralleling wind forcing components off Labrador. Additionally, periods of high severity were found to be preceded by reasonably well-defined maxima in the strength index associated with the ENSO phenomenon. It was proposed that the latter phenomenon was indicative of shifts in the global atmospheric pressure distribution which initiate shifts in the Icelandic Low. Variations of the Icelandic Low affect both the indicative (sea-ice extent and temperature) and causative (windage and wind stress anomaly) parameters.

Quantitative testing of these ideas required first, the minimizing of the effects of observational noise in the raw severity record. This was done using a three-level classification system of "rationalized" severity. Criteria were established for associating portions of the range of variability of each parameter with portions of the rationalized severity range by requiring equal fractional probability for corresponding three level severity and prediction parameter categories. Later, some relaxation of this partitioning requirement was allowed to reflect realistic parameter measurement uncertainties and to optimize hindcast success.

The results of the comparisons indicated that the January sea-ice extent indicator made only one or two errors (depending on the specific partitioning boundaries) over a 25-year period of reliable data values. Likewise, excellent agreement was achieved on a binary (two-level prediction) basis with the ENSO strength

predictor although the small number (5) of strong ENSO events included in the study period make the postulated connection highly speculative.

The remarkable coincidence of the ice extent and rationalized severity record suggests that not only is severity prediction possible but, to a considerable extent, it has already been achieved.

The sea-ice extent indicator and the ENSO indicator would appear to have the potential for offering predictions at least 3 to 6 months in advance of events. Better definition of the strong ENSO-severity linkage could extend the prediction data back to the fall or summer preceding the iceberg season. A key feature of the ice extent predictor is its conservative nature, whereby it was never observed to predict a low severity in a year of high severity.

Nevertheless, the possibilities for error remain as indicated by the two-level over-prediction of iceberg severity for the 1975 season. Recommendations for research directed at further improvement and the development of an overall understanding of the large-scale iceberg and sea-ice transport problem are given in the following section.

## 5.2 RECOMMENDATIONS

Upgrading of the data bases pertinent to all four boxes in Figure 3 is essential if we are to make further progress in developing a capability to predict large-scale changes in the numbers of icebergs and amounts of sea-ice which reach southern Canadian waters. A quantitative understanding of the patterns and statistics of the ice movements requires:

1. Improved survey resolution to obtain better measures of both the populations available in the secondary source regions and the true numbers of icebergs surviving to the 48th parallel. Surveys should emphasize completeness of coverage in all areas observed to have significant iceberg populations. Distinctions should be made between icebergs which are mobile or temporarily grounded in mobile pack ice and those which are trapped within fast ice zones.
2. The establishment of the precise connection between sea-ice extent and iceberg severity requires better documentation of the interannual and shorter term variability of sea-ice movement. Such documentation is

now available from the NOAA images collected for the winters of 1980-1981, 1981-1982, 1982-1983 and 1984-1985. Processing capabilities are now becoming available to extract velocity time series measurements from these data sources with sufficient accuracy to establish the linkage between flow parameters and sea-ice extent. Satellite imagery or ice chart analysis should also be carried out to establish whether the Gaussian distribution of the upstream (Davis Strait) ice extent becomes significantly modified at more southern latitudes to the proposed (Ebbesmeyer, Okubu and Helseth, 1980) exponential form, characteristic of the extinction region of a forward diffusing quantity.

3. Major advances in the understanding of time-dependent changes in the numbers of icebergs present in a deteriorating body of iceberg-laden ice. Empirical studies would appear to offer the only practical means of handling the large-scale calving problem. The design of programs is possible utilizing present IIP and AES surveillance data in connection with a small number of satellite-tracked, beacon-marked icebergs which could give the needed relationship between non-advective changes in iceberg numbers as a function of location, sea state and water temperature.
4. Active contact and cooperation with research on teleconnection and global pressure fluctuation phenomena in order to further possibilities for longer term prediction.
5. Stress anomaly calculations similar to those performed by Thompson and Hazen (1983) for individual months of the iceberg season to identify years in which significant cross-flow movements of the iceberg populations would have been expected in the Labrador Sea. Comparisons of the results with the predictor and severity variability would allow estimation of the probability and criteria for late modification of predicted severity levels.
6. In conjunction with point 2. above, a better understanding of the winter oceanographic and sea-ice regime off the continental shelves bordering Davis Strait, Labrador and northern Newfoundland. Separate sea-ice and current-monitoring research studies presently under way at the Bedford Institute of Oceanography, (G. Symonds, J. Lazier, pers. comm.) will

provide valuable information towards this long-term objective. A more integrated approach, directed at studying the marginal ice zone dynamics over a representative portion of the area of interest, would be invaluable in understanding the underlying transport processes relevant to iceberg severity.

## 6. REFERENCES

Note: Some of the following entries were not specifically referred to in the text. However they are included here since they may be of use to the reader with general and specific interests in iceberg severity studies.

Alekseev, A.P., B.P. Kudlo, V.N. Yakovlev, A.F. Fedoseyev, and A.A. Barinov, 1972. Some aspects of water circulation in the northwest Atlantic in 1960-1969. ICNAF Spec. Pub. No. 8, pp. 149-166.

Anderson, C., 1971. The flow of icebergs along the Canadian east coast. Proceedings of the Canadian Seminar on Icebergs held at the Canadian Forces Maritime Warfare School, CFB Halifax, December 6-7, 1971. pp. 52-62.

Anderson, I., 1984. Iceberg deterioration model. Report of the International Ice Patrol Services in the North Atlantic Ocean, 1983 season. U.S. Coast Guard Bull. No. 69, pp. 67-73, ill.

Barnett, T.P., 1985. Variations in near-global sea level pressure. J. Atm. Sci, 42(5), pp. 478-501.

Berlage, H.P., 1966. The Southern Oscillation and world weather. Mededel. Verhand., 99, Koninkl. Nederl. Meteor. Inst., 152 p.

Berlage, H.P. and H.J. DeBoer, 1960. On the Southern Oscillation, its way of operation and how it affects pressure patterns in the higher latitudes. Geofis. Pura. Appl., 46, pp. 329-351.

Birch, J.R. and D.B. Fissel, 1984. Drifting buoy measurements off the Labrador coast August to December, 1983. Prepared for Petro-Canada, Calgary, Alberta by Arctic Sciences Ltd., Sidney, B.C. 35 p. plus appendices.

Birch, J.R., D.B. Fissel and J.R. Marko, 1983. An analysis of surface drifter and iceberg motion off Labrador in winter. Vol. 1. Unpubl. rep. by Arctic Sciences Ltd., Sidney, B.C. for Petro-Canada, Calgary, Alberta, 65 p. plus appendices.

Bjerknes, J., 1966. A possible response of the atmospheric Hadley circulation to equatorial anomalies of ocean temperature. Tellus, 18, pp. 820-829.



- Bradley, R.S., 1973. Seasonal climatic fluctuations on Baffin Island during the period of instrumental records. *Arctic* 26(3), pp. 230-243.
- Brooks, L.D., 1977. Iceberg and current drift using the Nimbus 6 satellite. *Offshore Tech. Conf.*, Houston, TX, May 2-5, pp. 279-286.
- Burmakin, V.V., 1972. Seasonal and year to year variations in water temperature in the Labrador and Newfoundland areas. *ICNAF Spec. Publ. No. 8*, pp. 63-70.
- Canpolar Consultants Ltd., 1985. Pack ice/iceberg drift. Report prepared for SeaConsult Ltd. 11 p.
- Caviedes, C.N., 1975. El Nino 1972: its climatic, ecological, human and economic implications. *Geogr. Rev.* 65, pp. 493-509.
- Challender, E.R., 1947. In: International Ice Observation of Ice Patrol Service in the North Atlantic Ocean - season of 1946. *U.S. Coast Guard Bull. No. 32*.
- Chandrasekhar, 1943. Stochastic problems in physics and astronomy. *Reviews of Modern Physics*, 15, pp. 1-89.
- Chen, W.Y., 1982. Assessment of Southern Oscillation sea-level pressure indices. *Mon. Wea. Rev.* 110, pp. 800-807.
- Chen, T and X. Shi, 1984. Climatic anomalies in the South China Sea during the 1982-1983 El Nino. *Tropical Ocean-Atm. Newsletter No. 26*, pp. 11-12.
- Corkum, D.A., 1971. Performance of formula for predicting the iceberg count off Newfoundland. *J. of Appl. Meteorl.*, 10(3), pp. 605-607.
- Défant, A., 1924. Die Schwankungen der atmospherischen Zirkulation uber dem Nordatlantischen Ozean im 25-jahrigem Zeitraum 1881-1905. *Geogr. Ann.*, 6, pp. 13-41.
- Dickson, R.R., H.H. Lamb, S.A. Malmberg and J.M. Colebrook, 1975. Climatic reversal in northern North America. *Nature*, Vol. 256, pp. 479-482.

- Diemand, D. and J.H. Lever, 1986. Iceberg mass loss mechanisms and their implications for deterioration modelling. Canadian East Coast Workshop on Sea Ice, held at Bedford Institute of Oceanography, Dartmouth, N.S., January 7-9, 1986.
- Dinsmore, R.P., 1972. Ice and its drift in the north Atlantic Ocean. Intern. Commission for the Northwest Atlantic Fisheries. Spec. Publ. 8, pp. 89-128.
- Ebbesmeyer, C.C., A. Okubo and J.M. Helseth, 1980. Description of iceberg probability between Baffin Bay and the Grand Banks using a stochastic model. Deep-Sea Res. Part A. Oceanographic Research Papers: 27A: pp. 975-986.
- Eguiguren, D.V., 1894. Las Nuvias de Piura. Bol. Soc. Geogr. Lima 4(7-9), pp. 241-258.
- El-Tahan, M., Venkatesh, S. and El-Tahan, H., 1984. Validation and quantitative assessment of the deterioration mechanisms of Arctic icebergs. In: Proc. Third International Symposium on Offshore Mechanics and Arctic Engineering, New Orleans, Feb. 12-17, 1984, Vol. III, pp. 18-25.
- Enfield, D.B. and R. Lukas, 1984. Low-frequency sea level variability along the South American coast in 1981-83. Tropical Ocean-Atm. Newsletter No. 28, pp. 2-4.
- Fissel, D.B., 1980. Satellite-tracked iceberg movements in Baffin Bay and Lancaster Sound, summer 1978 and 1979. Unpub. Data Rep. No. 7, Arctic Sciences Ltd., Sidney, B.C. for Petro-Canada, Calgary, Alberta, unpaginated.
- Fissel, D.B. and D.D. Lemon, 1982. Analysis of physical oceanographic data from the Labrador shelf, 1980. Volumes I and II. Unpublished manuscript by Arctic Sciences Ltd., Sidney, B.C. for Petro-Canada, Calgary, Alberta. 156 p. plus unnumbered appendices.
- Forbes, H.O., 1914. Notes on Molina's pelican (Pelecanus thagus). Ibis, Ser. 10(2), pp. 403-420.
- Frijlinck, C.P.M., 1925. Bijdrage tot het probleem der Klimatwisselingen. Nat. Utr. 45, pp. 372-374.

- Greenland Technical Organization, 1979. Environmental conditions offshore west Greenland. Vol. IV - Icebergs. Greenland Tech. Org., Danish Hydraulic Inst., Horsholm, Denmark, 130 p. plus appendices.
- Groissmayr, F., 1939. Schwere und leichte Eisjahre bei Neufundland und Vorwetter. An. der Hydr. und maritimen Meteorl., 67(1), pp. 26-30.
- Guillen, O., 1967. Anomalies in the waters off the Peruvian coast during March and April 1965. Stud. Trop. Oceanogr. (Miami) 5, pp. 452-465.
- Halpern, D., 1984. Upper ocean heat content in the eastern equatorial Pacific during the 1982-1983 ENSO event. Tropical Ocean-Atm. Newsletter No. 24, pp. 14-16.
- Hare, F.K. and M.K. Thomas, 1974. Climate Canada. Wiley Publishers Canada, Toronto, 256 p.
- Hengeveld, H., 1981. Labrador iceberg baseline study. Atmospheric Environment Service, Ice Branch.
- Hildebrandsson, H.H., 1897. Quelques recherches sur les centres d'action de l'atmosphère. Kon. Svenska Vetens. Akad. Handl. No. 29, 36 p.
- Hisard, P. and C. Henin, 1983. The 1982-1983 warm upwelling season in the Canary Current off Dakar. Tropical Ocean-Atm. Newsletter No. 19, pp. 12-13.
- Horel, J. and J.M. Wallace, 1981. Planetary-scale atmospheric phenomena associated with the Southern Oscillation. Monthly Weather Review, 109, pp. 813-829.
- Hoskins, B.J. and D. Karoly, 1981. The steady linear response of a spherical atmosphere to thermal and orographic forcing. J. Atmos. Sci., 38(6), pp. 1179-1196.
- Hutchinson, G.E., 1950. Survey of existing knowledge of biogeochemistry. 3. The biogeochemistry of vertebrate excretion. Bull. Am. Mus. Nat. Hist. 96, 554 p.
- Idyll, C.P., 1973. The anchovy crisis. Sci. Am. 228(6), pp. 22-29.

- Intera Environmental Consultants, 1982. Historical SLAR iceberg data base ceation (Labrador Sea, 1978-1980). Report for Atmospheric Environment Service.
- Job, J.J., 1978. Moving unprotected icebergs to southern continents. In: Iceberg Utilization, A.A. Husseiny, ed. Pergamon, New York, pp. 503-527.
- Julian, P.R. and R.M. Chervin, 1978. A study of the Southern Oscillation and Walker circulation phenomenon. Mon. Weather Rev. 106, pp. 1433-1451.
- Ketchen, H.G., 1977. Iceberg populations south of 48°N since 1900. In: Report of the International Ice Patrol Service in the North Atlantic Ocean, U.S.C.G. Bull. No. 63, CG-188-32, pp. C1-C6.
- Kinsman, B., 1957. Proper and improper use of statistics in geophysics. Tellus IX, pp. 408-418.
- Kutzbach, J.E., 1970. Large-scale features of monthly mean Northern Hemisphere anomaly maps of sea-level pressure. Mon. Wea. Rev., 98, pp. 708-716.
- Lavalle, Y. Garcia J.A., De, 1917. Informe preliminar sobre la causa de la mortalidad anormal de las aves ocurida en el mes de marzo del presente ano. Mem. Cia. Adm. Guano, Lima 8.
- Lavalle, Y. Garcia J.A., De, 1924. Estudio de la emegracion y mortalidad de las aves guaneras. Mem. Cia. Adm. Guano, Lima 15.
- Lazier, J.R.N., 1982. Seasonal variability of temperature and salinity in the Labrador Current. J. Marine Res. 40: pp. 341-356.
- Lobell, M.G., 1942. Some observations on the Peruvian coastal current. Trans Am. Geophys. Union 23, pp. 332-336.
- Marko, J.R., J.R. Birch and M.A. Wilson, 1982. A study of long-term satellite-tracked iceberg drifts in Baffin Bay and Davis Strait. Arctic 35(1), pp. 234-240.
- Martec, 1982. Project iceberg statistics. Final Report. Unpublished manuscript by Martec Limited, Halifax, Nova Scotia for Petro-Canada, Calgary, Alberta. 134 p.

- Mears, E.G., 1944. The ocean current called "The Child". Annu. Rep. Smithson. Inst., 1943, pp. 245-251.
- Mecking, L., 1906. Die Eisdrift aus den Bereich der Baffin Bay beherrscht von Strom und Wetter. Veröff Inst. Meereskunde, 7, pp. 1-132.
- Mecking, L., 1907. Die Treibeiserscheinungen bei Neufundland in ihrer Abhängigkeit von Witterungsverhältnissen. An. der Hydr. und maritimen Meteorl., 35(8), pp. 348-355, (9) pp. 396-409.
- Meinardus, W., 1904. Über Schwankungen der nordatlantischen Zirkulation und ihre Folgen. An. Hydro., 32, pp. 353-362.
- Meserve, J.M., 1974. U.S. Navy Marine Climatic Atlas of the World. Naval Weather Service Detachment. Doc. NAVAIR 50-1C-528. U.S. Gov't Printing Office, Washington, D.C., 371 p.
- Mitchell, J.M., 1963. On the world-wide pattern of secular temperature change. In: Changes of Climate. Arid Zone Research XX, UNESCO Paris, pp. 161-181.
- Mitchell, J.M., 1971. The effect of atmospheric aerosols on climate with special reference to temperature near the earth's surface. J. of Appl. Meteorl. 10, pp. 203-214.
- Morgan, C.W., 1974. Long-term trends in the iceberg threat in the northwest Atlantic. In: Report of the International Ice Patrol Service in the North Atlantic Ocean - season of 1971. U.S. Coast Guard Bull. 57, CG-188-26, Dept. of Transportation, pp. 15-26.
- Murphy, R.C., 1923. The oceanography of the Peruvian littoral with reference to the abundance and distribution of marine life. Geogr. Rev. 13, pp. 64-85.
- Murphy, R.C., 1926. Oceanic and climatic phenomena along the west coast of South America during 1925. Geogr. Rev. 16, pp. 26-54.
- Murray, J.E., 1968. The drift, deterioration and distribution of icebergs in the North Atlantic Ocean. The Ice Seminar, CIM Special Vol. 10, Calgary, Alberta.

- Murty, T.S. and P.A. Bolduc, 1975. Prediction of the severity of iceberg season in the northwest Atlantic Ocean. 1975 Offshore Technology Conference, May 5-8, Houston, TX, proceedings. - Dallas, TX: Offshore Technology Conference, 1975, Vol. 3, pp. 785-794, ill.
- Namias, J., 1969. Seasonal interactions between the North Pacific Ocean and the atmosphere during the 1960's. Mon. Weather Rev. 97, pp. 173-192.
- Namias, J., 1972. Influence of Northern Hemisphere general circulation on drought in northeast Brazil. Tellus, 24, pp. 336-343.
- Namias, J., 1976. Some statistical and synoptic characteristics associated with El Nino. J. Phys. Oceanogr., 6, pp. 130-138.
- Namias, J., 1980. Case studies of exceptional climate in United States 1975-1979 air-sea interactions. In: Climatic Variations and Variability: Facts and Theories, A. Berger (ed). D. Reidel Publ. Co., Dordrecht, Holland, pp. 369-398.
- Nobre, P., A.D. Moura and C.A. Norbe, 1985. Planetary-scale circulation anomalies associated with droughts over northeast Brazil. Tropical Ocean-Atm. Newsletter, No. 30, pp. 11-13.
- Opsteegh, J.D. and H.M. Van Den Dool, 1980. Seasonal differences in the stationary response of a linearized primitive equation model: prospects for long-range forecasting? J. Atmos. Sci., 37, pp. 2169-2185.
- Perchanok, M., Kot, Edworthy, Singh and Comfort, 1982. SLAR/SAR image analysis, east coast Labrador and Newfoundland. Report prepared by Arctec Canada Ltd.
- Petrie, B. and C. Anderson, 1983. Circulation on the Newfoundland continental shelf. Atmosphere-Ocean 21: pp. 207-226.
- Petro-Canada, 1982. Offshore Labrador Initial Environmental Assessment. Calgary, Alberta. 572 p.

- Post, L.A., 1956. The role of the Gulf Stream in the prediction of iceberg distribution in the North Atlantic. *Tellus*, 8(1), pp. 102-111, ill.
- Putnins, P., 1970. The climate of Greenland. In: *Climates of the Polar Regions, Word Survey of Climatology, Vol. 14, Ch. 2*, S. Orvig (ed), pp. 3-128.
- Quinn, W.H., 1974. Monitoring and predicting El Nino invasions. *J. Appl. Meteorol.*, 13, pp. 825-830.
- Quinn, W.H., 1976. Use of Southern Oscillation indices to assess the physical environment of certain tropical Pacific fisheries. In: *Proceedings of the NMFS/EDS Workshop on Climate and Fisheries, Columbia, Mo., April 26-29, 1976*, pp. 50-70. U.S. Dep. Commer., NOAA, Natl. Mar. Fish. Serv. - Environ. Data Serv.
- Quinn, W.H., D.O. Zopf, K.S. Short and R.T.W.K. Yang, 1978. Historical trends and statistics of the Southern Oscillation, El Nino, and Indonesian droughts. *Fishery Bull.* 76(3), pp. 663-678.
- Quinn, W.H. and D.O. Zopf, 1984. The unusual intensity of the 1982-1983 ENSO event. *Tropical Ocean-Atm. Newsletter No. 26*, pp. 17-20.
- Quiroz, R.S., 1983. The climate of the El Nino winter of 1982-1983, a season of extraordinary climatic anomalies. *Monthly Weather Rev.*, 111, pp. 1685-1706.
- Rasmusson, E.M., 1984. El Nino: the ocean/atmosphere connection. *Oceanus*, 27(2), pp. 5-12.
- Rasmusson, E.M. and T. Carpenter, 1982. Variations in the tropical sea-surface temperature and surface wind fields associated with the Southern Oscillation/El Nino. *Mon. Wea. Rev.*, 110, pp. 254-284.
- Robe, R.Q. and D.C. Maier, 1979. Long-term tracking of arctic icebergs. U.S. Coast Guard, R&D Center, Groton, Conn., Rep. No. CG-D-36-79, 35 p.
- Rogers, J.C., 1984. The association between the North Atlantic Oscillation and the Southern Oscillation in the northern hemisphere. *Mon. Wea. Rev.*, 112, pp. 1999-2015.

- Schell, I.I., 1940. Foreshadowing the severity of the iceberg season south of Newfoundland. *Bull. Amer. Met. Soc.* 21: pp. 7-10.
- Schell, I.I., 1950. Further notes on foreshadowing the severity of the iceberg season south of Newfoundland. Woods Hole Oceanographic Institution, Woods Hole, Mass.; Springfield, Va. Ref. Ser. 50-15.
- Schell, I.I., 1952a. Stability and mutual compensation of relationships with the iceberg severity off Newfoundland. *Trans. Am. Geophys. Union* 33 (1): pp. 27-31.
- Schell, I.I., 1952b. The problem of the iceberg population in Baffin Bay and Davis Strait and advance estimate of the berg count off Newfoundland. *J. Glaciology* 2 (11): pp. 58-59.
- Schell, I.I., 1962. On the iceberg severity off Newfoundland and its prediction. *J. of Glaciology*, 4(32), pp. 161-172.
- Schell, I.I., D.A. Corkum and E.N. Sabbagh, 1975. Recent climatic changes in the eastern North American sub-arctic. In: G. Weller and S.A. Bowling (ed) 24th Alaska Sc. Conf., Aug. 15-17, 1973, Pub. by U. Alaska, Fairbanks, pp. 76-81.
- Schott, G., 1904. Die Grosse Eistrift bei der Neufundlandbank und die Warmeverhältnisse des Meerwassers im Jahr. 1903. *Annalen der Hydrographie und maritimen Meteorologie*, Vol.32, pp. 277-287.
- Schweigger, E.H., 1961. Temperature anomalies in the eastern Pacific and their forecasting. *Soc. Geogr. Lima, Bol.* 78, pp. 3-50.
- Sears, M., 1954. Notes on the Peruvian coastal current. 1. An introduction to the ecology of Pisco Bay. *Deep-Sea Res.* 1, pp. 141-169.
- Shepard, G., 1930. Notes on the climate and physiography of southwestern Ecuador. *Geogr. Rev.* 20, pp. 445-453.
- Shepard, G., 1933. The rainy season of 1932 in southwestern Ecuador. *Geogr. Rev.* 23, pp. 210-216.
- Smith, E., 1931. The Marion Expedition to Davis Strait and Baffin Bay, 1928. *U.S. Coast Guard Bull. No.* 19, Pt. 3, 221 p.



- Soule, F. and E. Challenger, 1949. Discussion of some of the effects of winds on ice distribution in the vicinity of the Grand Banks and the Labrador Shelf. U.S. Coast Guard Bull. No. 33, CG-188-1, pp. 59-61.
- Soule, F. et al, 1950. Oceanography of the Grand Banks Region and Labrador Sea, 1948. U.S. Coast Guard Bull. CG-188-3: p. 78.
- Thompson, K.R. and M.G. Hazen, 1983. Interseasonal changes of wind stress and Ekman upwelling: North Atlantic, 1950-1980. Can. Tech. Rep. Fish. Aquat. Sci. No. 1214, 175 p.
- Thomson, R.E., 1984. El Nino, an equatorial phenomenon of global importance. Unpubl. rep., Institute of Ocean Sciences, Sidney, B.C., 51 p.
- Thomson, R.E., H.J. Freeland and L.F. Giovando, 1984. Long-term sea surface temperature variations along the British Columbia coast. Tropical Ocean-Atm. Newsletter No. 26, pp. 9-11.
- Trenberth, K.E., and D.A. Paolino, 1981. Characteristic patterns of variability of sea level pressure in the northern hemisphere. Mon. Wea. Rev., 109, pp. 1169-1189.
- Trites, R.W. and K.F. Drinkwater, 1985. Overview of environmental conditions in the Northwest Atlantic during 1983. NAFO Sci. Coun. Studies, 8, pp. 7-20.
- van Loon, H. and R.A. Madden, 1981. The Southern Oscillation. Part I: Global associations with pressure and temperature in northern winter. Mon. Wea. Rev., 109, pp. 1150-1162.
- Walker, G.T., 1924. World Weather II. Mem. India Meteor. Dep. 24, pp. 275-332.
- Walker, G.T., 1928. World Weather III. Mem. Roy. Meteor. Soc., 17, pp. 97-106.
- Walker, G.T. and E.W. Bliss, 1932. World Weather V. Mem. Roy. Meteor. Soc., 4, pp. 53-84.
- Walker, G.T., 1947. Arctic conditions and world weather. Q.J.R. Met. Soc. 73, pp. 226-256.

- Wallace, J.M. and D.S. Gutzler, 1981. Teleconnections in the geopotential height field during the northern hemisphere winter. *Mon. Wea. Rev.*, 109, pp. 784-812.
- Walsh, J.E., 1979. A data set on northern hemisphere sea ice extent. World Data Center-A for Glaciology (Snow and Ice). Report GD-2.
- Webster, P.J., 1981. Mechanisms determining the atmospheric response to sea surface temperature anomalies. *J. Atmos. Sci.*, 38(3), pp. 554-571.
- White, F.M., Spaulding, M.L. and Gominho, L., 1980. Theoretical estimates of the various mechanisms involved in iceberg deterioration in the open ocean environment. U.S. Coast Guard R&D Center Rep. CG-D-62-80, 126 p.
- Wooster, W.S., 1960. El Nino. Calif. Coop. Oceanic Fish. Invest. Rep. 7, pp. 43-45.
- Wooster, W.S., 1983. An index of anomalous SST in the eastern equatorial Pacific, 1970-1982. *Tropical Ocean-Atm. Newsletter*, pp. 4-5.
- Wyrтки, K., E. Stroup, W. Patzert, R. Williams and W. Quinn, 1976. Predicting and observing El Nino. *Science* (Wash., D.C.) 191, pp. 343-346.